Norwegian University of Life Sciences
Faculty of Environmental Sciences
and Natural Resource Management

Philosophiae Doctor (PhD)
Thesis 2018:84

Performance Degradation Studies on Field-Aged Solar Photovoltaic Modules

Ytelsesstudier på aldrende solceller

David Ato Quansah

Performance Degradation Studies on Field-Aged Solar Photovoltaic Modules

Ytelsesstudier på aldrende solceller

Philosophiae Doctor (PhD) Thesis

David Ato Quansah

Norwegian University of Life Sciences
Faculty of Environmental Sciences and Natural Resource Management

Ås (2018)

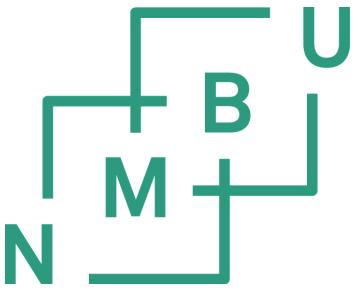

Thesis number 2018:84
ISSN 1894-6402
ISBN 978-82-575-1550-8

Supervisors

Professor Muyiwa Samuel Adaramola (Main Supervisor)
Renewable Energy Group
Faculty of Environmental Sciences and Natural Resource Management
Norwegian University of Life Sciences (NMBU)
P.O. Box 5003 NMBU, NO-1432 Ås, Norway

Dr. Gabriel Takyi (Co-Supervisor)
Senior Lecturer
Department of Mechanical Engineering
Kwame Nkrumah University of Science and Technology
Kumasi, Ghana

Evaluation Committee

Dr. Josefine Helene Selj
Research Scientist
Institute for Energy Technology
Instituttveien 18, NO-2007 Kjeller, Norway

Dr. David Mosser
Senior Researcher
EURAC Research – Institue for Renewable Enery,
Viale Druso Drususalle 1, I-39100 Italy

Associate Professor Thomas, Martinsen,
Renewable Energy Group
Faculty of Environmental Sciences and Natural Resource Management
P.O. Box 5003 NMBU, NO-1432 Ås, Norway

Acknowledgements

I am most grateful to Professor M. Sam Adaramola (my main supervisor) through whom I had the opportunity to study at one of Norway's prestigious institutions. I once more thank Professor Adaramola for his guidance and encouragement as my main supervisor, and also thank Dr Gabriel Takyi (co-supervisor) for his assistance. My visit to the Arizona State University (Photovoltaics Reliability Laboratory) in January 2015 gave me an early exposure to the subject of photovoltaic module degradation. I am grateful to Dr Gabriel Takyi for this.

To my wife Emmanuella and our children Nyamekye, Kwamena and Ewurama (who stayed only briefly), your sacrifices and support during this journey are forever appreciated. The financial and administrative support that I received from the Norwegian State Education Fund (Lånakassen - Quota Scholarship programme) and the Faculty of Environmental Sciences and Natural Resource Management (MINA) at NMBU towards my doctoral education is gratefully acknowledged. I am also grateful to my employer, the Kwame Nkrumah University of Science and Technology (KNUST), Ghana, for granting me study leave to enable me to complete my doctoral studies. Equipment support and administrative backstopping provided by The Brew-Hammond Energy Centre at KNUST was critical to the success of fieldwork in Ghana – this assistance is much appreciated! Again, at KNUST, assistance received from Mr. Isaac A. Edwin and Mr. Clement Appiah of the Solar Energy Applications Laboratory (SEAL) at various stages of this work is recalled with gratitude.

I am also indebted to various institutions in Ghana, which showed interest in this research and provided approval for their solar photovoltaic installations to be included in this study. These include the Ministry of Energy, Ghana Cocoa Board, Community Water and Sanitation Agency and the Social Security and National Insurance Trust.

Field assistance received from Mr Ekow Hagan, Madam Florence (a social worker at the Ga South Municipal Assembly in Ghana), Mr Joe Addae, Amadu Mahama (New Energy, Tamale), Mr Duut

Konlanbik (Nakpanduri), Mr Isaac Yamdogo (Navrongo/Paga), Mr Cornelius Yadle (Fielmon area). Support provided by Joseph Oti-Bioh (The Brew-Hammond Energy Centre) in conducting measurements in Northern Ghana (Napkanduri and Navrongo/Paga) is likewise acknowledged.

Back to Norway, my thoughts turn in gratitude to St Olav's Cathedral Parish in Oslo, where I found a home away from home, providing spiritual and emotional support throughout this journey, I am truly thankful for all these. To all the colleagues at MINA (Denis, Dawit, Mekdes, Nathan, Solrun, Thomas, Mengesteab, Yennie, Greyson and EVERYONE), thanks for your warm friendship.

Ad Majorem Dei Gloriam

David Ato Quansah
Ås Norway (September 2018)

TABLE OF CONTENTS

Abstract

Solar photovoltaic (PV) technology, in its variant forms, has evolved over the last four decades to become a mainstream energy technology for terrestrial applications, and is already playing an important role in national and regional energy systems around the world. As development increasingly becomes emissions-constrained, the role of solar PV (and renewable energy in general), takes on added significance and urgency. The transformation of the energy sector requires a major shift towards renewable energy (and efficient energy use). While solar PV plays an important role all scenarios and models of a low-carbon energy system, its deployment requires significant investments. Since the operating cost of solar PV systems is typically low, its life-cycle cost is dominated by the initial investment cost and it is therefore critical that the system delivers as expected, in order to realize an acceptable return on investment. Investment decision on the other hand relies on data regarding expected system performance and longevity.

While market development has been significantly aided by the development of standards such as the IEC 61215, the standard by itself does not provide assurance of longevity. The aim of this thesis is to make a scientific contribution to the understanding of solar PV performance degradation by studying field-exposed systems in Ghana within different sub-climatic contexts. The climatic delineation system adopted for this study was on the basis of latitude bands, and categorized as Humid (H) (lat. 0 - 6^{o}N), Sub-Humid Humid (SHH) (lat. 6 - 10^{o}N) and Sub-Humid Dry (SHD) (lat. 10 - 12^{o}N).

Sixty-five (65) mono- and poly-crystalline silicon (mc-Si and pc-Si) modules from twenty-nine (29) installations at different locations in all climate zones were assessed in studying long-term degradation effects. Early-period performance loss was assessed by examining time-series data on five co-located silicon and non-silicon based technologies. The results of this study were communicated in four journal articles (Papers 1 - 4). Paper 1 assessed 19-year-old polycrystalline modules deployed in off-grid battery-charging mode installed in climate category SHH, and found median degradation rate of 1.3%/year, dominated by losses in module fill factor (FF) followed by

losses in short-circuit current (I_{sc}). With the exception of minor bubbles observed on the front-side of the modules, no other visually observable defects (VODs) were found.

Paper 2 extended the scope of geo-climates and module technologies. It studied mono- and poly-crystalline systems from six locations in climate categories SHH and H. Degradation rates ranging from 0.8%/yr to 6.5%/yr were found for the systems. Fill factor losses were dominant in the most degraded modules (5%/yr and above). In general, however, I_{sc}-related defects such as delamination and encapsulant discolouration were the most prevalent defect. Poorly installed modules, and modules with no certification were found. The ages of the installations ranged from 6 - 32 years.

Paper 3 focused on the issue of early-period degradation and power loss in field-exposed modules. It studied five co-located PV module technologies, namely: mc-Si, pc-Si, a-Si (amorphous silicon), hybrid mc-Si/a-Si (Heterojunction with Intrinsic Thin layer - HIT) and CIS (Copper Indium Sulfide). Using system-level performance data and performance-ratio time-series regression, early losses (year 1) of up to 13.8% were found.

Paper 4 studied 16-year old mc-Si modules in Northern Ghana, of climate sub-category SHD and found degradation rate of 1.5%/yr. The losses were driven by I_{sc} losses (0.75%/yr), followed by FF losses (0.54%/yr). Dominant VODs were encapsulant browning and degraded adhesive of the junction-box.

Overall, climate-based aggregation of the results of this thesis show long-term linear annual degradation rate (median) of 1.4%/yr, 1.5%/yr and 1.8%/yr for SHH, SHD and H climate categories respectively. These results do not support typical industry claims of 80% (minimum) of a module's rated power within 20-25 years.

Sammendrag

Solar fotovoltaik(PV)-teknologi, i alle forskjellige varianter, har utviklet seg de siste fire tiårene til å bli en vanlig energiteknologi for landbaserte applikasjoner, og spiller allerede en viktig rolle i nasjonale og regionale energisystemer rundt omkring i verden. Etter hvert som utviklingen i økende grad blir utslippsbegrenset, får solar PV (og fornybar energi generelt), en større betydning og et større hastverk.

Transformasjonen av energisektoren krever et stort skifte mot fornybar energi (og effektiv energibruk). Mens solar PV spiller en viktig rolle i alle scenarier og modeller av et lav-karbon-energisystem, krever distribusjonen betydelige investeringer. Siden driftskostnadene for solar-PV-systemer vanligvis er lave, er deres livssykluskostnader dominert av den opprinnelige investeringskostnaden, og det er derfor av avgjørende betydning at systemet leverer som forventet for å realisere en akseptabel avkastning på investeringen. På den annen side avhenger investeringsbeslutningen av data på forventet systemytelse og levetid.

Selv om markedsutviklingen har fått vesentlig støtte av utviklingen av standarder som IEC 61215, gir standarden i seg selv ingen garanti for lang levetid. Målet med denne avhandlingen er å gi et vitenskapelig bidrag til å forstå solar PV ytelsesforringelse ved å studere feltbaserte systemer i Ghana innenfor ulike subklimatiske forhold. Det klimatiske avgrensningssystemet bestemt for denne studien var basert på breddegrader, og kategorisert som fuktig (H) (lat. 0 - 6^{o}N), sub-fuktig fuktig (SHH) (lat. 6 - 10^{o}N) og sub-fuktig tørr (SHD) (lat. 10 - 12^{o}N).

Sekstifem (65) mono- og polykrystallinske silisium-(mc-Si og pc-Si) moduler fra tjueni (29) installasjoner på forskjellige steder i alle klimasoner ble vurdert ved å studere langsiktige nedbrytningseffekter. Ytelsestap i tidlige faser ble vurdert ved å undersøke tidsseriedata på fem samlokaliserte silisium- og ikke-silisiumsbaserte teknologier. Resultatene av denne studien ble

kommunisert via fire artikler i vitenskapelige journaler (Artikkel 1 - 4). Artikkel 1 vurderte 19-årige polykrystallinske moduler som ble utplassert i off-grid batteriladningsmodus som ble installert i klimakategori SHH, og fant en median nedbrytningshastighet på 1,3% / år, dominert av tap i modulfyllingsfaktor (FF) etterfulgt av tap i kortslutningsstrøm (I_{sc}). Med unntak av mindre bobler observert på forsiden av modulene, ble det ikke funnet andre visuelt observerbare feil (VODer).

Artikkel 2 utvidet omfanget av geoklima og modulteknologi. Den omhandlet mono- og polykrystallinske systemer fra seks steder i klimakategoriene SHH og H. Det ble funnet degraderingshastigheter fra 0,8% / år til 6,5% / år for systemene. Tap av fyllingsfaktorer var dominerende i de mest degraderte modulene (5% / år og mer). Generelt var imidlertid I_{sc}-relaterte mangler som delaminering og misfarging av innkapslingen den mest utbredte feilen. Dårlige installerte moduler, og moduler uten sertifisering ble funnet. Installasjonenes alder varierte fra 6 til 32 år.

Artikkel 3 fokuserte på spørsmålet om tidlig degradering og krafttap i felteksponerte moduler. Den omhandlet fem samlokaliserte PV-modulteknologier, nemlig: mc-Si, pc-Si, a-Si (amorft silisium), hybrid mc-Si / a-Si (Heterojunction med Intrinsic Thin layer - HIT) og CIS (kopperindiumsulfid). Ved bruk av ytelsesdata på systemnivå og tidsserieregresjon på ytelsesforhold, ble det funnet tidlige tap (år 1) på opptil 13,8%.

Artikkel 4 omhandlet 16-årige mc-Si-moduler i Nord-Ghana, i klima-subkategorien SHD og fant en nedbrytningshastighet på 1,5% / år. Tapene ble drevet av I_{sc} -tap (0,75% / år), etterfulgt av FF-tap (o,54% / år). Dominerende VODs var bruning av innkapslingen og degradert festemiddel i sikringsboksen. Klimabasert aggregering av resultatene av denne oppgaven viser langsiktig lineær nedbrytning på 1,4% - 1,8% / år, (median) og støtter ikke industriens påstander om 80% (minimum) av modulens graderte kraft innen 20-25 år.

List of Papers

Paper 1	**David A. Quansah**, Muyiwa S. Adaramola, Gabriel Takyi, Isaac A. Edwin (2017). Reliability and Degradation of Solar PV Modules—Case Study of 19-Year-Old Polycrystalline Modules in Ghana. *Technologies* **2017**, *5*(2), 22. http://www.mdpi.com/2227-7080/5/2/22/htm
Paper 2	**David A. Quansah** and Muyiwa S. Adaramola (2018). Comparative study of performance degradation in poly- and mono-crystalline-Si solar PV modules deployed in different applications. *International Journal of Hydrogen Energy Volume 43, Issue 6, 8 February 2018, Pages 3092–3109.* https://doi.org/10.1016/j.ijhydene.2017.12.156
Paper 3	**David A. Quansah** and Muyiwa S. Adaramola (2019). Assessment of early degradation and performance loss in five co-located solar photovoltaic module technologies installed in Ghana using performance ratio time-series regression. *Renewable Energy Volume 131, 8 February 2019, Pages 900-910 https://www.sciencedirect.com/science/article/pii/S0960148118309145*
Paper 4	**David A. Quansah** and Muyiwa S. Adaramola (2018). Ageing and Degradation in Solar Photovoltaic Modules: An Assessment of 16-year-old modules installed in Northern Ghana. *Solar Energy 173 (2018), pages 834–847* https://doi.org/10.1016/j.solener.2018.08.021

Other Papers

David A. Quansah, Muyiwa S. Adaramola, George K Appiah, Isaac A. Edwin (2017). Performance analysis of different grid-connected solar photovoltaic (PV) system technologies with combined capacity of 20 kW located in humid tropical climate. *International Journal of Hydrogen Energy Volume 42, Issue 7* https://doi.org/10.1016/j.ijhydene.2016.10.119

David A. Quansah and Muyiwa S Adaramola (2016). Economic Assessment of a-Si and CIS Thin Film Solar PV Technologies in Ghana. *Sustainable Energy Technologies and Assessments (Elsevier), Volume 18, pages 164–174*. http://www.sciencedirect.com/science/article/pii/S2213138816301308

David A. Quansah, Muyiwa S Adaramola, Lena D Mensah (2016). Solar Photovoltaics in sub-Saharan Africa - Addressing Barriers, Unlocking Potential. *Energy Procedia 106 (2016) 97 – 110*. http://www.sciencedirect.com/science/article/pii/S1876610216316666

D. A. Quansah, M. S. Adaramola and G.Takyi (2016). Preliminary Assessment of Degradation in Field-Aged Multi-Crystalline Silicon PV Modules Installed in Hot-Humid Climate of Mid Ghana. ***32nd European Photovoltaic Solar Energy Conference and Exhibition (EUPVSEC)****, 20 - 24 June 2016, Munich Germany*. http://www.eupvsec-proceedings.com/proceedings?paper=38517

1. INTRODUCTION

1.1 Renewable Energy and the Global Development Challenge

Following periods of aggressive industrialization spanning decades in the 20th century and its associated carbon emissions, a strong and growing awareness has emerged in the last few decades, that, such development models are not only unsustainable, but also risk pushing the planet beyond its carrying capacity and causing irreversible changes in biogeochemical cycles that are vital for the survival of human and other life-forms [1] [2]. An early and major alarm bell was sounded in the 1970s with the publication by the Club of Rome, of the report titled “Limits to Growth” [3]. This report (Limits to Growth) modelled economic development and resource consumption patterns and scenarios, and concluded that the prevailing development trajectory needed a paradigm shift.

In the past few years, this understanding (of the need for different development models) has deepened and there is a wide consensus, that, development must proceed along low-carbon pathways if the planet were to avoid going beyond the “tipping-point” [4]. It has been demonstrated, that, economic growth can indeed be decoupled from carbon emissions and even energy consumption, and that, increased economic output does not necessarily imply increased energy consumption and carbon emissions ([4] [2] [5]). Significant unanimity has emerged on this view. Since the energy sector has been implicated as a major contributor to GHG emissions, major international (and national) initiatives have been designed to reduce and roll-back the sector's contribution to anthropogenic emissions. Key energy sector emissions-reduction strategies include the rapid adoption and upscaling of technologies in renewable energy, energy efficiency and conservation, and carbon capture and storage [5].

A recent IRENA (International Renewable Energy Agency) assessment suggests that renewable energy (RE) and energy efficiency technologies could contribute up to (40%) of anticipated emissions reduction by the year 2050 [5]. It foresees the contribution of RE to total final energy consumption (TFEC), increasing from 18% in 2015 to 25% in 2050 under a reference business-as-usual scenario.

However, to accomplish the goal of rapid slow-down and reversal of atmospheric greenhouse gas accumulation, the transition of the energy sector is urgent. The sector must move away from emission-intensive fossil fuels and ramp-up the deployment of renewable energy technologies, to constitute 65% of TFEC by 2050 [5].

At the same time, billions of the world's inhabitants are deprived of access to electricity and modern forms of cooking fuel, and remain poor. For these people to escape the vicious cycle of poverty, the role of electricity and modern cooking fuels are indispensable. Consequently, the global energy challenge becomes one in which the multiple goals of energy access (pre-requisite for poverty reduction), economic growth and emissions reduction are pursued at the same time [6]. The Sustainable Energy for All (SE4ALL) initiative is one of such global initiatives which attempts to demonstrate the viability of pursuing these multiple goals in a non-contradictory manner. The SE4ALL initiative that aims to mobilize various actors to achieve, by 2030, universal access to modern energy services, doubling the share of renewable energy in the global energy mix and doubling the rate of improvement in energy efficiency [6]. For example, studies by the International Labour Organization (ILO) and the European Commission (EC) ([7]) have shown, that, while transitioning from traditional fossil fuels based energy systems to renewable energy could indeed result in some job losses, it also opens up opportunities that could create even more new jobs.

1.2 Renewable Energy Investment and Technology-Related Risk

The development of renewable energy resources requires significant investments. IRENA and OECD/IEA [8] have estimated cumulative additional investments requirements of about $29 trillion in order to achieve global decarbonisation targets between 2015 and 2050. Investment due-diligence requires an understanding of the risk-return profiles to facilitate informed decisions. This thesis aims to make a scientific contribution towards understanding performance evolution of solar photovoltaic modules based on field studies in different geo-climatic zones of Ghana. The longevity of products and their useful economic life is important in all sectors of socio-economic activity. Reliable products

are those that perform their intended functions without failure over a specified time under stated conditions [9].

Reliability is of particular importance in the energy sector, as failure to deliver expected power (leading to possible curtailment) is costly to society, due to the enormous disruption it imposes on public life and economic activities. For technologies such as Solar PV, for which capital expenditure (CAPEX) overwhelmingly dominates the Life Cycle Cost (LCC), there are very few options available for mitigating the impact of technology failure (or underperformance) on ROI (return on investment) [10]. This is in contrast with technologies such as diesel generators and gas turbines (high OPEX), for which financial losses could be mitigated by scaling back fuel purchases should technological failure occur. The foregoing underscores the importance of assessing technology-related risks with regards to solar PV technology, with the view to obtaining a better understanding of these risks as to permit their realistic quantification in risk-return profiling as well as the evaluation of minimization techniques (through R&D efforts).

In the past 10 - 15 years, studies in this domain have received significant attention. In 2006, research by Osterwald et al [11] found just about nine references that had examined the subject of performance degradation in photovoltaic modules. By 2013, however, Jordan and Kurtz [12] reported over 100 studies reporting close to 2000 degradation rates from various regions of the world. An even greater number of studies have since been reported in a 2016 update by Jordan et al [13]. This increase, notwithstanding, an important observation has been made by several authors ([12], [11], [14]) regarding the geographical imbalance in available studies and research. While such studies provide actors along the value-chain with useful data for various purposes (basic cell/module design, system integration, financial modelling, etc.) ([12] [15]), it also has application in some new approaches to module reliability testing and lifetime prediction. For instance, in the so-called qualification plus testing, Wohlgemuth and Kurtz [16], have suggested that field-tested “veteran” modules whose performance are known could be used as base or control designs against which to test new module designs and thus provide insight into how long they could last on the field.

Following global trends, and actuated by its own domestic needs and priorities, Ghana has since the early 1980s pursued alternate sources of energy to grow its economy, diversify energy sources and reduce poverty. Solar PV has been an integral and important part of this pursuit – by virtue of the country's location along the equator, in the so-called sub-belt region of the world. Actual deployment of photovoltaics in Ghana is traced back to the mid-1980s. Its early utilization, promotion and challenges are documented by Adanu [17], Essandoh-Yeddu [18]and Edjekumhene et al [19]. In its first strategic national energy plan (2006 – 2020), the important role of photovoltaic technology was once more emphasized ([20]). Following the passage of Ghana's renewable energy law in 2011, several licenses (of them provisional) have been acquired by prospective developers of solar power projects, with proposed installed capacities exceeding 1000 MW ([21]). Even though concerns have been raised about stability of the national electricity grid with increasing shares of variable renewable energy (VRE) resource based technologies such as solar (and wind), the number of licenses obtained points to a strong interest by investors. While some work has been done on time-series based operational performance of solar photovoltaic technology in Ghana ([22], [23]), including an early study (in the 1990s) by Adanu [24]; no work (until now) is available in the open literature regarding module performance degradation and how performance metrics evolve over time under the climatic conditions of Ghana.

1.3 Aim and Objectives

Against this background, it is the aim of this thesis to make a scientific contribution to the subject of photovoltaic module performance degradation, by studying systems installed in different sub-climatic zones of Ghana and in different applications.

Specific Objectives

1. To determine the long-term performance degradation rate of photovoltaic modules in different sub-climatic zones of Ghana.
2. To assess PV module degradation modes and correlate with performance loss.

3. To evaluate early-period degradation in PV installations using system-level data.

Contribution and Significance of Study

It is expected, that, the results of this study will aid in the development of the PV market in Ghana by empowering actors to make more confident long-term yield projections and generate more realistic financial scenarios for prospective projects. Data from this study could also be used in selecting benchmark module designs against which to compare new and novel module designs in module lifetime prediction. Degradation and failure mechanisms identified in this study can help system integrators in improving system-level design and installation techniques. In module qualification tests such as IEC 61215, future reviews could benefit from this work, as data from this work could help in the development of region- or climate-specific test series. Finally, this thesis also contributes to efforts at addressing issues of data under-representation from countries in Africa.

1.4 Degradation in Solar Photovoltaic Modules

Gautam and Kaushika (2002), using probabilistic modelling estimate, that, crystalline silicon solar cells could last up to 165 years [25]. In reality, however, the cells in a solar PV array are interconnected in several thousands to give the desired current and voltage output and are further subject to environmental and operational stresses, which significantly affect their longevity [25]. These environmental and operational stresses include UV radiation, humidity, high/low temperatures, temperature cycling and high voltage. Additional factors such as snow, hail, wind, dust, sand and gases act either alone or in various combinations to impose stress on various components of PV modules. Ferrara and Philipp [26] have grouped constituent materials in a typical PV module into four categories, namely: polymers, metals, glass and semiconductor. These four materials are found in about seven major components in a PV module, i.e., front cover (glass), module frame (metal), encapsulant (polymer), solar cell (semiconductor), backsheet (polymer), fingers/interconnects/cables (polymer/metal), junction box (polymer/metal).

These materials and components are subject, on diurnal and seasonal basis, to the aforementioned environmental and operational stresses. For example, a combination of high winds and sand in desert locations could result in aberration of the front glass surface and lead to irreversible reduction in optical transmission of the module. Quintana et al [27], in studying PV module degradation have identified five major drivers of performance loss and categorized them as: degradation of packaging materials, loss of adhesion, degradation of cell/module interconnects, degradation caused by moisture intrusion and degradation of the semi-conductor device itself (Figure 1). These processes are triggered by complex combinations of environmental and operational stresses [28] (Figure 1).

Degradation factors have also been categorized as either intrinsic or extrinsic, where the former refers to factors that originate from the production process, and the latter, a result of factors that are external to the manufacturing process (climatic and operational related factors) [26] [29] [30]. Bogdanski and Herman [31] have provided another classification of PV module degradation, based on four "major processes". These processes include diffusion (e.g. water ingress), thermo-mechanical stresses (e.g. temperature changes and unequal coefficient of thermal expansion), photo-thermal degradation (acting on polymeric materials) and static/dynamic mechanical stresses (e.g. by wind and snow) [31].

Even though physicochemical pathways and mechanisms that relate these stresses and the degradation/failure modes are not fully understood, accelerated stress tests in laboratories (e.g. IEC 61215 [32]) have replicated many of the degradation modes which have been observed in field-exposed modules and therefore provide some evidence of cause-effect relationships.

For example, thermal cycling tests in IEC 61215 series, have reproduced the impact of high temperature and temperature variation to which field-exposed modules are subjected, which tend to cause defects such as solder-bond failures, broken interconnects and broken cells ([26] [33], [16]). Such defects are expected to be prominent in regions of high temperature and rapid temperature fluctuations. Damp Heat (DH) test (IEC 61215), in which the combined action of high humidity and temperature (as pertains in hot-humid regions) on fielded modules is simulated, has reproduced

degradation modes such as delamination and corrosion. Other tests in the sequence are designed to reproduce known degradation and failure modes such as junction box failure, snail tracks, front glass breakage, potential induced degradation and EVA discolouration [33].

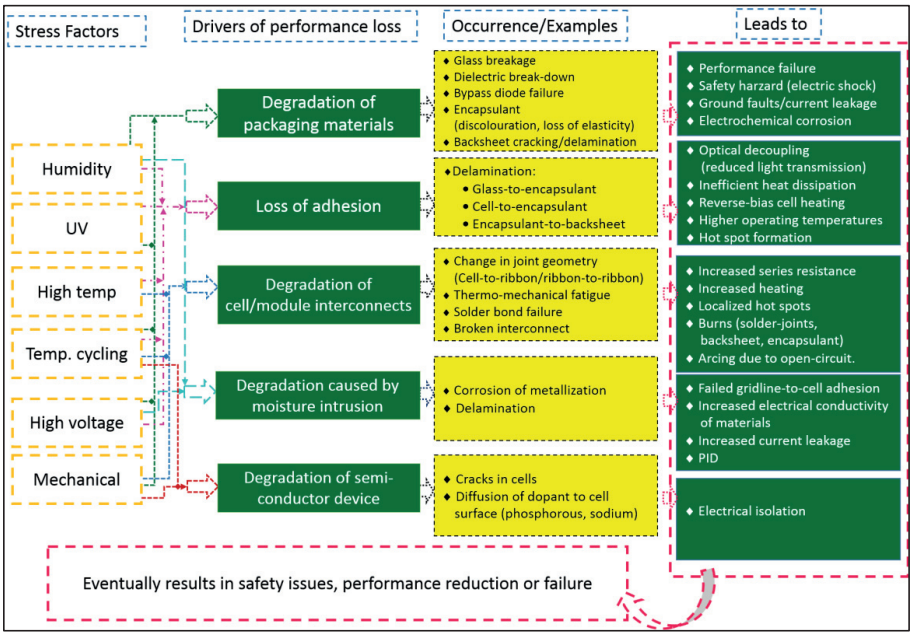

Figure 1: Environmental and operational factors responsible for module degradation and failure

1.5 PV Module Qualification and Durability Issues

Currently, the IEC (International Electrotechnical Commission) module type approval tests, the IEC 61215 [32] for crystalline silicon and its counterpart IEC 61646 [34] for thin film, have become widely accepted market entry labels for PV modules. They are however limited in the assurance that they provide. For instance, for a particular design, a manufacturer typically sends only eight selected modules for testing in accredited laboratories. This has led some industry analysts to raise questions regarding statistical sampling method for test modules and inferential validity of test results [35]. It has been argued [35], that, for millions of modules that come from production lines for a given design, a one-time selection of eight pieces, by the manufacturer for testing purposes might not be a sufficient

quality assurance measure. Nevertheless, the IEC 61215 and other module qualifications tests have been hailed for significant reduction in infant mortality failures and for providing some "minimum" assurance of module quality for market entry [36] [37]. Indeed, the IEC 61215 and (IEC 61646) have been credited for the commercial success of solar PV in terrestrial applications [38].

In spite of this success, qualification tests in themselves do not provide any guarantee that the product will last on the field and perform as expected [38] [28]. As noted by Wohlgemuth [38], these tests are indeed, not designed to provide such assurances. They rather aim to rapidly detect initial short-term reliability issues (such as infant failures) [38] [28] in the tested modules. However, investors (and system owners) are not only concerned about avoiding infant failures in PV modules, they are also concerned about the longer-term performance of PV installation as to realize the anticipated return on investment (ROI).

Manufacturers have usually assured clients of a minimum of 80% of rated module power over a stated period. The warranty periods have evolved from 10 years in the 1990s to the current industry standard-practice of 25 years. The 25-year warranty was first introduced by Siemens in 1997 ([39]) and has since become the industry benchmark. As the PV market grows, investors demand greater assurance of product reliability and durability. Manufacturers have responded by providing assurances such as insurance-backed warranties and early-period performance guaranteed [40] [41].

A challenge with the traditional 20-25 year guarantee had been, that, degradation rate is assumed to be linear, and a loss, for example, of 15% of module power within the five years of field-exposure was insufficient to trigger warranty claims since overall performance remains above the critical 80%. Industry response to this has been the introduction of multi-staged warranties that provide assurance of up to 97% of module power within the first year [41]. Warranty provisions can therefore be triggered if modules lose more than 3% of power within the first year [42]. Following major bankruptcies and collapse of PV module manufacturers in the period 2010 – 2013, the usefulness of warranties issued by defunct companies came to the fore ([43]). The introduction of insurance-backed

warranties is therefore designed to assure other actors in the value-chain of the validity of the warranties, even in the event of the manufacturers folding up before the 25-year period is up.

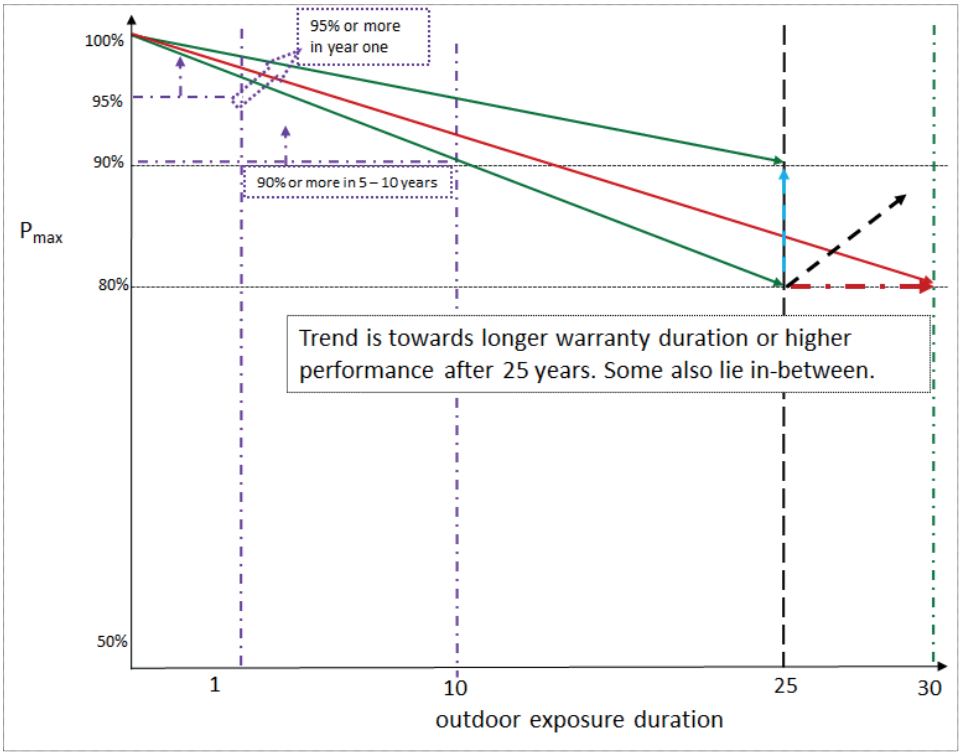

Figure 2: Trends in module warranty provisions (not drawn to scale)

Currently, warranty provisions on modules are being extended, with some manufacturers maintaining the 25-year period, but assuring higher than 80% of module power in this period (a vertical extension– Figure 2). Others have maintained the 80% of P_{max}, but extended the duration beyond 25 years (horizontal extension – Figure 2). Still, others have provisions which lie between these first two categories – i.e. extending both duration and the assured P_{max}. This thesis therefore examines both early-period and long-term performance loss in photovoltaic modules.

2. MATERIALS AND METHOD

The methodology used in accomplishing the objectives of this thesis is elaborated in this section. As

outlined in Figure 3, it involved identification of installations of interest (particularly early installations), filtering of the information obtained, visiting the selected installations for measurements, analysing data obtained and communicating results in the form of manuscripts and journal publications.

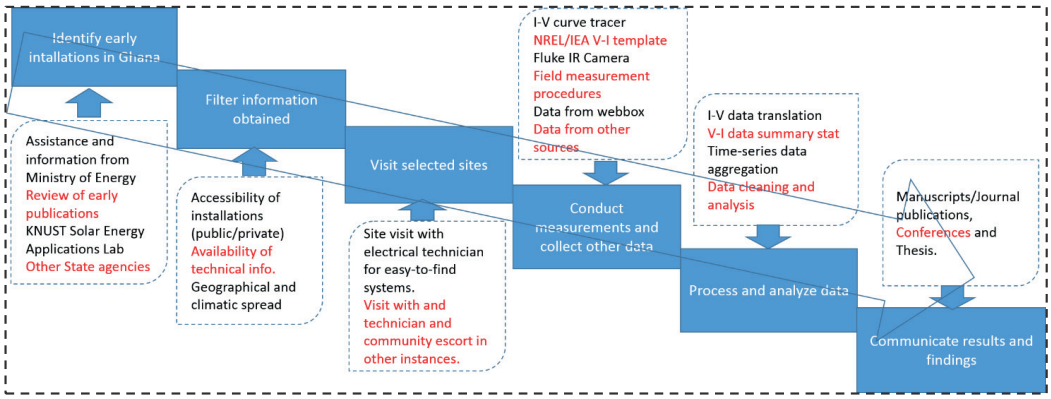

Figure 3: schematic of the research methodology

2.1 Identification and Selection of Installations

Identification and selection of installations around the country was fundamental to this study and as such, much attention was paid to this stage of the research. Journal articles, workshop presentations and technical reports on the early deployment of solar PV in Ghana were reviewed, with the view to obtaining information (locational, ownership, etc.) on early installations in the country. These documents include: Wereko-Brobby and Opam [44], Nasson et al [45], UNDP/GEF [46], Adanu [17], Essandoh-Yeddu [47] and Edjekumhene et al [19]. These documents revealed, that, early installations were mostly either institution-owned (e.g. those owned by the Ghana Cocoa Marketing Board, (now Ghana COCOBOD) Adanu [17], Essandoh-Yeddu [47]) or government-facilitated through bi- and multi-lateral arrangements (e.g. systems installed in Northern Ghana Nasson et al [45], UNDP/GEF [46]). Besides the Government Ministry responsible for energy, the active role of the Solar Energy Applications Laboratory at the Kwame Nkrumah University of Science and Technology (KNUST)

in the early uptake of solar PV in Ghana was established from the documents reviewed (e.g. Nasson et al [45], UNDP/GEF [46], Edjekumhene et al [19]). Additional information was therefore obtained from these sources. Within constraints of available resources (budget, time and personnel), installations were purposively selected to encompass module technology, geo-climatic location, age of installation and mounting method (such as ground, roof and roof).

Practical considerations such as the availability of community escort, receipt of official permission for institution-owned installations and safe access to installation terminals for measurement influenced the selection of installations for study. Early installations were of particular interest, as they have spent much time withstanding climatic stresses after initial exposure. Characteristics of modules studied for long-term power degradation are presented in Table 1. For the purpose of this research, long-term exposure was construed to mean (module) exposure for 5 years or more, taking a cue from [11] and [14], who have found, that, beyond 3 – 5 years of exposure, long-term linear degradation trends are established, as the effect of seasonal variation is smoothened.

Table 1: Characteristics of Modules Encountered in the Research – Long-term degradation

Module Type	Manufacturer	Module Technology	Max. Power (P_{nom})	Short Circuit Current (I_{sc})	Open Circuit Voltage (V_{oc})	Impp	Vmpp
ASE-50-PWX-D	ASE GmbH, Germany	pc-Si	49.5	3.10	21.6	2.85	17.4
HS.40.1 N	HOLEC HH, Netherlands	pc-Si	36.0	2.30	22.0	2.1	17.0
Isofoton I-110/12	Isofoton, Spain	mc-Si	110.0	6.76	21.6	6.32	17.4
Isofoton I-100	√	mc-Si	100.0	6.54	21.6	5.74	17.4
Isofoton I-50	√	mc-Si	50.0	3.27	21.6	2.87	17.4
Baodin Solar	TT Baodin Group, China	pc-Si	50.0	3.20	21.6	2.90	17.2
aleo 150-M5i	Aleo Solar GmbH, Germany	mc-Si	150.0	4.93	43.3	4.35	34.9
aleo S_03	√	mc-Si	165.0	5.10	43.5	4.64	35.8

In some instances, manufacturer nameplate data was insufficient for the definition of reference module performance features; hence, in such instances, field data was complemented with data from

the database of the photovoltaic system design and simulation software PVSYST® [48]. For some modules, nameplate data was inadequate, and additional information was unavailable in the reference databases available (Figure 4). This challenge was surmounted by contacting entities that inherited the legal rights and liabilities of the module manufacturers as well as renowned solar energy research institutes in the host country of the manufacturer. For example, the assistance of the Dutch energy research centre, ECN, was sought in obtaining reference data on the HOLEC HH modules examined in Paper 2 (as the manufacturer is defunct).

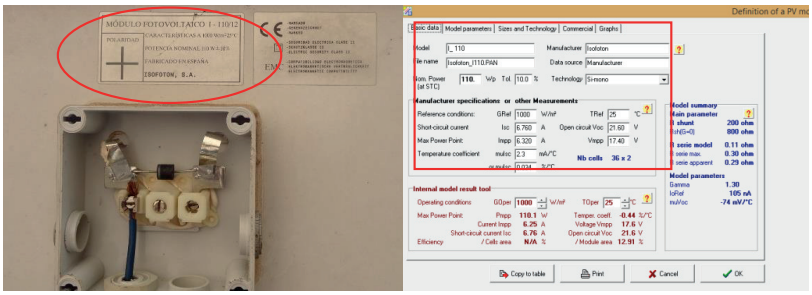

Figure 4: Example of field data complemented with data from PVSYST®

In all, sixty-five 65 modules from twenty-nine (29) solar PV installations at different locations across Ghana were studied in the long-term performance degradation assessment. Figure 5 shows the locations in Ghana from which measurements were conducted. A similar national-scale study in India, covered 68 modules at 26 different locations [49].

For early-period performance degradation, a 20 kWp experimental grid-connected installation comprising five different co-located technologies was studied. This was the only such installation in the country, based on information available in the open literature as well as the researcher's knowledge of the renewable energy ecosystem in the country. Module technologies comprised polycrystalline silicon (pc-Si), monocrystalline silicon (mc-Si), amorphous silicon (a-Si), hybrid mc-Si/ a-Si (Heterojunction with Intrinsic Thin layer - HIT) and Copper Indium disulphide (CIS) technologies. They are separately connected to the 220 V distribution utility grid via SB3800 Sunny

Boy inverters. The installation is equipped with sensors for monitoring module temperature, irradiance and other environmental parameters. An integrated data-logger stores the system performance, environmental and operational data every 5-minutes. Characteristics of the modules are presented in Table 2.

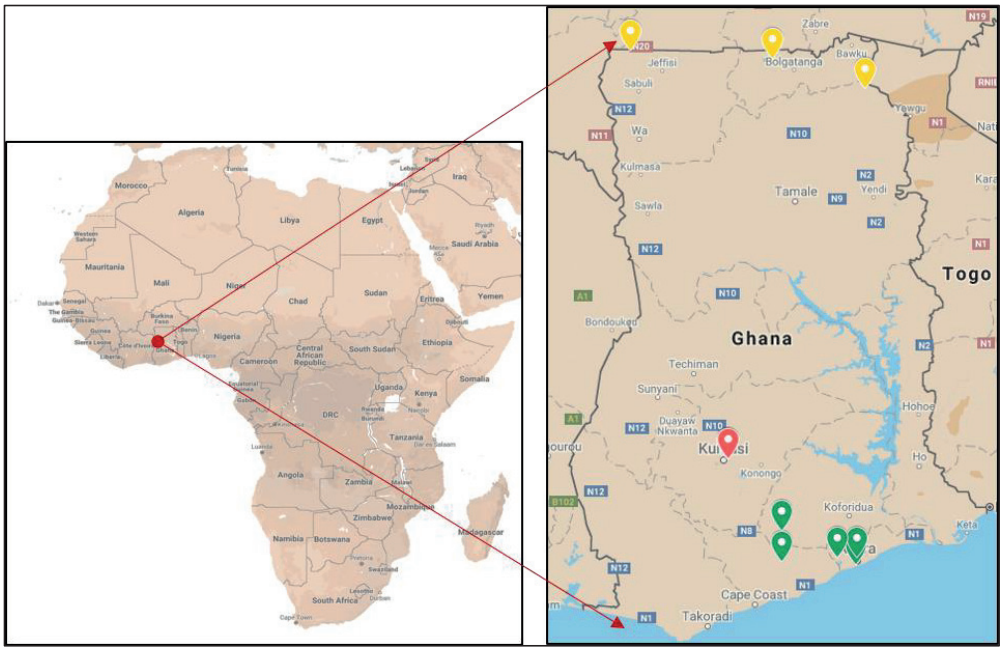

Figure 5: Map of Ghana showing location of installations studied (shown in green, yellow and red highlights)

Table 2: Characteristics of Modules Encountered in the Research – Early-period degradation

Module Type	Manufacturer	Module Technology	Peak Power (P_{nom})	Short Circuit Current (I_{sc})	Open Circuit Voltage (V_{oc})	Impp	Vmpp
Schott Poly 225	Schott Solar GmbH	pc-Si	225.0	8.24	36.7	7.55	29.8
Schott Mono 190	√	mc-Si	190.0	5.46	45.2	5.22	36.4
Schott ASI 100	√	a-Si	100.0	3.85	40.9	3.25	30.7
Sanyo H250	Panasonic Group	mc-Si/ a-Si	250.0	7.74	43.1	7.18	34.9
Sulfurcell SCG50–HV 50	Sulfurcell Solartechnik GmbH	CIS	50.0	1.65	50.0	1.35	37.5

2.2 Climate Categorization and Characteristics

The Koppen-Geiger classifications of climates is one of the most widely used. Ghana's land mass falls within latitude 5 ^{o}N - 11 ^{o}N and longitude 3 ^{o}W - 1 ^{o}E, and by the Koppen-Geiger classification, its climate is classified as tropical climate (A) of the monsoon (Am) type and savanna with dry winter (Aw) type. This implies that the average temperature of the coolest month is above 18 ^{o}C and precipitation in the driest month is less than 60 mm [50]. However, sub-classifications of climatic conditions are often necessary for various purposes (e.g. agro-meteorology, disease prevalence). One such sub-classification, provided by Beckley et al. [51], is adopted for this study. Beckley et al. [51] classify Ghana's climate from latitude 0 – 6 ^{o}N as Humid (H), from latitude 6 – 10 ^{o}N as Sub-Humid Humid, and latitude 10 – 12 ^{o}N as Sub-Humid Dry (SHD). These climate zones encompass five agro-ecological zones (rain forest, semi-deciduous forest, Guinea savannah, Sudan savannah and coastal savannah). In Figure 5, sub-climatic zoning of the locations of study are colour-coded as Green (Humid), Red (Sub-Humid Humid) and Yellow (Sub-Humid Dry). Representative long-term climatic data of the study locations were obtained from climatological databases and are presented in Figures 6 and 7. They show monthly variation of solar irradiation, ambient temperature, and relative humidity for Accra (Humid), Kumasi (Sub-Humid Humid) and Navrongo (Sub-Humid Dry).

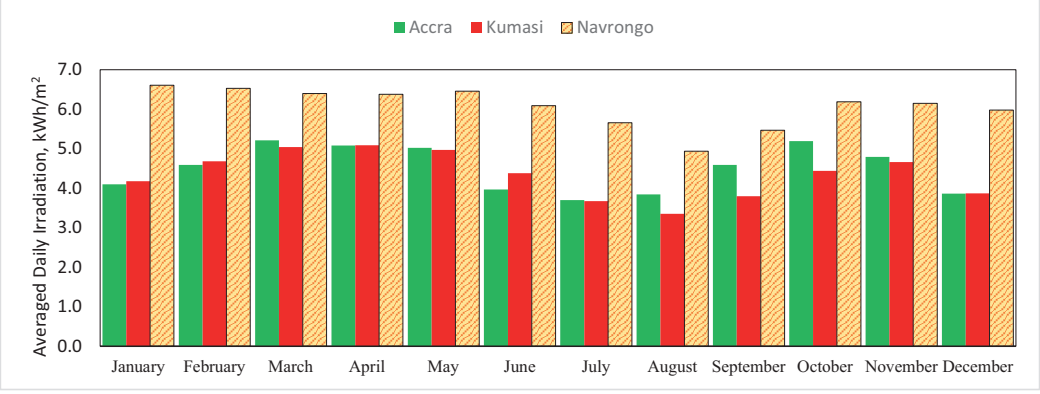

Figure 6: Monthly averaged daily solar irradiation at study areas (kWh/m^2) [52]

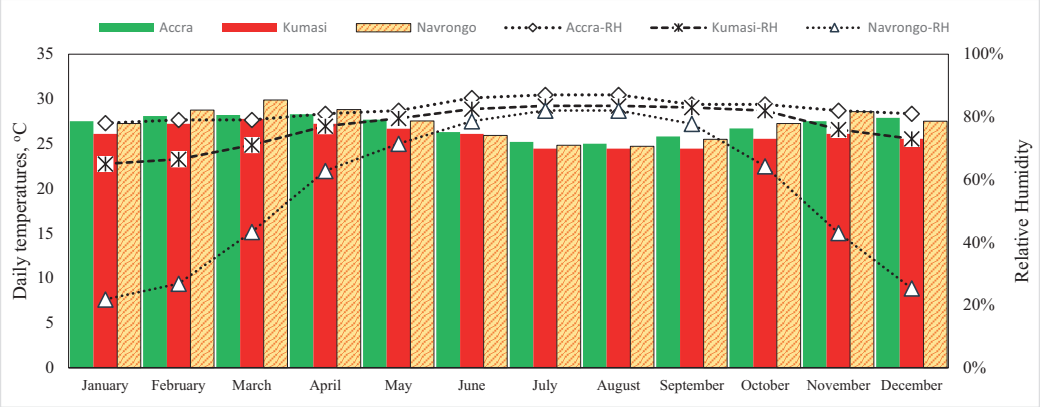

Figure 7: Average monthly ambient temperature and relative humidity at areas of study [52]

2.3 Equipment and Field Measurements

Field current-voltage (I-V) measurements on the solar modules were conducted with a TRI-KA® I-V curve tracer and its accompanying TRI-SEN® for the measurement of irradiance, module temperature and inclination. The current and voltage measurement range of the TRI-KA® are 0.1 – 15 A and 1 – 1000 V respectively and have measurement uncertainty of ±1% (for both current and voltage). The TRI-SEN® has irradiance and temperature measurement range of 100 – 1200 W/m^2 and 0 – 100 ºC respectively, with uncertainties of ±3% and ±5%. Thermal images were acquired with a Fluke® TI400 infrared camera. A Canon EOS 1100D camera was used to obtain photo-shots of the physical condition of the modules encountered in order to enable reporting on visually observable defects. The Canon EOS 1100D camera was also used to capture geo-location of installations, as it has an integrated GPS signal receiver. Following IEC 61215 [32] recommendation on outdoor measurement of maximum power, a minimum irradiance level of 700 W/m^2 was set during field measurements. Furthermore, to reduce angle of incidence effects, measurements were taken between the hours of 10 am and 2 pm – the solar window. This was also the time window, within which irradiance levels above 700 W/m^2 were typically available, as the climate in Ghana is generally cloudy and characterized by low clearness index [53].

2.4 Visually Observable Defects (VODs)

Defects visible to the eye often provide useful clues to underlying material-level degradation. For instance, the degradation of the encapsulant material results in a visually observable yellowing/browning, which leads to losses in short-circuit current of modules. Visual inspection is therefore widely used as relatively inexpensive method, in conjunction with other techniques for PV system performance monitoring and diagnosis. Work conducted by the IEA/NREL (IEA Photovoltaic Power Systems Programme (PVPS) Task 13) has resulted in a widely used visual inspection checklist for PV systems, which makes it possible for researchers to use consistent vocabulary to describe observed defects [33]. Such consistency in the description of module-related defects minimizes subjectivity and enables, to an extent, the comparison of visual inspection results from different sources. This IEA/NREL template was adopted in reporting defects observed in this research. It broadly categorizes defects according to the component of the PV module in which they are observed. For instance, defects linked to the front-side of the module includes: formation of bubbles, delamination and discolouration (yellowing or browning) (Table 3).

Table 3: Categorization of some commonly observed module defects [33]

PV Module Component	Potential Defects
Front of PV module	Bubbles, delamination, yellowing/browning and glass breakage.
PV cells	Discoloured anti-reflection, broken cell and cracked cell.
Cell metallization	Burned, oxidized, snail tracks
Frame	Bent, broken, scratched, misaligned
Back of module	Delaminated, bubbles, yellowing, scratches, burn
Junction box	Loose, oxidation, corrosion
Wires – connectors	Detachment, brittle, exposed electrical parts

2.5 Calculations

2.5.1 Long-term degradation

Since photovoltaic modules are rated under Standard Test Conditions (STC), (i.e. irradiance – 1000 W/m^2, module temperature – 25 ^{o}C and air mass – 1.5), it is often necessary to translate measured field data back to STC to enable comparison with initial or reference performance data. A number of approaches exist in the open literature for accomplishing this task of translating module performance from one set of conditions to another (e.g. [54]). These approaches, although are of comparable accuracy [55], do come with varying data requirements for implementation. For example, equations such as those proposed by Tsuno et al. [56] require measurements at constant irradiance with temperature variation, and vice versa. Yet, these conditions are not easy to achieve under outdoor conditions (unlike indoor laboratory tests) and hence limit the applicability of some available correlations. Nevertheless, it has been demonstrated (Herrmann & Wiesner [57]), based on results from round-robin tests that the translation accuracy of various methods currently in use (both algrbraic and numeric) are comparable, noting, that conditions of measurement tend to be critical. They recommended a minimum irradiance level of 600 W/m^2 for acceptable results. Similar conclusions have been reached by [58] who after studying IEC 60891 translation methods found that irradiance distribution and temperature at a location had more impact on translation accuracy than the particular translation method selected.

In this thesis, expressions proposed by Kaplanis & Kaplani [59]and Herrmann & Wiesner [57] were adopted for translation of measured field data to STC. The relationship between the measured open-circuit voltage, V_{oc1} (at module temperature Tc and Irradiance I_T) that at STC (V_{oc0}) is given by Eqn. 1.

$$V_{oc1} = V_{oc0} - n_s \times 2.3 \times 10^{-3} \times (T_c - 25^o C) + \frac{kT_c}{q} lnC \quad (1)$$

where:

$C = \frac{I_T}{10^3}$

$T_c = cell\ temperature$

$k = Boltzman\ Constant = 1.38 \times 10^{-23}\ J/K$,

$n_s = number\ of\ cells\ in\ series$,

$q = electron\ charge = 1.602 \times 10^{-19}\ C$, and

$I_T = irradiance\ in\ {}^{W}/_{m^2}$

The short-circuit current at STC, I_{sc0}, is calculated from Eqn. 2:

$$I_{sc1} = I_{sc0} \times (1 + h_f \times (T_c - 25^o C)) \times \frac{I_T}{10^3} \quad (2)$$

Where:

$$h_f = 6.4 \times 10^{-4} K^{-1}$$

The maximum power at STC, P_{STC}, is computed from I_{sc0}, V_{oc0} and the measured fill factor (FF) as (Eqn. 3):

$$P_{STC} = FF \times I_{sc0} \times V_{oc0} \quad (3)$$

The linear, long-term annual linear degradation rate is then computed as (Eqn. 4):

$$DR = \left(\frac{P_{STC\_Ref} - P_{STC}}{y_f}\right) \times 100\% \quad (4)$$

Where P_{STC_Ref} and P_{STC} are respectively, the initial (reference) module power output (all at STC) and the power output after y_f years of field exposure. By analogous reasoning, degradation rates of open-circuit voltage, short-circuit current and fill factor are determined.

2.5.2 Early-period degradation

The assessment of early-period degradation employed time-series performance-ratio regression for five (5) co-located photovoltaic technologies located in Kumasi and installed in a grid-connected mode (Paper 3). Performance ratio (p_r) is a composite metric that compares the final yield (y_f) of a

PV system to its reference yield (y_r) (Eqn. 5). The final yield normalizes the power output (P) to the installed capacity (P_{inst}), while the reference yield normalizes available irradiance (G) to irradiance at STC conditions, G_o (i.e. 1000 W/m^2). It allows the comparison of systems of different sizes installed at different locations, and may be defined for various time intervals (e.g. hourly, daily, monthly or yearly).

$$p_r = \frac{y_f}{y_r} = \frac{P/P_{inst}}{G/G_o} \tag{5}$$

A temperature-corrected performance ratio is often defined (Eqn. 6) to account for temperature-related losses and seasonal effects. It uses the temperature coefficient of power to adjust the performance ratio while the module operates off the STC temperature of 25 ^{o}C.

$$p_{rT} = \frac{p_r}{1+\gamma(T-25)} \tag{6}$$

Time-series based analysis, even for long-term degradation studies, is preferred (instead of discrete data points), as it provides a more complete picture of the evolution of module performance with time. Moreover, it permits the visualization of any non-linearities in degradation rates with time; for example, the initial module degradation, and the occurrence effect of major defects such as glass breakage, hot-spots and breaks in PV cells.

Linear regression, based on monthly median p_r and p_{rT} values, was used in estimating losses in the five technologies within the first year of exposure. The degradation rate (DR) was then computed using Eqn. 7, where m is the slope of the least-squares regression line and c is the intercept.

$$DR = \frac{m \times 12}{c} \times 100\% \tag{7}$$

3. OVERVIEW OF RESULTS

The findings of this research have been communicated in four papers/manuscripts and are summarized in this section. Papers 1, 2 and 4 dealt with the subject of long-term degradation (Table 4), while Paper 3 studied early-period performance loss.

3.1 Long-term performance degradation

Paper 1 ([60]) studied a 19-year-old off-grid battery-charging pc-Si installation in Kumasi, of climate sub-category SHH. It found a degradation rate of 1.3%/yr of maximum power, which was dominated by losses in fill factor and short-circuit current. Paper 2 ([15]) expanded the geographic scope of the study to systems from climate sub-categories SHH and H, and studied more diversified installation types, including grid-connected systems, water-pumping systems and off-grid battery-charging systems. The systems were aged between 6 and 32 years and included both mc-Si and pc-Si technologies (Paper 2). The degradation rates found in Paper 2 were varied, showing median P_{max} losses in the range of 0.8%/yr - 6.5%/yr. The northern part of Ghana features some of the highest levels of irradiation in the country and as such, Paper 4 [61]studied installations in that part of the country. Median module degradation rates of 1.4%/yr – 1.6%/yr were found and were dominated by losses in short-circuit current. In all, twenty-two (22) installations from three communities were studied in Northern Ghana (climate sub-category SHD). The number of modules examined in each category and the weighted age of the installations are shown in Figure 8.

Table 4: Summary of Key Results from Papers

Paper	Module Tech.	Application	Field-years	Climate	Mounting Type	Losses (Median), %/year			
						P_{max}	I_{sc}	V_{oc}	FF
Paper 1	pc-Si	Battery-Charging	19	SHH	Rack-mounted	1.3%	0.4%	0.2%	0.8%
Paper 2	pc-Si	Battery-Charging	32	H	Pole-mounted	0.9%	0.4%	0.1%	0.6%
	pc-Si	Battery-Charging	10	H	Roof-flushed	6.5%	3.5%	0.5%	4.4%
	mc-Si	Grid-Connected	16	√	Rack-mounted	1.9%	1.2%	0.5%	0.5%
	pc-Si	Grid-Connected	10	SHH	Roof-flushed	1.3%	0.4%	0.4%	0.4%
	mc-Si	Water-Pumping	11	H	Pole-mounted	0.8%	0.2%	0.4%	0.3%
	mc-Si	Water-Pumping	6	H	√	5.3%	2.3%	0.2%	3.2%
Paper 4^	mc-Si	Battery-Charging	16	SHD	√	1.6%	0.9%	0.3%	0.6%
	√	√	16	√	√	1.4%	0.7%	0.4%	0.5%
	√	√	16	√	√	1.6%	0.7%	0.4%	0.5%

^ *Based on results from 3 major communities of study*

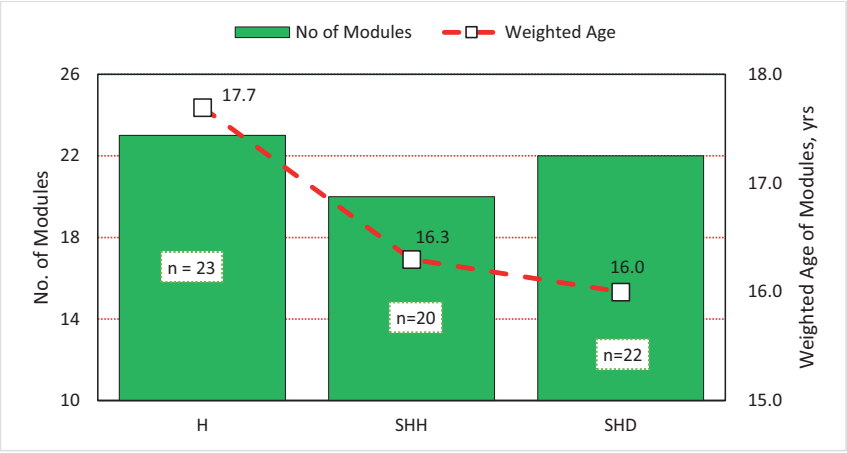

Figure 8: No. of modules in various climates and weighted field-age

3.2 Early-period degradation

Early-period degradation and performance loss in five co-located grid-connected PV module technologies were studied in Paper 3 ([62]). The results (based on a 14-month observation period) show performance loss in the range of 8% - 13.8% (based on performance ratio) and 6.1% - 13.7% (based on temperature-corrected performance ratio – Figure 9). Performance loss was highest for a-Si and least for CIS. The two x-Si technologies (mc-Si and pc-Si) showed losses of 6.1% and 8.0% respectively within first year of exposure, while HIT declined by 11%. The results are presented in Figure 9. Degradation rates of 0% – 4% have been reported for x-Si modules within first year of exposure [63] while 10% – 30% performance decline is reported for a-Si within a similar period [64]. Except for a-Si, the degradation rates found in this assessment are higher than those reported in the literature. This observation could be due to the fact that system-level data was used and partly due to the inability of the current method to offset the contribution of soiling losses.

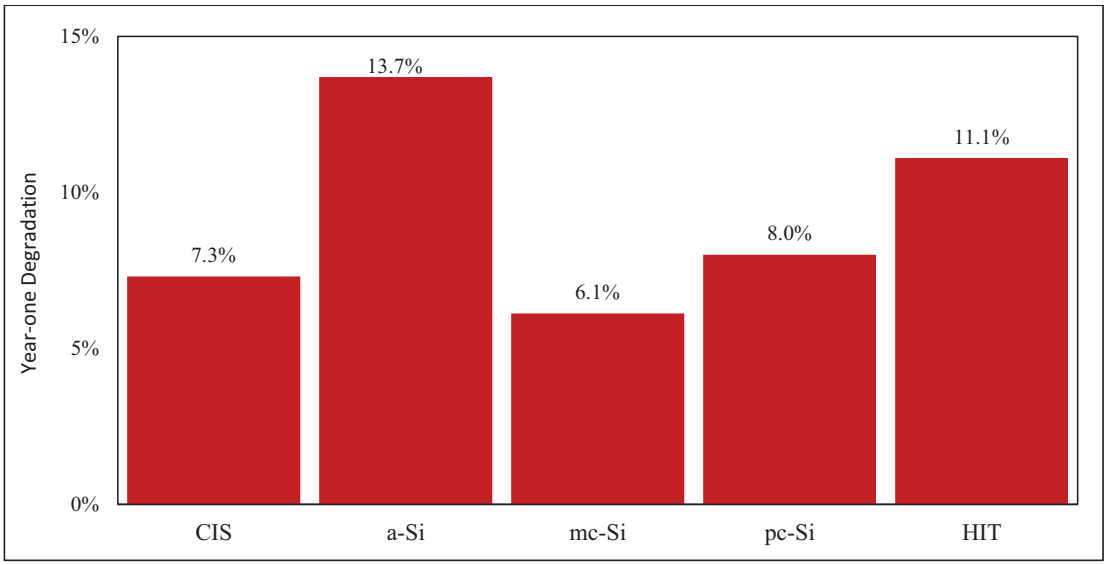

Figure 9: Early-period performance loss (based on temperature-corrected PR-ratio)

3.3 Geo-climate based synthesis of results (Long-term degradation)

As the impact of climatic conditions significantly impact module operation and degradation, the results obtained from long-term degradation studies (Papers 1, 2 and 4) are aggregated and presented in Figures 10 – 12 according to climatic sub-categories (H, SHH and SHD). For the response variable (P_{max}) and explanatory variables (I_{sc}, V_{oc} and FF), the distribution of actual degradation rates in all three climate sub-categories are shown (in these Figures). In Figures 10 – 12, the minimum, maximum and median values are highlighted. The Humid (H) climate sub-category shows the highest median power loss - of 1.8%/yr -, compared with 1.43%/yr and 1.5%/yr for the Sub-Humid Humid (SHH) and Sub-Humid Dry (SHD) categories respectively. P_{max} losses in categories H and SHD are dominated by I_{sc} losses (1.1% and 0.8% respectively), while losses in SHH category are dominated by FF losses (0.89%). The range of degradation rates found in the Humid climate category is much wider than the others (e.g. 0.8%/yr – 7%/yr for P_{max}). The extreme end of the range was due to the impact of some "uncertified" modules which were also poorly installed and had degraded substantially (this is described in more detail in Paper 2). In all climate categories, the annual linear

degradation rates found in this study are substantially higher than values of 0.5% - 0.8% reported from major meta-analytical reviews [12] [13] [11]. A further comparison may be drawn with a similar nation-wide study in India, which found degradation rates of 1.17%/yr and 1.43%/yr for mc-Si and pc-Si respectively [49].

Installations in climate sub-categories H (Accra area) and SHH (Kumasi area) appear to endure a stronger combined effect of high temperature and high humidity through out the year, compared with systems installed in the SHD climate (Navrongo area) (Figure 7). On the other hand, installations in the SHD climate are exposed to a greater effect of high temperature and UV (ultra violet) radiation exposure. Consequently, one may expect the degradation and failure modes reproduced by the dump-heat test in the IEC 61215 (stage 10.13) sequence to be more prevalent in field aged installations in the Southern to mid part of the country (humid and sub-humid humid) than in the Northern part (sub-humid dry). By analogous reasoning, the effects of TC200 (IEC 61215 stage 10.11) is likely to be more prevalent in installations in the SHD climate than in H and SHH.

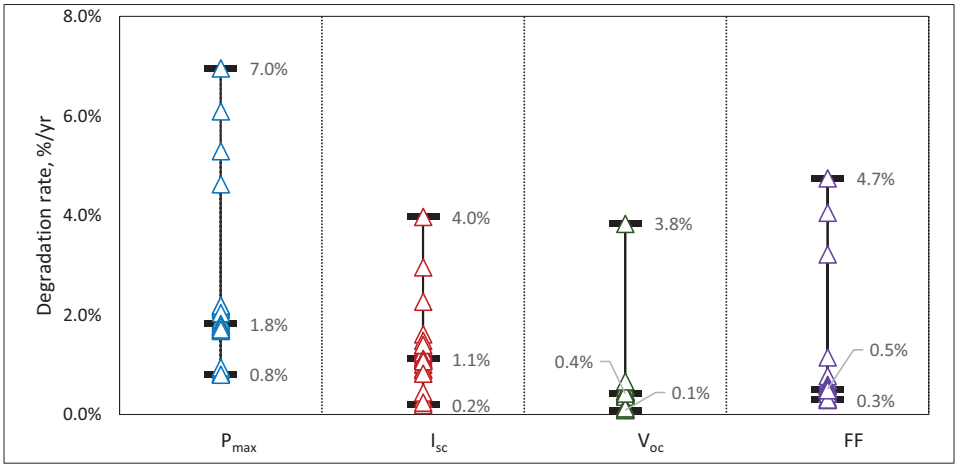

Figure 10: Degradation in *Humid* climate category

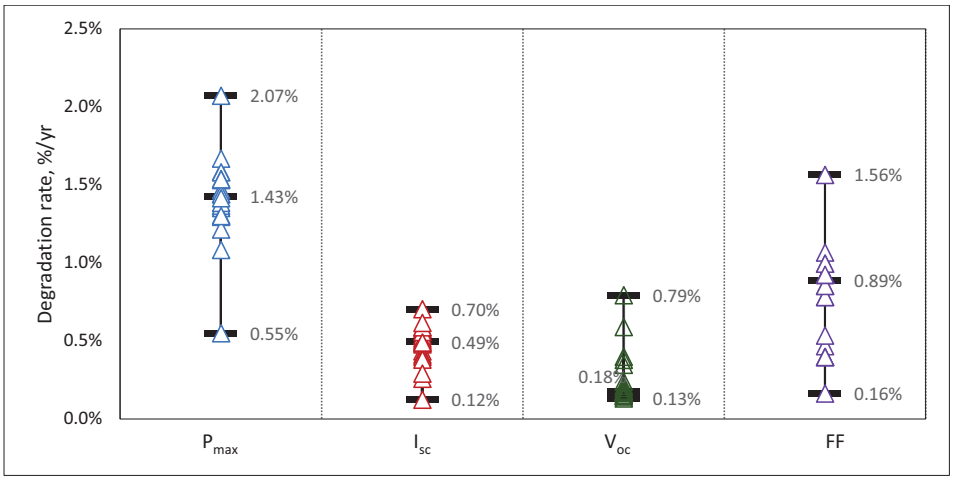

Figure 11: Degradation in Climate SHH category (Diversity of installations.)

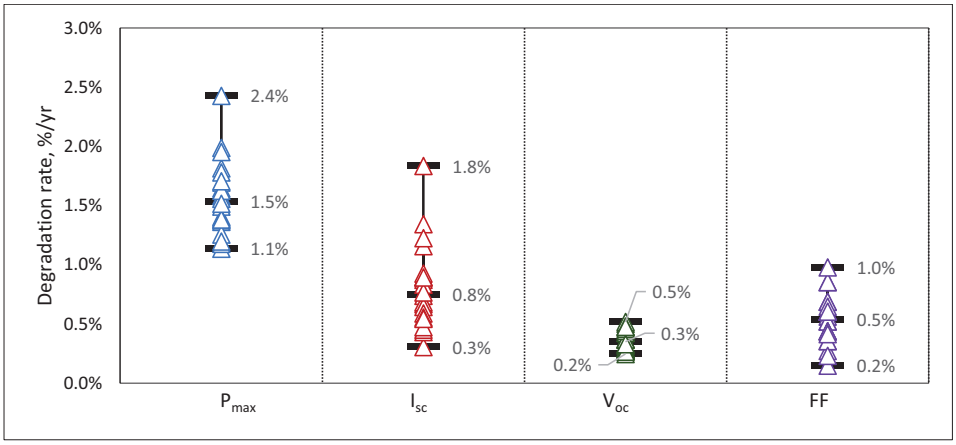

Figure 12: Degradation in Climate SHD category

Correlation between module power loss and explanatory variables are explores in Figures 13 – 15. They show, that, in all climates Isc and FF have stronger correlation with power loss in all climates compared with Voc.

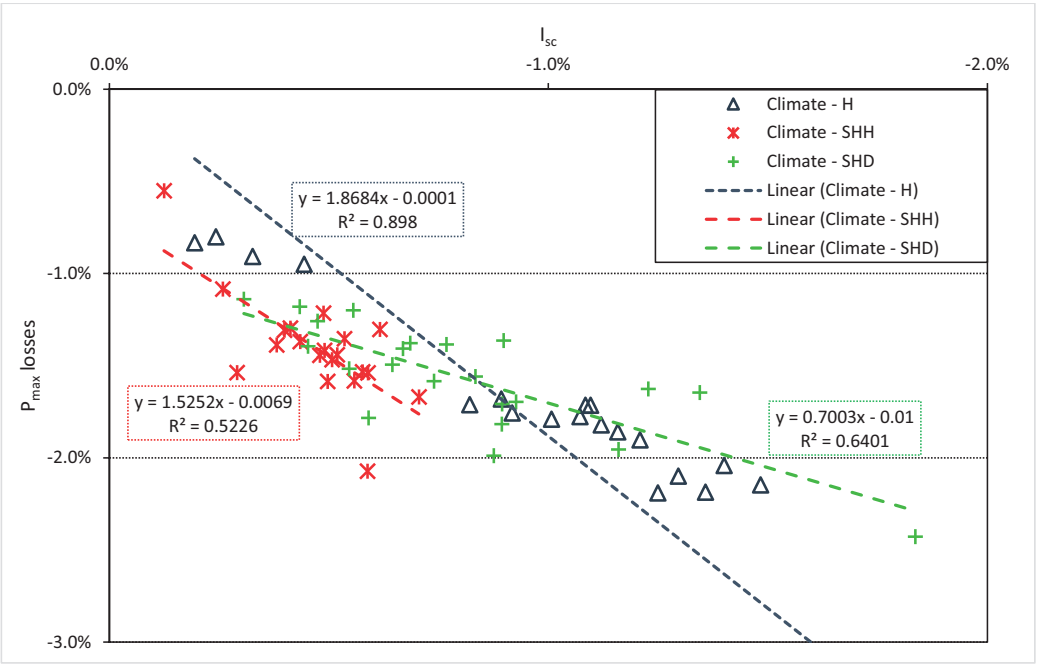

Figure 13: Correlation between module power loss and short-circuit current in various sub-climates

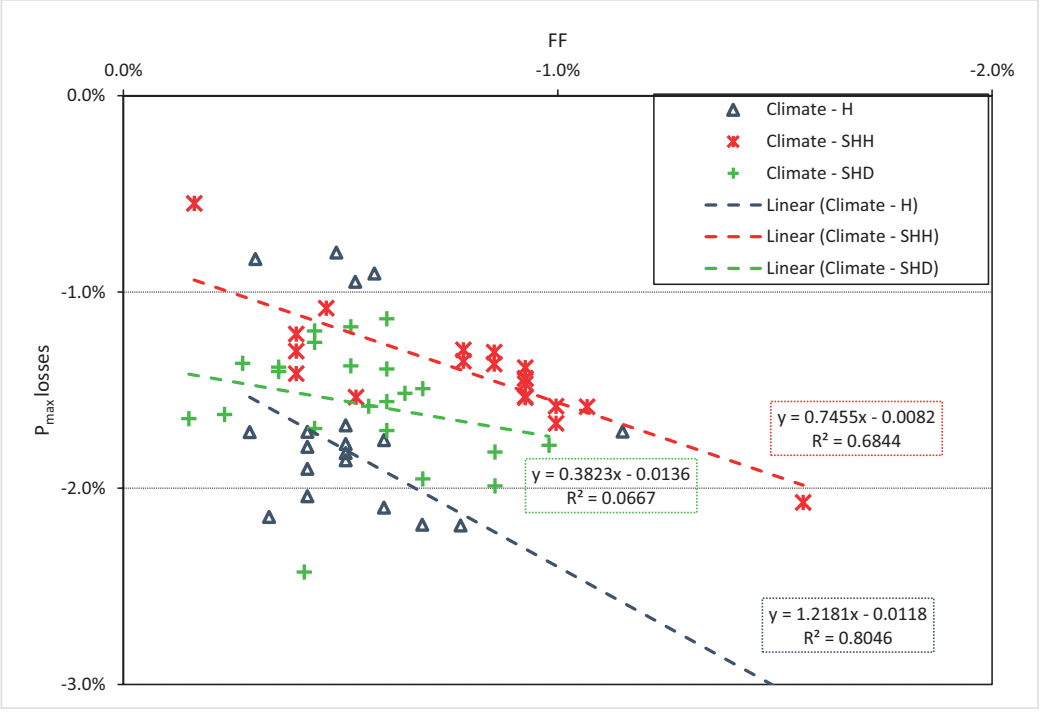

Figure 14: correlation between module power loss and fill factor losses in various sub-climates

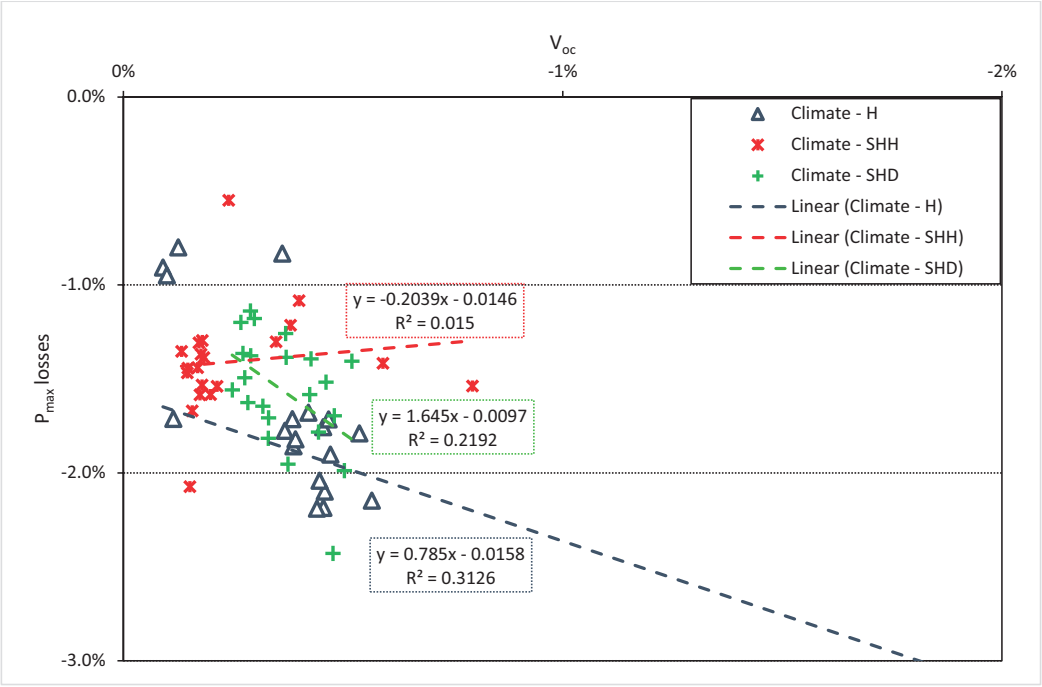

Figure 15: correlation between module power loss and open-circuit voltage in various sub-climates

The results from these studies suggest that installations with lowest degradation rate (0.8%/yr, see Table 4) may be expected to take 25 years before its maximum power falls below 80% of rated output (Figure 16). However, based on median degradation rates found for the different climate sub-categories (1.43% – 1.8%/yr), it would take a much shorter period to (11 - 14 years) to reach this critical threshold (Figure 16). Nevertheless, crossing the warranty threshold does not imply the end of a module's useful life [35].

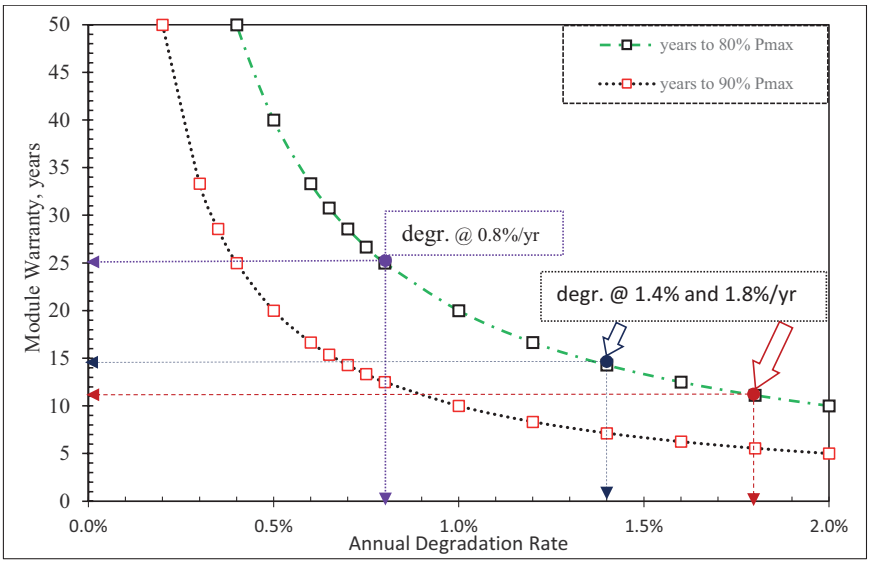

Figure 16: Module degradation curves showing duration to 80% P_{max}. Adapted from [60]

3.4 Visual Observable Defects (VODs)

Visually observable defects (VODs) were documented in all three climate categories, using the classification in Table 3. Overall, front-side defects were dominant, followed by defects related to cell metallization and junction box (Figure 17). A module could exhibit more than one defect in a given category; for instance at, the front side of the module, defects such as delamination, formation of bubbles and glass breakage could all be observed in a given module. Figure 18 shows some VODs that were documented in the study (browning, delamination, corroded metallization, snail tracks, burn marks in junction box, degraded j-box adhesive shattered and front-glass). From Figure 17, front-of-module defects were the most prevalent in all climate categories. Additionally, modules in climate category H recorded more VODs than other climates. A further breakdown of front-of-module defects are shown in Figure 19 and show encapsulant browning and delamination as the most dominant VODs across all three climate categories.

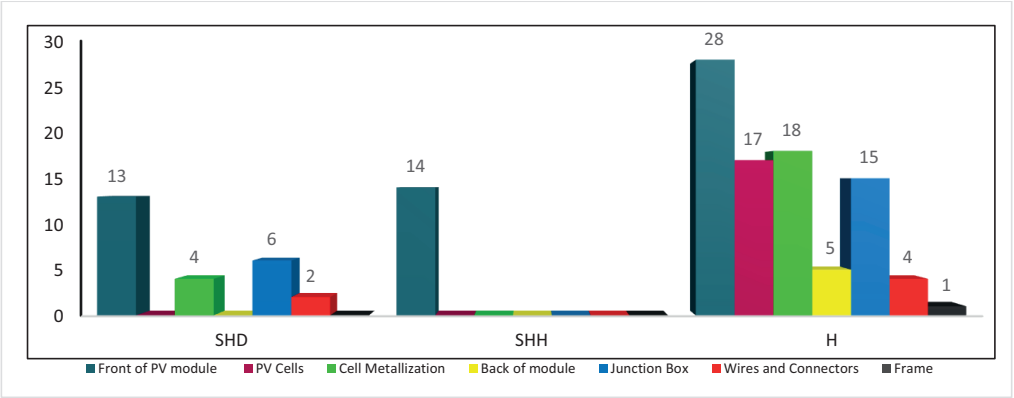

Figure 17: Count of defects found in module components in different climate categories

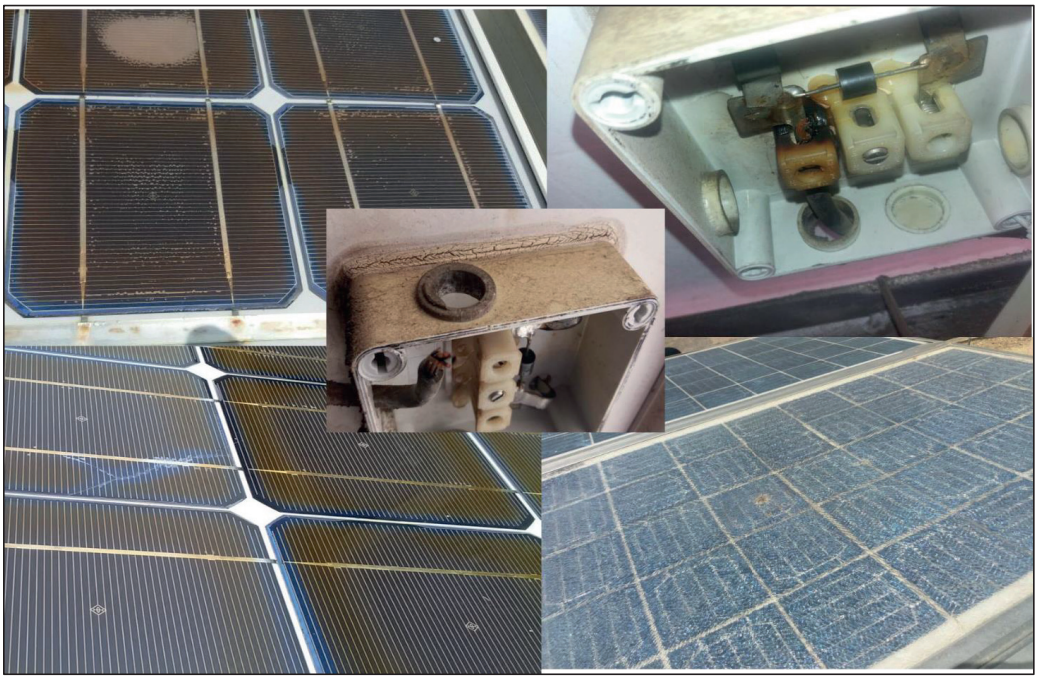

Figure 18: Some defects observed modules

Although climate SHH had high incidence of bubbles on the front-side, these were minor in extent (of the order of 1-mm diameter) and did not appear to have had much impact on power loss based on the contribution of I_{sc} and FF losses (Paper 1). No other defects were visible.

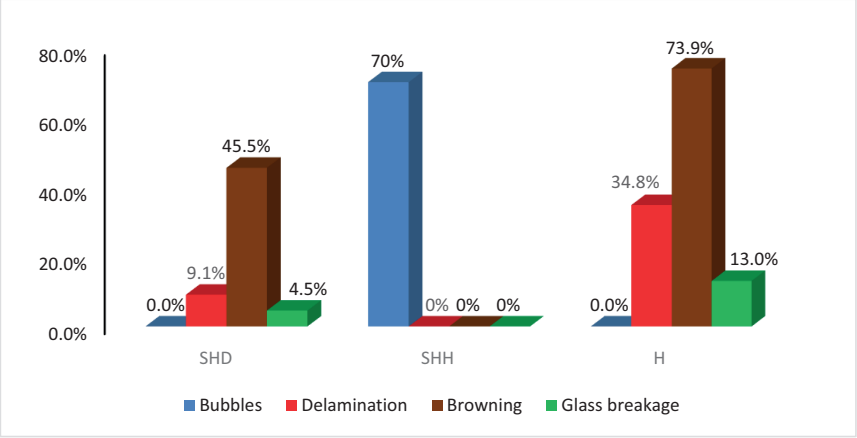

Figure 19: Details of front-of-module VODs observed in various climate categories

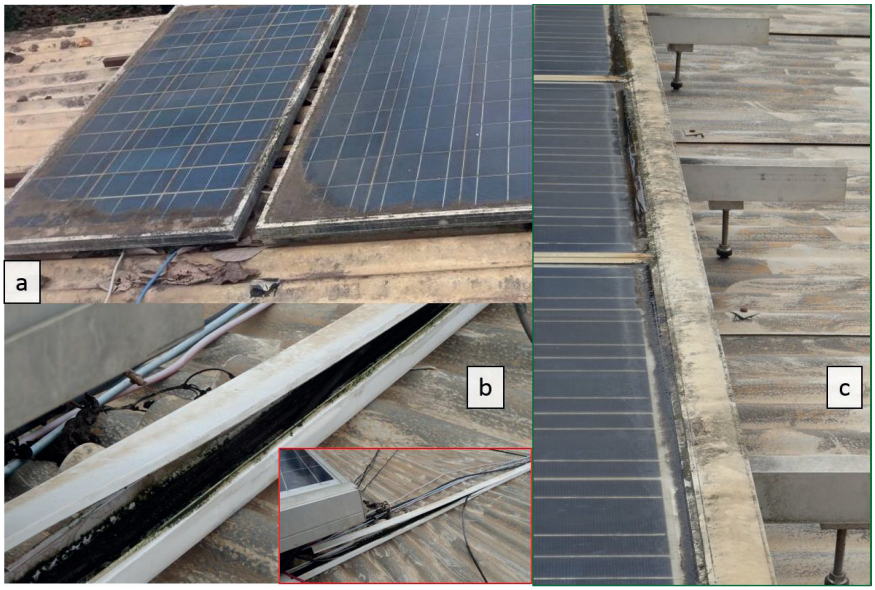

a) Low-tilt roofflushed modules with extensive soiling b) Cable ducts retaining water (with inset). c) Installation frame impeding water run-off.

Figure 20: Examples of installation defects and consequent effects

Also observed were obvious installation flaws, which, with the benefit of time, had demonstrated the impact it could have on module performance and potentially on electrical safety of module (Paper 2). For instance, modules installed at low tilt angle (6^{o}) were observed, which had been significantly affected by soiling, as water run-off during rains were impeded (Figure 20). Consequently, these

modules suffered major shunting and FF losses. Also observed were cable ducts in which rainwater had collected (Figure 20) as well as modules with wrong nameplate labelling and without certification labels (Paper2).

4. CONCLUSION, POLICY IMPLICATIONS AND FUTURE WORK

This section summarizes the main findings of this thesis in view of the broad aim and objectives outlined in Section 1.3, and reflects briefly on policy and application-related implications of the findings. To extend the scope of this study, improve on its methodological limitations and inspire new areas of research, some thoughts on future research direction are also provided.

4.1 Conclusions

The overarching aim of this research was to make an original scientific contribution to the subject of PV module performance degradation by studying systems installed in different climate sub-categories of Ghana. Although some studies on operational performance of solar PV modules in Ghana can be found in the open literature (e.g. [24], [22], [23]), this study has been the first known attempt to examine PV module performance degradation in Ghana. Moreover, this research has attempted, for the first time, a national -scale assessment to yield a more complete picture of module degradation in different climate zones of the country. Three climate sub-categories were defined for this purpose, delineated by latitude bands, as Humid (0 ^{o}N – 6 ^{o}N), Sub Humid Humid (6 ^{o}N – 10 ^{o}N) and Sub Humid Dry (10 ^{o}N – 12 ^{o}N). The long-term performance degradation sub-objectives focused on crystalline silicon (mc-Si and pc-Si) modules at different geo-locations, while the early-period study used time-series data from five different co-located technologies (a-Si mc-Si, pc-Si and HIT (mc-Si/a-Si)).

4.1.1 Findings from early-period degradation studies

Early-period degradation ranged between 6.1% and 13.8%, depending on technology (and method). While the degradation rate found for a-Si (13.8%) was relatively lower than many found in the open literature (10 – 30%), those found for x-Si technologies (including HIT) turned out to be higher than degradation rates reported by other researchers, and higher than 0 – 4% early degradation that is usually contained in multi-staged warranties provided by manufacturers. The lower degradation rate

found for a-Si could be the result of lower post-stabilization period degradation rate, since this research did not establish the stabilization time for a-Si. On the other hand, the use of system-level performance data and the inability to isolate the impact of dust/soiling is thought to be responsible for the higher rates for x-Si. However, these losses could also be a more realistic view of early-period losses that rooftop systems in Ghana could incur, compared with lower rates reported mostly from carefully-controlled experimental test-beds with regular module cleaning. This subject requires further investigation, particularly by eliminating non-degradation related losses such as soiling or temporary shading.

4.1.2 Findings from long-term degradation studies

A wide range of degradation rates were observed for the sixty-five modules studied in all three climates in the long-term degradation study. The annual degradation rates for individual modules ranged from 0.8% - 7%/yr, 0.55% - 2.07%/yr and 1.1% - 2.4%/yr for Humid (H), Sub-Humid Humid (SHH) and Sub-Humid Dry (SHD) respectively. The corresponding median values observed were 1.8%, 1.43% and 1.5% respectively for H, SHH and SHD climate categories respectively. Losses in short-circuit current dominated power loss in the Humid and Sub-Humid Dry climates (1.1%/yr and 0.8%/yr respectively); while losses in fill-factor drove power loss in the Sub-Humid Humid climate category (0.89%/yr). The P_{max} degradation rate found in this study are substantially higher than median and mean values of 0.5%/yr - 0.8%/yr which have been reported from meta-analytical studies as being representative of crystalline silicon (x-Si) modules. Although there is the need to expand the number of modules studied, the results of this research suggest, that, modules installed in Ghana will generally take less than 15 years to fall below 80% of initial power. This duration could be as short as 11 years (based on median degradation rate of 1.8%/yr).

Visually observable defects (VODs) were most prevalent in the Humid (H) climate, with occurrences registered in all seven of the module defect categories defined. Front-of-module and cell metallization defects were dominant. The Sub-Humid Dry (SHD) climate was next in VODs and had occurrences

in four out of seven defect categories. These were dominated by front-of-module and junction-box related defects (mostly, degraded adhesive). The H climate appears to impose more stresses than other climates due to the combined effect of high humidity and high temperature. This is consistent with the comparatively high incidence of module delamination and browning observed in climate H and the high contribution of I_{sc} losses to power degradation.

Meanwhile, in the Sub-Humid-Humid climate, VODs were observed in only one defect category (front-of-module); and, although they occurred in 70% of modules, they were minor bubbles (of the order of 1-mm diameter) and had a smaller impact on power losses as evidenced by the lower contribution of Isc losses compared with FF losses. The superior contribution of FF losses to power decline, suggests increased series resistance within the module. Thermo-mechanical fatigue and breakage in solder bonds/interconnects are not readily visible to the unaided eye and therefore account for the lower record of VODs in the SHH climate.

Installation and workmanship flaws, which accelerate module performance degradation were observed and documented in this study. Modules without any certification label (e.g. IEC 61215) were also encountered.

4.2 Implications of Findings

1. Overall, long-term degradation rates found, for both technologies (mc-Si and pc-Si), in all climates (H, SHH and SHD), age brackets, mounting type and various applications (grid-connected, battery-charging and water-pumping) suggest, that, photovoltaic module degradation rate in Ghana is higher than is typically suggested by PV modelling tools. Furthermore, they are higher than median values found by Jordan and Kurtz [12] in a global meta-study and throw open the question of realistic degradation in PV module performance and financial modelling. Even though studies that use nameplate data as reference data have been found to present systematically higher degradation rates, the findings of this study

suggest, that the 0.5%/year rule-of-thumb may not be applicable for Ghana, and possibly this part of the world. **Policy Implication:** Additional and continuing studies are needed to generate reference data for modelling in the PV industry in Ghana.

2. Performance of the 30+ year old modules, still performing at more than 70% of their rated capacity, provides the research community with a possible reference design against which to compare new and novel designs, in the quest to provide greater assurance to the PV industry [16]. Even though the manufacturer (HOLEC HH) is not in existence any longer, the design could be studied and replicated. **Policy Implication:** Typical 20-25 year economic life used in techno-economic analysis could be a conservative assumption in some instances.

3. Although some of the 30+ year modules were still performing well, electrical insulation of the cables in these modules had degraded significantly, raising questions about the safety, as well as end-of-life management approaches for solar PV modules. **Policy Implication:** Regulations that provide for end-of-life management of PV modules are needed. Although photovoltaic technology is a cleaner energy-producing technology compared with fossil-fuel fuel based options, the expected upsurge in installations could end up creating an environmental catastrophe, if appropriate regulations are not passed and implemented, to encourage the development of a PV-based circular economy.

4. The worst performing module encountered (the Baodin solar module), also had installation problems, as the modules were installed at a tilt angle (about 6^{o}) which impeded water run-off during rains and significantly increased the risk of water/moisture intrusion. Current-voltage characterization of this module revealed significant shunting and loss of fill factor. It also did not have any qualification label, even though tests such as IEC 61215 were available at the time of installation. **Policy Implication:** Quality workmanship is vital, in addition to quality products. Developing and enforcing regulations in this direction will protect consumers from sub-substandard products and workmanship, and boost confidence in the

burgeoning PV market in Ghana.

4.3 Methodological Limitations and Future Work

The data used in the long-term degradation study were based on discrete field measurements, rather than continuous observation; which is the preferred approach, as the latter provides a more complete picture of the temporal evolution of performance degradation. Some of the installations (particularly, those studied in Paper 1 and Paper 4) had been in open circuit mode during some periods of their exposure, the impact of these no-load periods on the degradation rates found in this research could not be isolated. The long-term modules studied were for crystalline silicon only. Data used in assessment of early-period degradation were from only one climate category and based on system level data rather than actual module-level I-V curves, which could be more accurate. A proper isolation of effects (e.g. climate) with controlled variables could not be carried out. Future government projects could be planned to integrate R&D aspects, which allow improvements in the methodology applied. While the results may have been influenced by the dominance of modules from one manufacturer, it also provided a common and stronger basis for comparison across geo-climatic zones. Specifically, the following themes are envisaged in future work:

- Intensification of data (by climate, application, technology, age and mounting type).
- Development of a multi-criteria economic decision tools for solar PV installation management.
- Study on awareness levels of warranty provisions and experiences with triggering them.
- Ongoing monitoring of accessible installations to provide insight into the inter-annual performance decline.
- Application of UAV and imaging techniques in solar PV monitoring (team up with research groups active in this area).
- Establishment of well-maintained experimental testbeds with I-V instrumentation to generate data in support of PV industry in Ghana.

References

[1] UN, “Report of the World Commission on Environment and Development: Our Common Future,” UN, 1987.

[2] UNDESA, “A guidebook to the Green Economy - Issue 1: Green Economy, Green Growth, and Low-Carbon Development – history, definitions and a guide to recent publications,” UNDESA, 2012.

[3] D. H. Meadows, D. L. Meadows, J. Randers and W. W. I. Behrens, The Limits to Growth, New York: Universe Books, 1972.

[4] IPCC, “Renewable Energy Sources and Climate Change Mitigation: Special Report of the Intergovernmental Panel on Climate Change,” Cambridge University Press, New York, 2012.

[5] IRENA, “Global Energy Transformation: A roadmap to 2050,” International Renewable Energy Agency (IRENA), Abu Dhabi, 2018.

[6] UN, “Sustainable Energy for All Website (SE4All),” 2011. [Online]. Available: http://www.se4all.org/sites/default/files/l/2013/09/SG_Sustainable_Energy_for_All_vision_final_clean.pdf. [Accessed 19 Feb 2016].

[7] ILO; EC, “Skills and Occupational Needs in Renewable Energy,” International Labour Organization, Geneva, 2011.

[8] OECD/IEA; IRENA, “Perspectives for The Energy Transition - Investment Needs for a Low-Carbon Energy System,” IEA Publications, Paris, 2017.

[9] G. Yang, Life Cycle Reliability Engineering, New Jersey: John Wiley & Sons, 2007.

[10] IEA-PVPS, “Technical Assumptions Used in PV Financial Models - Review of Current Practices and Recommendations,” IEA, Paris, 2017.

[11] C. Osterwald, J. Adelstein, J. del Cueto, B. Kroposki, D. Trudell and T. Moriarty, “Comparison of Degradation Rates of Individual Modules Held at Maximum Power,” in *4th IEEE World Conference on Photovoltaic Energy Conversion*, Hawaii, 2006.

[12] D. C. Jordan and S. R. Kurtz, “Photovoltaic Degradation Rates—an Analytical Review,” *PROGRESS IN PHOTOVOLTAICS,* p. 12–29, 2013.

[13] D. C. Jordan, S. R. Kurtz, K. VanSant, Newmiller and Jeff, “Compendium of photovoltaic degradation rates,” *Progress in Photovoltaics: Research and Applications,* vol. 24, no. 7, p. 978–989, 2016.

[14] A. Phinikarides, N. Kindyni, G. Makrides and G. E. Georghiou, “Review of photovoltaic degradation rate methodologies,” *Renewable and Sustainable Energy Reviews,* vol. 40, p. 143–152, 2014.

[15] D. A. Quansah and M. S. Adaramola, “Comparative study of performance degradation in poly- and mono-crystalline-Si solar PV modules deployed in different applications,” *International Journal of Hydrogen Energy,* vol. 43, no. 6, p. 3092–3109, 2018.

[16] J. H. Wohlgemuth and S. Kurtz, “Using Accelerated Testing To Predict Module Reliability,” in *Photovoltaic Specialists Conference (PVSC), 2011 37th IEEE*, Seattle, WA, USA, 2011.

[17] K. G. Adanu, “Photovoltaic electricity in Ghana—current use and potential for the future,” *Renewable Energy,* vol. 1, no. 5-6, pp. 823-826, 1991.

[18] J. Essandoh-Yeddu, “Photovoltaic R&D and applications in Ghana: current status and prospects,” in *Conference Record of the Twenty Fifth IEEE Photovoltaic Specialists Conference - 1996* , Washington, DC, USA, USA , 1996.

[19] I. Edjekumhene, S. B. Atakora, R. Atta-Konadu and A. Brew-Hammond, “Implememtation of Renewable Energy Technologies - Opportunities and Barriers (Ghana Country Study),”

UNEP/KITE, Roskilde, 2001.

[20] Energy Commission Ghana, "Strategic National Energy Plan 2006 – 2020: Main Report," Energy Commission Ghana, 2006.

[21] D. A. Quansah, M. S. Adaramola and E. K. Anto, "Cost-competitiveness of distributed grid-connected solar photovoltaics in Ghana: case study of a 4 kWp polycrystalline system," *Clean Technologies and Environmental Policy,* vol. 19, no. 10, p. 2431–2442, 2017.

[22] H. A. Koffi, V. C. K. Kakane, A. Kuditcher, A. F. Hughes, M. Adeleye and J. Amuzu, "Seasonal variations in the operating temperature of silicon solar panels in southern Ghana," *African Journal of Science, Technology, Innovation and Development,* vol. 7, no. 6, p. 485–490, 2015.

[23] D. A. Quansah, M. S. Adaramola and G. K. Appiah, "Performance analysis of different grid-connected solar photovoltaic (PV) system technologies with combined capacity of 20 kW located in humid tropical climate," *International Journal of Hydrogen Energy,* vol. 42 (2017), pp. 4626 - 4635, 2017a.

[24] K. G. Adanu, "Performance of a 268 Wp stand-alone PV system test facility," in *Proceedings of 1994 IEEE 1st World Conference on Photovoltaic Energy Conversion - WCPEC (A Joint Conference of PVSC, PVSEC and PSEC)*, Hawaii, 1994b.

[25] N. K. Gautam and N. D. Kaushika, "Reliability Evaluation of Solar Photovoltaic Arrays," *Solar Energy,* vol. 72, no. 2, p. 129–141, 2002.

[26] C. Ferrara and D. Philipp, "Why Do PV Modules Fail?," in *International Conference on Materials for Advanced Technologies 2011, Symposium O*, 2012.

[27] M. A. Quintana, D. L. King, T. J. McMahon and C. R. Osterwald, "Commonly Observed Degradation in Field-Aged Photovoltaic Modules," 2002.

[28] A. R. Hoffman and R. G. J. Ross, "Environmental qualification testing of terrestrial solar cell modules," in *Photovoltaic Specialists Conference; 13th; June 5-8, 1978*, Washington, DC, 1978.

[29] I. Berardonea, J. Lopez Garciab and P. M., "Analysis of electroluminescence and infrared thermal images of monocrystalline silicon photovoltaic modules after 20 years of outdoor use in a solar vehicle," *Solar Energy,* vol. 173, p. 478–486, 2018.

[30] C. E. Packard, J. H. Wohlgemuth and S. R. Kurtz, "Development of a Visual Inspection Data Collection Tool for Evaluation of Fielded PV Module Condition," NREL, Golden, 2012.

[31] N. Bogdanski and W. Herrmann, "Weighting of Climate Impacts on PV-module Degradation - Comparison of Outdoor Weathering Data and Indoor Weathering Data," in *26th European Photovoltaic Solar Energy Conference and Exhibition*, Hamburg, 2011.

[32] IEC, "Crystalline silicon terrestrial photovoltaic (PV) modules - Design qualification and type approval," IEC, 2005.

[33] IEA, "Review of Failures of Photovoltaic Modules," IEA/OECD, 2014.

[34] IEC, "Thin-film terrestrial photovoltaic (PV) modules - Design qualification and type approval," IEC, 2008.

[35] C. R. Osterwald and T. J. McMahon, "History of Accelerated and Qualification Testing of Terrestrial Photovoltaic Modules: A Literature Review," *Progress in Photovoltaics: Research and Applications,* vol. 17, p. 11–33, 2009.

[36] N. G. Dhere, "Reliability of PV modules and balance-of-system components," in *Conference Record of the Thirty-first IEEE Photovoltaic Specialists Conference, 2005.*, Lake Buena Vista, FL, USA, USA, 2005.

[37] D. L. King, M. A. Quintana, J. A. Kratochvil, D. E. Ellibee and B. R. Hansen, "Photovoltaic module performance and durability following long-term field exposure," *Progress in Photovoltaics: Research and Applications,* vol. 8, no. 2, p. 241–256, 2000.

[38] J. Wohlgemuth, “IEC 61215: What it is and isn’t,” NREL, 2012.

[39] M. A. Green, “Silicon Photovoltaic Modules: A Brief History of the First 50 Years,” *Progress in Photovoltaics: Research and Applications,* vol. 13, no. 5, p. 447–455 , 2005.

[40] Canadian Solar (USA) Inc., “PV Module Warranty and Warranty Insurance Comparisons: A Cornerstone Of Bankability,” Solar Southwest Florida, 2011.

[41] REC, “25-year linear power output warranty,” REC, 2013.

[42] J. Meydbray and F. Dross, “PV Module Reliability Scorecard 2016,” DNV GL, Oslo, 2016.

[43] GTM Research, “Rest in Peace: The List of Deceased Solar Companies,” GTM Research, 2013.

[44] C. Y. Wereko-Brobby and M. Opam, “The Application of Solar Photovoltaic Systems in Ghana,” in *Proceedings of the Biennial Congress of the International Solar Energy Society, 13–18 September 1987*, Hamburg, Federal Republic of Germany, 1987.

[45] J. Nassen, J. Evertsson and B. A. Andersson, “Distributed Power Generation versus Grid Extension: An Assessment of Solar Photovoltaics for Rural Electrification in Northern Ghana,” *Prog. Photovolt: Res. Appl.,* vol. 10, pp. 495-510, 2002.

[46] UNDP/GEF, “Renewable Energy-Based Electrcity for Rural Social and Economic Development (RESPRO),” 2002.

[47] J. Essandoh-Yeddu, “Current solar energy utilization in Ghana,” *Renewable Energy,* vol. 10, no. 2–3, pp. 433-436, 1997.

[48] PVsyst SA, “PVSyst Photovoltaic Software,” Satigny, 2012.

[49] NCPRE/Solar Energy Centre, “All-India Survey of Photovoltaic Module Degradation: 2013,” 2013.

[50] M. C. Peel, B. L. Finlayson and T. A. Mcmahon, “Updated world map of the Koppen-Geiger climate classification,” *Hydrology and Earth System Sciences Discussions,* pp. 439-473, 2007.

[51] C. S. Beckley, S. Shaban, G. H. Palmer, A. T. Hudak, S. M. Noh and J. E. Futse, “Disaggregating Tropical Disease Prevalence by Climatic and Vegetative Zones within Tropical West Africa,” *PLOS ONE,* vol. 11, no. 3, 2016.

[52] RETScreen International, *RETScreen Climate Database,* 2014.

[53] F. Akuffo and A. Brew-Hammond, “The frequency distribution of daily global irradiation at Kumasi,” *Solar Energy,* vol. 50, no. 2, pp. 145-154, 1993.

[54] IEC, “IEC 60891:2009 Photovoltaic devices - Procedures for temperature and irradiance corrections to measured I-V characteristics,” IEC, 2009.

[55] A. Carullo, F. Ferraris, A. Vallan, F. Spertino and F. Attivissimo, “Uncertainty analysis of degradation parameters estimated in long-term monitoring of photovoltaic plants,” *Measurement,* vol. 55, p. 641–649, 2014.

[56] Y. Tsuno, Y. Hishikawa and K. Kurokawa, “Translation Equations for Temperature and Irradiance of the I-V Curves of Various PV Cells and Modules,” in *IEEE 4th World Conference on Photovoltaic Energy Conference*, Waikoloa, Hawaii, 2006.

[57] W. Herrmann and W. Wiesner, “Current-Voltage Translation Procedure for PV Generators in the German 1,000 Roofs-Programme,” CiteSeerX, 2014.

[58] B. C. Duck, C. J. Fell, B. Marion and K. Emery, “Comparing Standard Translation Methods for Predicting Photovoltaic Energy Production,” in *Proceedings 39th IEEE Photovoltaic Specialists Conference, June 16-21, 2013*, Tampa Florida, 2013.

[59] S. Kaplanis and E. Kaplani, “Energy performance and degradation over 20 years performance of BP c-Si PV modules,” *Simulation Modelling Practice and Theory,* vol. 19, p. 1201–1211, 2011.

[60] D. A. Quansah, A. M. S., G. Takyi and I. A. Edwin, “Reliability and Degradation of Solar PV Modules—Case Study of 19-Year-Old Polycrystalline Modules in Ghana,” *Technologies,* vol. 5, no. 22, 2017b.

[61] D. A. Quansah and M. S. Adaramola, “Ageing and degradation in solar photovoltaic modules installed in northern Ghana,” *Solar Energy,* 2018b.

[62] D. A. Quansah and M. S. Adaramola, “Assessment of early degradation and performance loss in five co-located solar photovoltaic module technologies installed in Ghana using performance ratio time-series regression,” *Renewable Energy,* vol. 131, pp. 900-910, 2019.

[63] M. A. Munoz, A.-G. M. C, N. Vela and F. Chenlo, “Early degradation of silicon PV modules and guaranty conditions,” *Solar Energy,* no. 85(2011), pp. 2264-2274, 2011.

[64] M. Gostein and L. Dunn, “Light soaking effects on photovoltaic modules: Overview and literature review,” in *Photovoltaic Specialists Conference (PVSC), 2011 37th IEEE*, Seattle, WA, USA, 2011.

[65] B. Marion, S. Rummel and A. Anderberg, “Current-Voltage Curve Translation by Bilinear Interpolation,” *Progress in Photovoltaics: Research and Applications,* vol. 12, pp. 593-607, 2004.

Paper 1

technologies

MDPI

Article

Reliability and Degradation of Solar PV Modules—Case Study of 19-Year-Old Polycrystalline Modules in Ghana

David A. Quansah [1,2,3,*], Muyiwa S. Adaramola [1], Gabriel Takyi [2,3] and Isaac A. Edwin [2,3]

1 Renewable Energy Group, Faculty of Environmental Sciences and Natural Resource Management, Norwegian University of Life Sciences (NMBU), Ås (1432), Norway; muyiwa.adaramola@nmbu.no
2 The Brew-Hammond Energy Centre, College of Engineering, Kwame Nkrumah University of Science and Technology (KNUST), PMB, University Post Office, Kumasi, Ghana; gabrieltakyi@yahoo.co.uk (G.T.); edwinadjei@gmail.com (I.A.E.)
3 Department of Mechanical Engineering, College of Engineering, Kwame Nkrumah University of Science and Technology (KNUST), PMB, University Post Office, Kumasi, Ghana
* Correspondence: david.ato.quansah@nmbu.no; Tel.: +47-90-56-10-63

Academic Editor: Manoj Gupta
Received: 3 May 2017; Accepted: 12 May 2017; Published: 22 May 2017

Abstract: Fourteen (14) rack-mounted polycrystalline modules installed on the concrete roof of the solar energy applications laboratory at the Kwame Nkrumah University of Science and Technology (KNUST) in Ghana, a hot humid environment, were assessed after 19 years of continuous outdoor exposure. The physical state of the modules was documented using a visual inspection checklist. They were further assessed by current-voltage (I-V) characterization and thermal imaging. The modules were found to be in good physical state, except some bubbles on front side and minor discolouration/corrosion at edge of the cells. Compared with reference values, the performance decline of the modules observed over the exposure period was: nominal power (P_{nom}), 21% to 35%; short circuit current (I_{sc}), 5.8% to 11.7%; open circuit voltage (V_{oc}) 3.6% to 5.6% and 11.9% to 25.7% for fill factor (FF). It is hoped that this study will provide some helpful information to project developers, manufacturers and the research community on the long-term performance of PV modules in Ghana.

Keywords: solar PV; module; degradation; characterization; I-V Curve

1. Introduction

The phenomenal and sustained growth of solar photovoltaics (PV) in recent years is well-documented [1–9]. Indeed, this growth extends to other renewable energy technologies such as wind, bioenergy, hydropower and geothermal. The drivers for this growth are widely acknowledged to include, climate policy, technology improvements and energy security considerations. Research and development (R&D) efforts have paid off in the form of increased efficiencies at both cell and module levels. For example, cell efficiencies reported in major laboratories for crystalline silicon have increased from 13% in the 1970s to over 26% in 2016 [10,11], doubling in the period, and thus approaching the theoretical thermodynamic limit of 34% (Shockley-Queisser limit) [12,13] for single crystal silicon cells at standard test conditions. Advances in thin-film and multi-junction cell technologies have been even more rapid. The cell-to-module efficiencies for these cell technologies have also improved to 99% (in 2015) and is projected to exceed 103% by 2026 because of improvement in light management techniques [14].

As research laboratories and industry players focus on improving solar-to-electric conversion efficiencies, there is increasing acknowledgement of the need for data on the performance of systems that have already been deployed across the various climates and geographical regions of the world.

A characteristic feature of solar PV (and other renewables) is the high upfront cost per installed power. Once installed, reliable performance and durability of the system enables it to generate electricity (kWh), which represents a benefit to the investor/system owner. Reliability is understood as the probability that an item, in this case the solar PV module, will continue to perform its intended function without failure for a specified period of time under stated conditions [15,16]. Durability, on the other hand, has to do with how long the product will last under normal operating conditions [17].

For the solar PV investor, reliable operation of the PV modules and their durability as per warranty conditions, are important for the realization of the expected return on investment. Module manufacturers, similar to other product manufacturers, attempt to assure buyers of their products by providing warranties. The warranties on PV modules have evolved from 5 years in the 1980s, through 10–20 years in the 1990s to current industry standard practice of 80% of peak power for 25 years [18]. Some manufacturers provide 2-stage (and other multi-stage) warranties. These warranties are typically in the range of 90%–95% peak power in the first 5–10 years and thereafter, 80%–87% of peak power up to year 25 [19]. REC Solar [20], for example, provides a 97% performance guarantee on its modules within the first year of exposure and 80.2% of peak power by the end of the 25th year.

For current standard 25 year warranty (80% of peak power) to hold, modules must, on the average, degrade at not more than 0.8%/year (Figure 1). However, industry players are seeking to extend warranty periods to 30 years [21], which would imply a maximum average annual performance decline of no more than 0.65% (Figure 1).

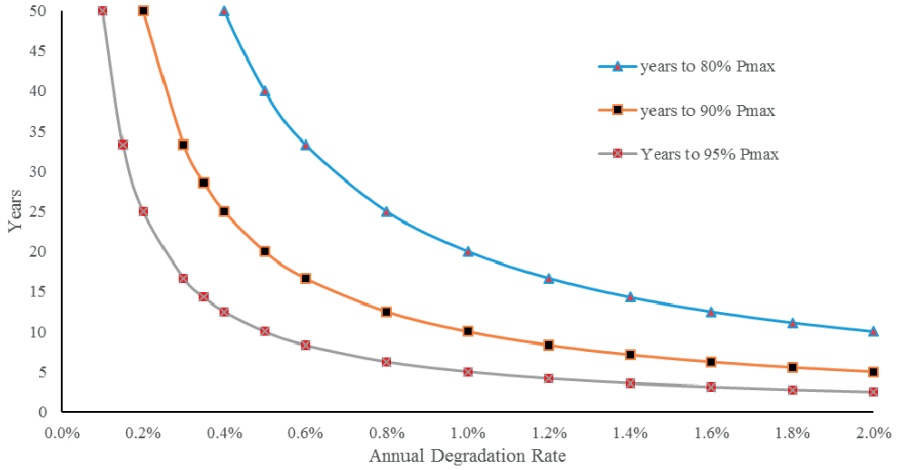

Figure 1. Module warranty periods and degradation rates.

Solar PV warranties typically encounter two major hurdles. First, is the enforceability of the warranties [22]. This is largely attributable to the rapidly evolving landscape that has led to the extinction of many manufacturers, with others filing for bankruptcy. This extinction was most noticeable in the period 2010–2013, when, in the US alone, over 50 companies either collapsed or filed for bankruptcy protection [23]. Warranties provided by defunct companies on PV modules sold therefore become difficult to enforce, particularly if the need for warranty claims arise after official liquidation. To address this first problem with the warranties, some manufacturers are now providing insurance-backed warranties [24–27]. These insurance products are, however, certain to add to the cost of modules to the buyer.

The second difficulty with the warranties is the more fundamental question of physical basis. Current testing and qualification regimes such as the IEC 61215 [28] for crystalline Silicon modules and IEC 61646 [29] for thin film modules employ techniques such as accelerated ageing and stress

tests with the view to detecting the presence of known failure or degradation modes in the intended environments [30]. These qualifications tests can however not predict or guarantee product life under field conditions. They are indeed not designed for such a purpose [30,31]. Qualification tests instead seek, among other answers, to find design and process flaws and have been credited with significantly reducing infant mortality among PV modules [32]. It has been suggested [18], that recent studies based on field exposure is providing some basis for and validation of 25-year warranties; however, an overwhelming majority of modules have hardly lasted 25 years on the field to prove the validity of the warranties. Figure 2 shows that, over 80% of modules installed today have been installed in the last 5 to 6 years.

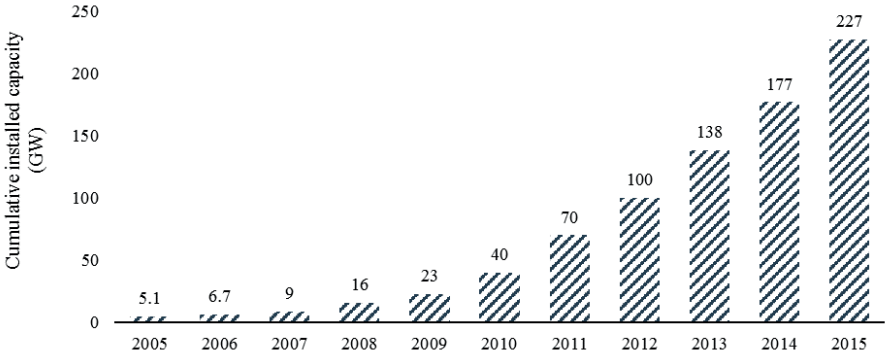

Figure 2. Global module installations over the years. Data REN21 [8].

To compound this problem further, the technologies themselves are undergoing significant material level changes. For example, [33–35] reported that crystalline Silicon (c-Si) wafer thickness has reduced from 400 µm in 1990 to 180 µm in 2015, while silicon usage has declined from 16g/Wp in 2004 to less than 6g/Wp in 2015. The metallization is also moving away from silver to less expensive options such as copper, nickel and zinc [34].

Therefore, monitoring and assessment of fielded modules provide useful insight and feedback for module manufacturers and R&D institutions and reduces uncertainties for solar PV investors. A number of researchers have undertaken, over the years, to study the long-term outdoor performance, degradation and failure of solar PV modules around the world. Notable authors in this area include Lorenzo et al. [36], Bandou et al. [37], Ndiaye et al. [38], Jordan and Kurtz [18], Quintana et al. [39], Skoczek [40], Skoczek et al. [41], Kahoul et al. [42] and Ferrara and Daniel [43]. The literature identifies major causes and modes of module degradation and failure to include [18,39]: degradation of packaging materials, loss of adhesion, degradation of cell/module interconnects as a result of thermomechanical fatigue, degradation due to moisture intrusion and degradation of semiconductor device [39]. These defects tend to result in reduced module output, safety issues and sometimes complete failure. Nevertheless, as noted by Jordan et al. [44], it may be surmised, that, degradation in performance characteristics of modules have some dependence on local conditions and climate zone. Yet, there are no reports on degradation rates and failure modes of PV modules in many climate zones [44,45]. Indeed, as demonstrated by authors such as Jordan et al. [44] and Phinekarides et al. [45], who compiled globally reported degradation rates and overlaid them on global maps (using the Koppen climate classification), there is very little reported from Africa, with nothing at all in the vast majority of climate classifications.

According to Peel et al. [46], Africa's climate comprises mainly of three (3) of the Koppen-Geiger climate types-A, B and C. Ghana's climate is classified as tropical climate (A) of the monsoon (Am) and savanna with dry winter (Aw) types. This implies that the average temperature of the coolest month of

the year is above 18 °C. In terms of precipitation, the tropical monsoon climate's driest month records less than 60 mm of precipitation but the precipitation is greater than or equal to h.

Where

$$h = 100 - \frac{\text{Total annual precipitation (in mm)}}{25} \quad (1)$$

Precipitation in tropical savanna climate is less than 60 mm in the driest month and also less than h (as defined in Equation (1)) [46]. Further microclimate sub-classifications of the country have also been made based on agro-ecological characteristics of various zones and is used by organizations such as the UN Food and Agriculture Organization (FAO) [47]. These sub-classifications are: Rain Forest, Deciduous Forest, Forest-Savannah Transition, Coastal Savannah and Northern (Interior) Savannah which comprises Guinea and Sudan Savannahs [47].

It should be noted, however, that, whereas the Koppen-Geiger classification scheme is based on temperature and precipitation, for solar PV performance and durability issues additional parameters such as humidity, temperature variation (thermal cycling), altitude and air salinity are important as well [43]. For consistency and comparability of analysis, consolidation of climate categories sometimes becomes necessary. In the work of Jordan et al. [44], tropical climates such as Aw and Af are broadly classified together with Cfa (Temperate hot summer without dry season) and consolidated as hot and humid. This present work adopts this climate categorization. Another climate categorization of interest is that which was used for the All-India Survey of Photovoltaic Module Degradation: 2013 [48].

This paper seeks to contribute to filling this gap (long-term performance of PV modules and degradation in Africa) and presents results of assessment conducted on an 19-year old polycrystalline solar PV installation at the Kwame Nkrumah University of Science and Technology (KNUST) in Ghana.

2. Materials and Methods

2.1. Site Description and Climate

As shown in Figure 3, Kumasi is a hot and humid climate with average daily temperature ranging from 24.4 °C in July to 27.8 °C in March and relative humidity of 65% in January to 83.5% in July [49]. Hence, accordingly, Kumasi is climate condition can be classified as Aw using Koppen classification. This climate would be categorized as "warm and humid" per classifications used in [48].

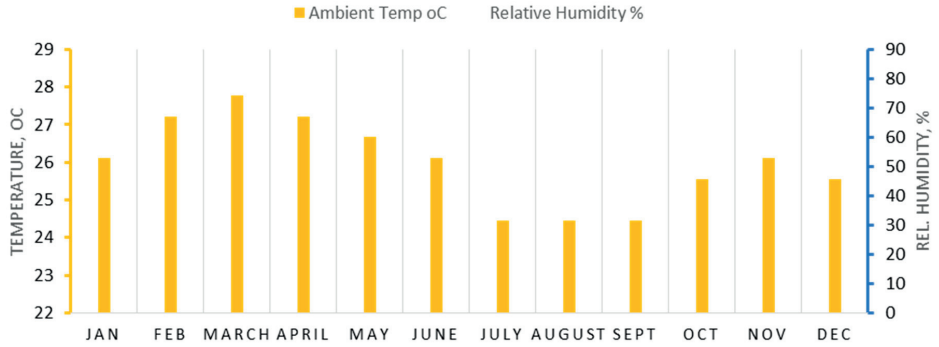

Figure 3. Monthly Average Temperature and Humidity in Kumasi. Data from [49].

Daily solar irradiation on horizontal surface in Kumasi ranges from 3.35 kWh/m^2 in August to 5.09 kWh/m^2 in April and monthly precipitation in the year varies from a low of 25 mm in December to a high of 218 mm in June (Figure 4). Wind speeds are generally low and ranges from average 1.5 m/s to 2.6 m/s at this location [49].

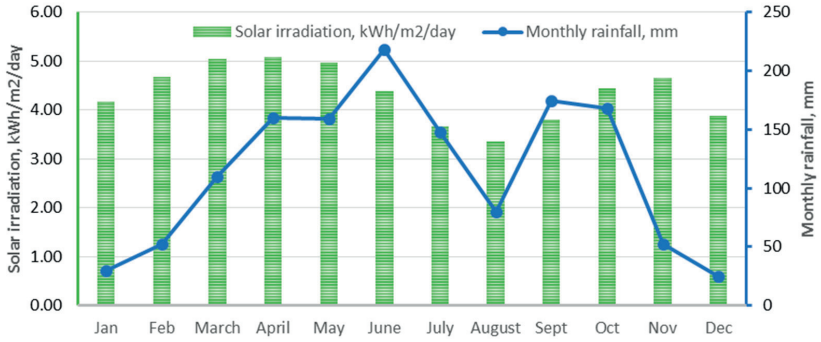

Figure 4. Daily solar irradiation and precipitation for Kumasi. Data from [49,50].

2.2. Description of Installation

The system under study was installed in 1998 and comprises of fourteen (14) ASE-50-PWX-D modules, manufactured by ASE GmbH (Putzbrunn, Germany). They were initially installed as part of joint project on solar-driven centrifugal pumps between the Institute of Machine Design, Hydraulic Turbomachinery and Hydrodynamics at the Technical University of Berlin (Germany) and the Department of Mechanical Engineering, Kwame Nkrumah University of Science and Technology (Ghana). The modules have for some time now been used in off-grid mode and charges a 400 Ah which provides power to selected loads at the Solar lab at the College of Engineering.

The system is mounted on a metallic frame on top of a concrete roof with about 1 m clearance above the roof and hence, ensures good ventilation of the modules. Each module comprises 36 cells and has nominal power of 49 W (a total of 686 Wp). The module material comprises tempered glass at the front (3.1 mm), EVA (ethylene vinyl acetate) encapsulant, polymer backsheet and aluminium frame [51]. Performance parameters of the modules are shown in Table 1.

Table 1. Reference module parameters.

Parameter	Value
Nominal Power (P_{nom}), W	49.50
Short-circuit current (I_{sc}), A	3.10
Open-circuit voltage (V_{oc}), V	21.60
Current at maximum power point (I_{mpp}), A	2.85
Voltage at maximum power point (V_{mpp}), V	17.40
Efficiency	10.3%

The modules were qualified under the CEC ESTI (European Solar Test Installation) 503 Standard. The cell design comprises two bus bars and 40 grid lines, organized in a rectangular pattern around four (4) centres on the two bus bars (Figure 5). In addition to the rectangular grid patterns, four (4) grid lines are also observed to run across the cells in both horizontal and vertical directions (Figure 5).

The modules are oriented toward south with a fixed inclination of approximately 15° to the horizontal. For the purpose of the assessment and measurements, the modules were labelled from PWX1 to PWX 14 as shown in Figure 6.

During the measurements, the modules were electrically isolated to permit access to the terminals of the modules. Even though there was no cleaning schedule in place for the modules, the rains had done some cleaning of the module surface during the period of measurement. Nonetheless, to further eliminate impact of dust on the measurement, the module surfaces were cleaned with clean water and allowed to dry before measurements were made.

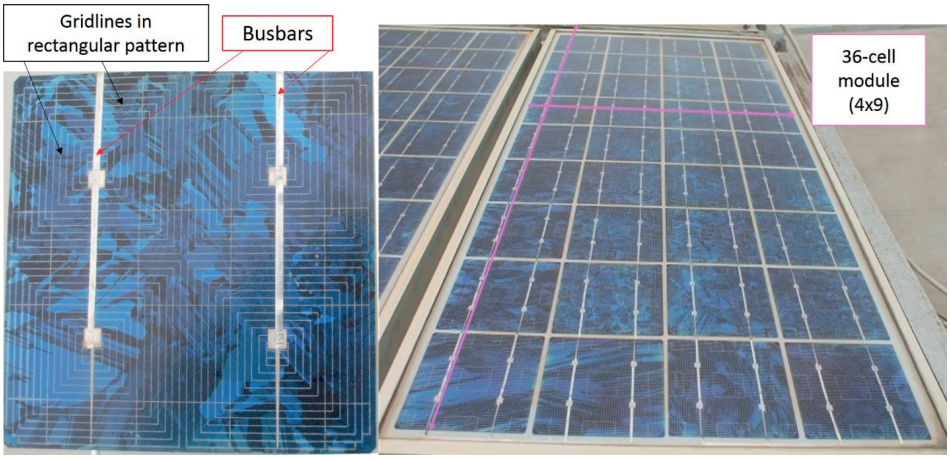

Figure 5. A photograph of the solar cell (**left**) showing its metallization and the module (**right**) showing number of cells.

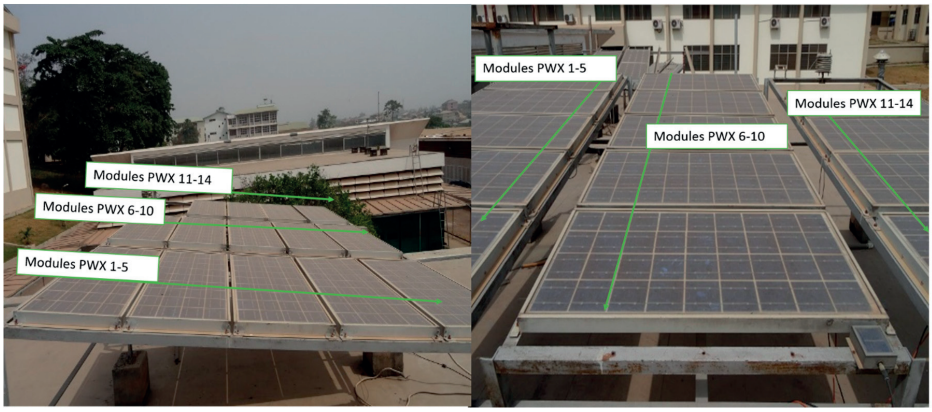

Figure 6. Picture of installation from different views showing modules labelled as PWX 1–14.

2.3. Inspection and Measurements

Field assessment of solar PV modules usually employs techniques such as visual and physical inspection, I-V (current-voltage) characterization, bypass diode test, insulation testing and thermal imaging to help detect defects in the modules [41]. Some defects, such as micro-cracks in cell structure may not be visible to the eye and require more advanced techniques such as electroluminescence imaging to detect. However, the I-V curve tracing is the most widely used technique in outdoor electrical characterization of solar PV modules [52].

In this study, three methods, which are visual inspection, I-V characterisation and thermal imaging were used. The visual inspection of the modules was undertaken using the widely-applied field visual inspection template by NREL/IEA [32]. This sought to systematically document any visually observable defects on the various components of the modules (such as front glass, back sheets, junction boxes, metallization, encapsulation and frames) and interconnections following 18 years of outdoor exposure.

Many known PV module defects (encapsulant browning, solder bond degradation, hot spot formation, etc.) also lead to changes such as increased series resistance, lowered shunt resistance, low transmittance of front glass and encapsulant (and optical decoupling) which tend also have characteristic signatures on I-V curves. The I-V characterization of the modules under study was undertaken using a TRI-KA I-V curve tracer. The TRI-KA IV tracer works together with TRI-SEN which measures irradiance, module temperature and module inclination angle. In-plane irradiance and module temperature are necessary for the translation of the current-voltage measurements to other reference conditions, such as STC (Standard Test Conditions–i.e., 25 °C, 1000 W/m^2 and AM 1.5). Module current is known to be a strong function of irradiance, while voltage on the other hand, has a stronger dependence on temperature. The TRI-SEN maintains a wireless communication with the TRI-KA during the measurements.

The TRI-KA I-V tracer has a voltage and current measurement range of 1–1000 V, and 0.1–15 A, respectively, with uncertainty of ±1% (for both current and voltage). The TRI-SEN measures temperature in the range 0–100 °C (±3% uncertainty) and irradiance in the range 100–1200 W/m^2 (±5% uncertainty).

The key parameters used for assessment include the nominal power (P_{nom}), short-circuit current (I_{sc}), open circuit voltage (V_{oc}) and fill factor (FF). It must be noted, that maximum power (P_{max}), which is the product of I_{sc} and V_{oc} is never generated, as the I-V curve (see Figure 7) is never rectangular. The peak power may therefore be viewed as a fraction of the maximum power. This fraction is the fill factor.

A Fluke® TI400 thermal camera was used to obtain thermal images of the modules in forward bias mode at I_{sc}. The emissivity of the camera was set to 0.85 since the module surface is glass. This was to help assess temperature inhomogeneity and possible hotspots in the modules.

2.4. Calculations and Data Analysis

A modified version of IEC 60891 (Procedures for temperature and irradiance corrections to measured I-V characteristics.) I-V data translation method, developed by the Joint Research Centre (JRC) of the European Commission and applied in the German 1,000 Roofs Solar Programme [53,54] was used. The equations are presented below (Equations (2)–(5)):

$$I_{SC,2} = I_{SC,1}[1 + \alpha(T_2 - T_1)]\frac{G_2}{G_1} \tag{2}$$

$$V_{OC,2} = V_{OC,1}\left[1 + a\ln\frac{G_2}{G_1} + b.(T_2 - T_1)\right] \tag{3}$$

$$I_2 = I_1\left(\frac{I_{SC,2}}{I_{SC,1}}\right) \tag{4}$$

$$V_2 = V_1 + (V_{OC,2} - V_{OC,1}) + R_s(I_1 - I_2) \tag{5}$$

where: I is current (A); I_{sc} is short-circuit current (A); G is irradiance (W/m^2); T is module temperature (°C), V is voltage (V) and V_{oc} is open-circuit voltage (V). In these equations, subscripts 1 and 2 refer respectively to measured values and values at reference conditions. The constant parameters and their default values, which are valid for crystalline silicon, are defined and given as:

- α is a dimensionless temperature coefficient of I_{sc} (default value is 0)
- b is dimensionless temperature coefficient of V_{oc} (default value is -0.004)
- a is dimensionless irradiance correction factor (default value is 0.06) and
- R_s is series resistance (Ω) (default value is 0)

Although a number numeric and algebraic approaches exist (e.g., IEC [55], Smith et al. [56], Tsuno et al. [57] and Marion [58]) for translating I-V data from measured to desired reference conditions

(such as STC), many of these require the determination of coefficients, which in turn require controlled conditions such as constant irradiance and constant temperature; conditions which are difficult to obtain under field conditions, making the equations difficult to implement. The approach proposed by JRC therefore presents a balance between accuracy and practicability and has uncertainty of about 4%.

Standard manufacturer reference electrical parameters are normally reported at STC conditions. However, outdoor conditions differ, and sometimes the irradiance is well below this reference. Work by Anderson [59], has shown that translating to STC from low irradiance values and high temperature comes with lower levels of accuracy. In this present study, effort was therefore made to obtain I-V measurements at irradiance levels that were as close as possible to 1000 W/m^2. The standardization could in principle also be undertaken to other reference conditions, such as to the nearest irradiance level for which reference I-V data is available.

The I-V characteristic curve of the ASE-50-PWX-D module at different irradiance levels was obtained from PVSyst solar PV module database (Figure 7) [51] due to the fact that that the manufacturer label on the module only showed the peak power. PVSyst uses the well-known 1-diode model to generate I-V curves. For reasons of completeness and consistency of data and following the example of Abete et al. [18], even though the manufacturer label on the module has 49 W as peak power rating, 49.5 W (with short-circuit current of 3.1 A and open circuit voltage 21.6 V) based on the 1-diode model of PVSyst is used in this paper as the baseline. This will result in the assessment of power degradation being slightly overstated (by approximately 1%). The use of models to simulate baselines for module degradation studies is discussed further by [52]. The decline in key characteristics of the modules was computed by comparing the standardized performance data with the baseline values.

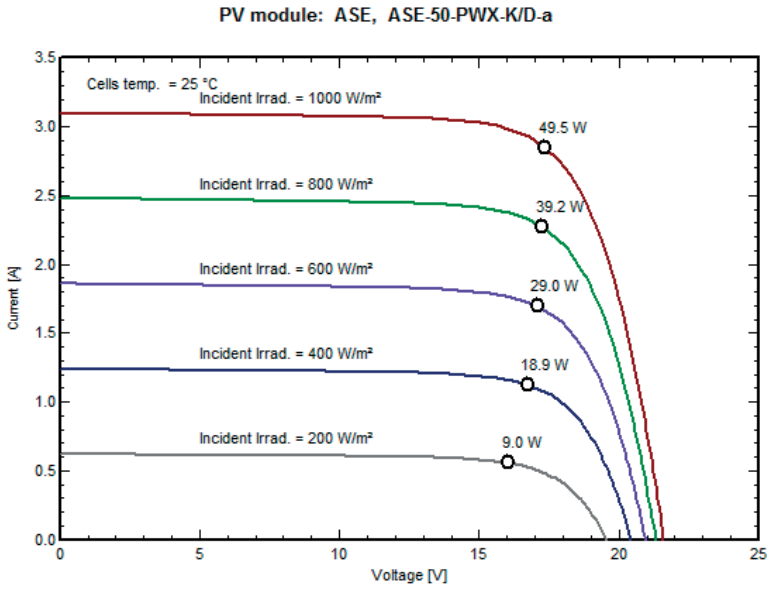

Figure 7. I-V curve of ASE-50-PWX-D module at different irradiance levels. Data–PVSyst SA [51].

3. Results and Discussion

3.1. Visual and Physical Inspection

The visual inspection documented the visually observable condition of the modules. The summary is presented in Table 2. Accompanying pictures are shown in Figures 8–11. Generally, no major visually observable defects were seen on the front glass, backsheets, wires/connectors, the junction box, frame

and metallization. Some minor corrosion/discolouration at the edge of some cells was also observed (Figure 9).

Table 2. Visual inspection observations.

Component	Observation(s)
Front Glass	Front glass was smooth and dusty prior to cleaning with water; no damage or cracks were observed. Minor occurrence of bubbles were observable on the front side of the module (Figure 8).
Backsheet	Minor discoloration observable from front glass (Figure 8)—this might be due to moisture ingress. Generally was like new. No wavy texture was observed, no chalking, burn marks or other damage was visible.
Wires/Connectors	no embrittlement or burns was observed.
Junction Box	Intact and well-attached, no loss of adhesion was observed, Figure 9 (opened by authors during study).
Frame	Minor discoloration was observed; no corrosion was found; frame adhesive was not visible and showed no signs of degradation; the bottom section of the frame was soiled and had accumulated over the years. Figure 10
Metallization	Bus-bars and cell interconnects showed no burns, discoloration or corrosion. Figure 10
PV Cell	The cells were observed to be in good condition. Light discolouration (<5%) could be seen at the edge of some of the cells when the image is magnified.

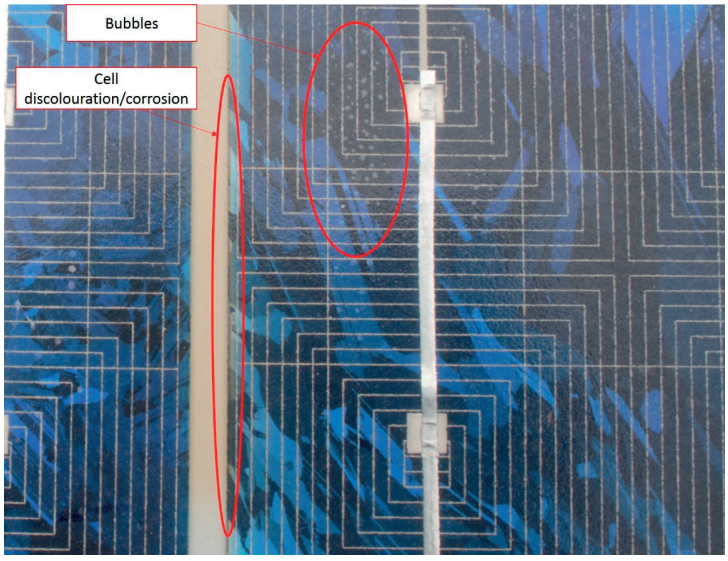

Figure 8. Minor discolouration of backsheet (Observable from front glass). Busbars and fingers in good condition.

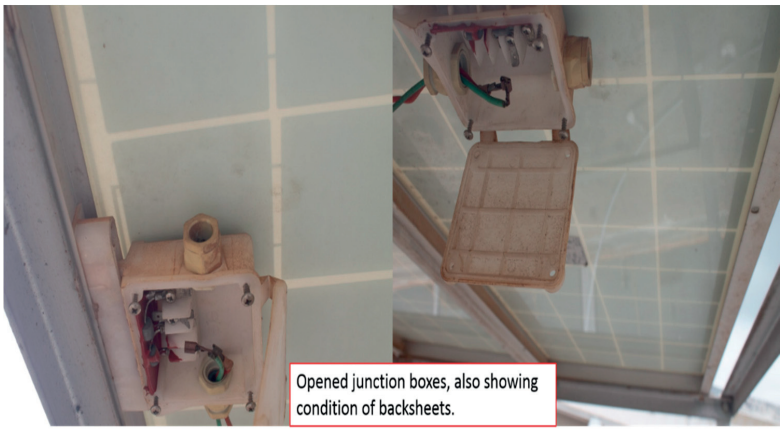

Figure 9. Junction box of modules, also showing backsheet.

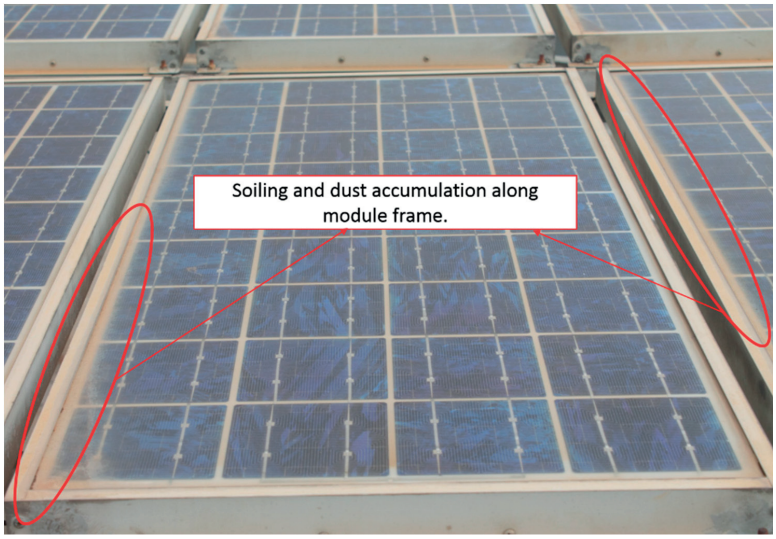

Figure 10. Soiling and dust accumulation along module frame.

3.2. Performance Measurements (I-V Curve)

Module temperatures during the measurements period ranged from 47.80 °C to 58.90 °C, while the irradiance conditions varied from 883 W/m^2 to 1020 W/m^2. The raw data, showing the different irradiance and temperature values are shown in Table A1 (Appendix A). For each module, the measurements were repeated 5 times. The values were standardized (to STC) using Equations (2)–(5). The key parameters, with their associated random errors are shown in Figures 11–13.

3.2.1. Peak Power

Overall on module-by-module basis, the power output had declined from 49.5 W to 32.2–39 W (with a median of 37.6 W) over the 19-year period of exposure (Figure 11). This represents a decline of 21.1%–35.0%, with a median of 24%. On an annual basis, the median degradation rate is 1.3%.

The advantage of using the median instead of the mean, is that, it minimizes the impact of outliers. Modules of this era (the 1990s) came with 10-year warranties; within which period 80% of the peak power was guaranteed [18]. This implied a maximum average annual degradation of 2% (see Figure 1).

Assuming a linear degradation rate for the modules, as suggested by [60], all the modules could be said to have met and exceeded warranty provisions. In addition, modules of the time came with tolerance of ±10% [18]; which implied that the peak power less 10%, (in this case 44.5 W) would still be within the purchase agreement. If this lower limit of the tolerance were used, 80% of peak power will translate to 35.6 W, in which case over 85% of the modules will still be operating above the minimum guaranteed output after 19 years of exposure. While some authors have defined module failure to mean an effect that degrades the module power, which is not reversed by normal operation or creates a safety issue [32], module life on the other hand, as noted by [30], does not lend itself to easy definition, as they could mean different things depending on the perspective. From a manufacturer's perspective, module life may be viewed in terms of financial liability period, whereas the user is not necessarily bound by this and may keep the module in service as long as it is safe, and meets or contributes to meeting their needs.

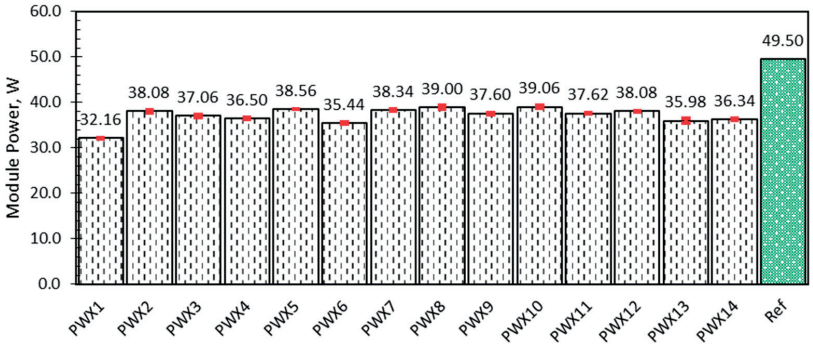

Figure 11. Peak power of modules at STC.

The coefficient of variation of the peak power of the 14 modules (computed as ratio of the population standard deviation to the mean) is 5%; indicating uniformity of ageing. Such uniformity of ageing has been viewed by authors such as Skoczek et al. [41] as an indicator of good quality control in the module manufacturing process. The power loss in module PWX1 is notably much higher than the remaining modules. Its power output had dropped to 32.2 W, much below the median value of 37.6 W; registering a decline of 35% compared with the median decline of 24% for the entire system. The nature of the I-V curve (discussed later in Section 3.2.4) may help in explaining the cause of the performance decline. Since module peak power is a function of short-circuit current, open-circuit voltage and fill factor; changes in power output must be explainable in terms of these parameters.

3.2.2. Short-Circuit Current

As shown in Figure 12, the short-circuit current of the modules declined from 3.1 A to between 2.74 A and 2.92 A, with a median value of 2.86 A. These represent, respectively declines of 5.8% to 11.7% and median of 7.9% over the 19-year period. On an annual basis, the median decline in the short-circuit current is 0.4%. Of particular note is module PWX6 (Figure 12), which showed a much sharper decline in short circuit current (0.6%/year). Bubble formation and delamination is suspected to be the cause of this observation. Overall, however, coefficient of variation was 2%. The short circuit current has a strong dependence on irradiance and hence a decline in short-circuit current could be due to optical transmission problems caused by factors such as module soiling, browning/yellowing of encapsulant and delamination which causes optical decoupling (mismatch of refractive indices).

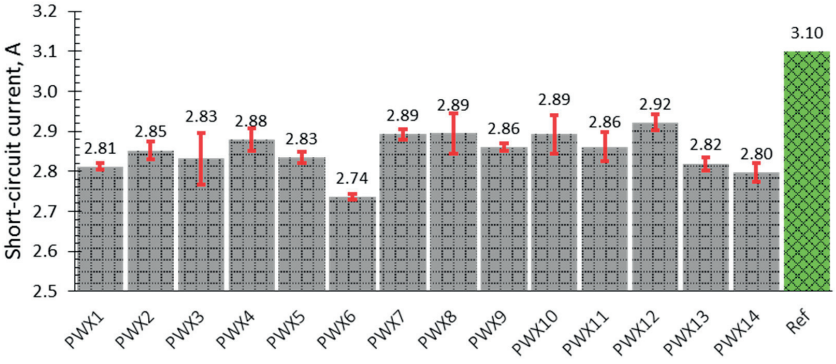

Figure 12. Short-circuit current of modules at STC.

3.2.3. Open-Circuit Voltage

The open-circuit voltage (V_{oc}) of the modules (Figure 13) ranged from a low of 20.4 V (PWX 14) to 20.8 V (PWX 5) and a median of 20.7 V. The decline from the nameplate rating of 21.6 V is 3.6% to 5.6% over the period with a median of 4.1%. The annual decline translates to 0.2% to 0.3% with median of 0.2%. The open-circuit voltage coefficient of variation is estimated as 1%. The annual degradation rate of the open circuit voltage is significantly less than the short-circuit current. Loss of V_{oc} usually attributed to degradation of the cells and shunting problems [43].

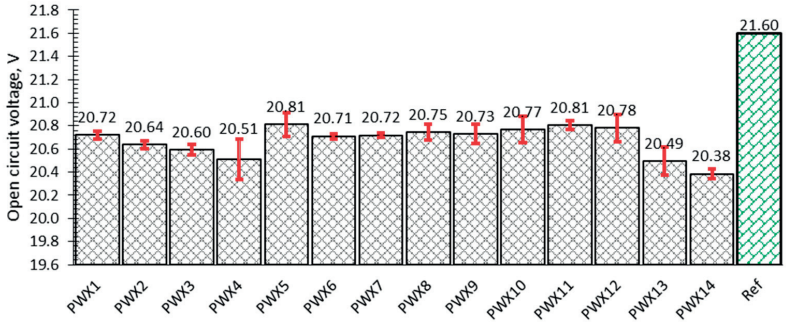

Figure 13. Open-circuit voltage of modules at STC.

3.2.4. Fill Factor

The fill factor of the modules (Figure 14) was in the range of 55% (PWX 1) to 65.2% (PWX 5). This represents a decline of 11.9% to 25.7% with a median of 14.3% over the period of exposure; compared with the original value of 74%. On an annual basis, this translates to 0.6%–1.4% and median of 0.8%. Even though the coefficient of variation of the fill factor of the modules is 4%, module PWX 1, exhibits markedly higher loss of fill factor compared with the rest of the modules. Figure 15, shows the I-V curves of the modules studied. The power loss of module PWX1 (Section 3.2.1), in particular, is traceable to fill factor loss. Loss of fill factor is generally attributed to increase in series resistance of the modules ([38,40]), arising from factors such as corrosion and thermo-mechanical fatigue of the solder bonds and interconnection. Indeed, the shape of the I-V curve arising from fill factor loss, as is the case with module PWX 1 (Figure 15), is reproducible from the 1-diode PV cell model by increasing the series resistance [61].

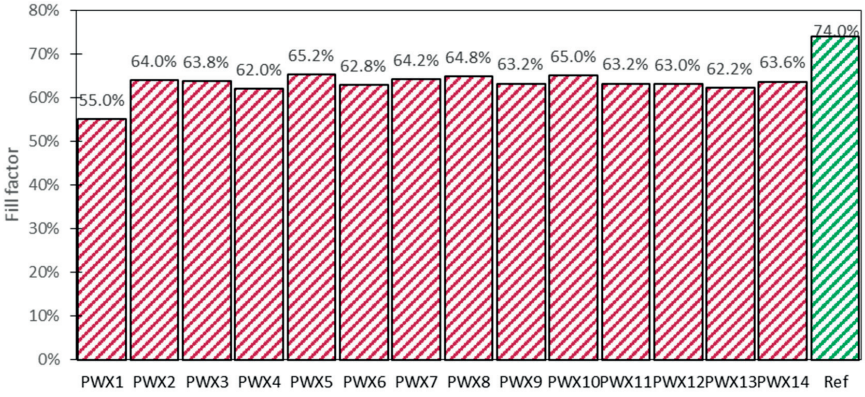

Figure 14. Fill factor of modules at STC.

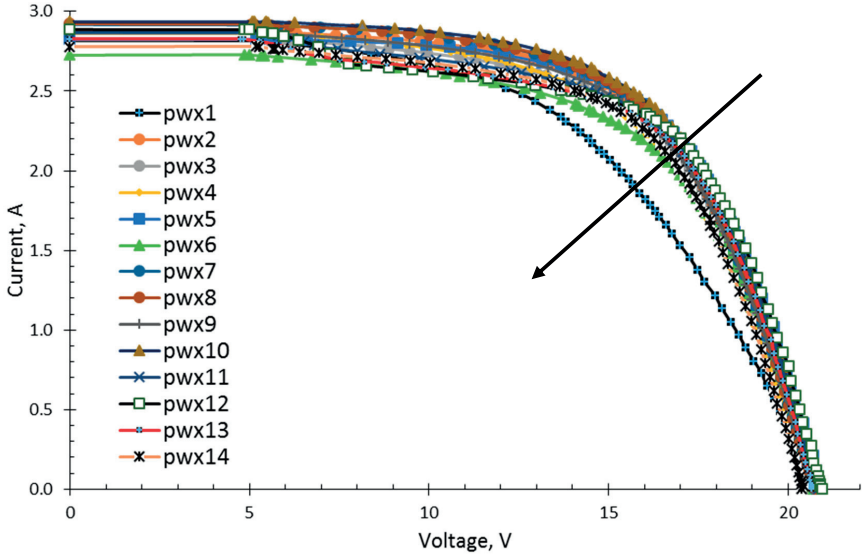

Figure 15. I-V curves of modules.

3.3. Thermal Imaging

Thermal imaging of the modules, forward-biased at I_{sc}, generally did not reveal much inhomogeneity in module surface temperature. Temperature distribution on the module surface showed difference of less than 5 °C for most modules, the exception being module PWX 1 which had cell temperature difference of about 10 °C at some sections of the module (Figure 16).

The general uniformity of temperature distribution and non-occurrence of hot-spots agrees with the point made earlier on the uniform ageing of the modules based on the co-efficient of variation of peak power and other key performance parameters.

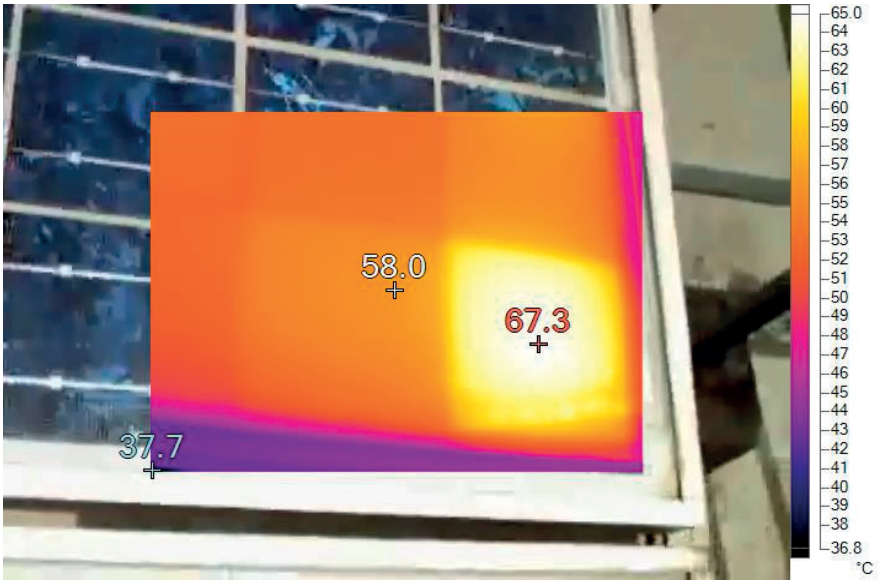

Figure 16. Surface temperature distribution—module PWX 1.

3.4. Accounting for Power Loss

As noted in Section 3.2.1, the peak power of the module is a function of short-circuit current, open-circuit voltage and fill factor. A plot of annual loss in peak power versus these parameters (I_{sc}, V_{oc} and FF) indicates that they are positively correlated (Figure 17).

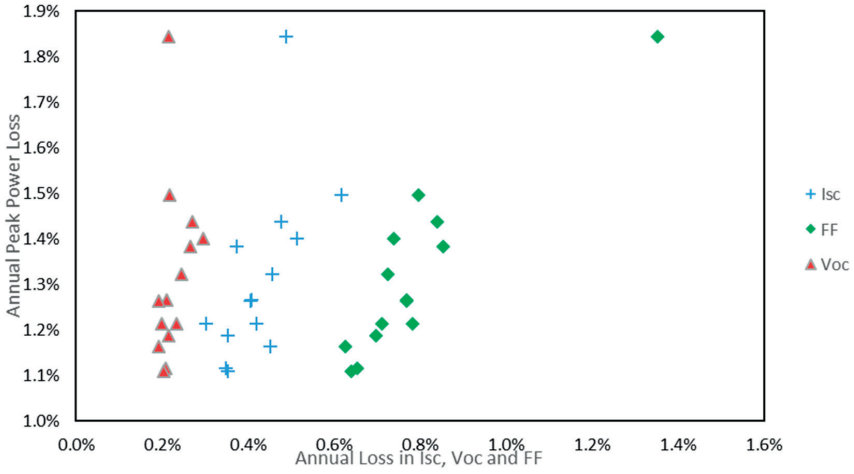

Figure 17. Annual power loss versus losses in I_{sc}, V_{oc} and FF.

A regression analysis indicates that I_{sc} and FF, together explain 97.5% of the variability in peak power (adjusted R-squared), Table 3. The loss of power is therefore attributable to losses in short-circuit current and fill factor, and to a lesser extent, on the open circuit voltage.

Table 3. Regression parameters (P_{nom} modelled by Isc and FF).

	Coefficients	Standard Error	t Stat	*p*-value
Intercept	0.002495398	0.000502317	4.96778	4.24×10^{-4}
I_{sc}	0.907725217	0.106155361	8.55091	3.45×10^{-6}
FF	0.869416269	0.050343898	17.26955	2.56×10^{-9}
Adjusted R Square: 0.975; F statistic: 256.2 Standard error: 0.000308;				

3.5. General Discussion

To put the current results into perspective, it is helpful to compare with similar studies. Jordan and Kurtz [18], conducting an analytical review of alomost 2000 reported degradation rates found in the literature, determined a median value of 0.61%/year degradation for multicrystalline Silicon modules installed prior to the year 2000, a total of 409 installations. In a more recent and updated work by an expanded team, Jordan et al. [60], based on a literature review, found that a median annual degradation rate of 0.6% (based on 683 observations) was reported for crystalline silicon modules installed in hot humid climates. Even though the median degradation (peak power) of the modules in this present study is higher (1.3%/year) than the median of reported in these reviews, it is consistent with rates reported of installations in the period 1990–2000, which were about 1%/year [60]. It should be noted also, that, the data used in the reviews do not have balanced geographical representation as acknowledged by the authors of the review. This geographical imbalance underscores the need for continuing effort to study systems that are installed in regions for which data is under-reported or not reported at all.

The dominance of short-circuit current and fill factor in driving the power loss of the modules is consistent with previous studies which have reported on this, including: Ndiaye et al. [38], Bandou et al. [37] and Jordan and Kurtz [18]. Bandou et al. [37] studied a 28-year old systen installed in the desert of Algeria and reported annual degradation of 1.22% in peak power, arising mainly from 0.78% in short circuit current and 0.56% in fill factor. Even though the study by Ndiaye et al. [38] had a rather short observation period (1.3–4 years), the results also confirm the dominance of short-circuit current and fill factor in power degradation.

4. Concluding Remarks

This study has examined the performance of fourteen (14) polysilicon modules, installed at KNUST in Kumasi Ghana, a hot and humid climate, after 19 years of outdoor exposure and under load. Systematic visual inspection, electrical characterization using current-voltage (I-V) tracing and thermal imaging were used to assess the modules. This paper concludes as follows:

- The physical condition of the modules was good, with no major visually observable defects on the front glass, back sheets, wires/connectors, junction box, frame and metallization. Some bubble on front side and minor discolouration at the edge of some cells were however observed upon magnification of images acquired.
- During the period of exposure (19 years), the median decline recorded in the performance parameters of the modules, compared with reference values were, respectively: *Peak Power (P_{nom})-24%, Short Circuit Current (I_{sc})-7.9%, Open Circuit Voltage (V_{oc})-4.1% and Fill Factor (FF)-14.3%*.
- On an annual basis, the median of the decline in performance parameters were: *P_{nom}-1.3%, I_{sc}-0.4%, V_{oc}-0.2% and FF-0.8%*.
- The module had a warranty of 10 years, with a tolerance of ±10%. At the median annual power degradation rate of 1.3%, the module has met and exceeded warranty expectations, even if the lower end of the tolerance was ignored.
- The reduction in nominal power is dominated by reduction in fill factor and short circuit current.

To contribute to filling the data gap on long-term PV module performance degradation in Ghana, future work will study modules installed in various micro-climatic zones of Ghana.

Acknowledgments: David A Quansah is grateful to the Quota Scholarship Programme of the Norwegian Government for sponsoring his Doctoral studies at NMBU Norway. He is also grateful to his employer, the Kwame Nkrumah University of Science and Technology (KNUST) for granting him study leave and equipment support. The authors are grateful to the Provost of the College of Engineering at KNUST for providing financial assistance towards data collection, and also to Research Assistants at The Brew-Hammond Energy Centre (Jacob and Henry) for their support during the measurements period.

Author Contributions: David A. Quansah, Muyiwa S Adaramola and G Takyi conceived and designed the experiments and developed the outline of the paper. David A. Quansah (with assistance of Isaac A. Edwin) conducted the measurements. Isaac A. Edwin contributed to the system description and provided the background to the installation. David A. Quansah did the analysis of the data and generated the first draft of the manuscript. All co-authors contributed review comments to the manuscript.

Conflicts of Interest: The authors declare no conflict of interest.

Appendix A

Table A1. Measured performance data at various irradiance and temperature (irradiance nearest 1000 W/m^2).

Module ID	T mod, °C	G, W/m^2	I_{sc} [A]	V_{oc} [V]	Impp [A]	Umpp [V]	P [W]	FF
PWX1	56.70	970.00	2.73	18.33	2.18	11.86	25.80	0.51
PWX2	58.80	937.00	2.69	18.14	2.25	13.34	30.00	0.61
PWX3	58.90	941.00	2.67	18.02	2.15	13.53	29.10	0.60
PWX4	58.90	949.00	2.72	18.10	2.25	12.83	28.80	0.59
PWX5	54.10	997.00	2.83	18.73	2.39	13.88	33.20	0.63
PWX6	50.10	1014.00	2.76	18.84	2.26	13.91	31.40	0.60
PWX7	51.10	958.00	2.79	18.73	2.30	14.01	32.20	0.61
PWX8	51.40	958.00	2.81	18.73	2.37	13.61	32.20	0.61
PWX9	57.40	960.00	2.74	18.27	2.22	13.74	30.40	0.61
PWX10	51.50	883.00	2.59	18.73	2.14	14.01	30.00	0.62
PWX11	57.30	964.00	2.76	18.42	2.25	13.67	30.70	0.60
PWX12	49.10	917.00	2.65	19.03	2.06	14.87	30.60	0.61
PWX13	47.80	962.00	2.71	18.90	2.22	14.28	31.70	0.62
PWX14	55.40	1020.00	2.81	18.19	2.38	13.46	32.00	0.63

References

1. IEA. *Projected Costs of Generating Electricity 2015 Edition*; IEA: Paris, France, 2015.
2. IEA. *Technology Roadmap: Solar Photovoltaic Energy 2014 edition*; OECD/IEA: Paris, France, 2014.
3. IEA. *World Energy Outlook*; OECD/IEA: Paris, France, 2013.
4. IRENA. *Africa 2030: Roadmap for a Renewable Energy Future*; IRENA: Masdar City, United Arab Emirates, 2015.
5. IRENA. *Solar PV in Africa: Costs and Markets*; IRENA: Masdar City, United Arab Emirates, 2016.
6. REN21. *ECOWAS Renewable Energy and Energy Efficiency Status Report*; ECREEE/UNIDO/REN21: Paris, France, 2014.
7. REN21. *Renewables 2015 Global Status Report*; REN21 Secretariat: Paris, France, 2015.
8. REN21. *Renewables 2016 Global Status Report*; REN21 Secretariat: Paris, France, 2016.
9. Fraunhofer ISE. *Photovoltaics Report*; Fraunhofer ISE: Freiburg, Germany, 2015.
10. NREL. *Best Research Cell Efficiencies*; NREL: Golden, CO, USA, 2016.
11. Yoshikawa, K.; Kawasaki, H.; Yoshida, W.; Irie, T.; Konishi, K.; Nakano, K.; Uto, T.; Adachi, D.; Kanematsu, M.; Uzu, H.; et al. Silicon heterojunction solar cell with interdigitated back contacts for a photoconversion efficiency over 26%. *Nat. Energy* **2017**, *2*, 17032. [CrossRef]
12. Solar Cell Efficiency Detailed Balance. Available online: http://www.pveducation.org/pvcdrom/detailed-balance (accessed on 16 May 2017).
13. Shockley, W.; Queisser, H.J. Detailed Balance Limit of Efficiency of p-n Junction Solar Cells. *J. Appl. Phys.* **1961**, *32*, 510. [CrossRef]
14. ITRPV/VDMA. *International Technology Roadmap for Photovoltaic 2015 Results*; ITRPV/VDMA: Frankfurt, Germany, 2016.

15. Yang, G. *Life Cycle Reliability Engineering*; John Wiley & Sons: Hoboken, NJ, USA, 2007.
16. ReliaSoft Corporation. About Reliability Engineering. 2016. Available online: http://www.weibull.com/basics/reliability.htm. (accessed on 18 May 2017).
17. Verma, A.K.; Ajit, S.; Karanki, D.R. *Reliability and Safety Engineering*; Springer: London, UK, 2016.
18. Jordan, D.C.; Kurtz, S.R. Photovoltaic Degradation Rates—an Analytical Review. *Prog. Photovolt. Res. Appl.* **2013**, *21*, 12–29. [CrossRef]
19. EnergySage Inc. *What to Know About a Solar Panel Warranty*; EnergySage Inc.: Boston, MA, USA, 2015.
20. REC Solar. 25-year Linear Power Output Warranty. Available online: http://www.recgroup.com/sites/default/files/documents/rec_fact_sheet_warranty_web_en_20130719.pdf (accessed on 16 May 2017).
21. King, D.L.; Quintana, M.A.; Kratochvil, J.A.; Ellibee, D.E.; Hansen, B.R. Photovoltaic module performance and durability following long-term field exposure. *AIP Conf. Proc.* **1999**, *462*, 565–571.
22. Srinivasan, S. Solar photovoltaics: Oligopsony, non-market decision-making and the paradoxical persistence of unprofitability. *Int. J. Green Econ.* **2013**, *7*, 116–147. [CrossRef]
23. GTM Research. Rest in Peace: The List of Deceased Solar Companies. Available online: http://www.greentechmedia.com/articles/read/Rest-in-Peace-The-List-of-Deceased-Solar-Companies?utm_source=Daily&utm_medium=Headline&utm_campaign=GTMDaily (accessed 18 May 2017).
24. CivicSolar Inc. Canadian Solar Warranty Insurance. Available online: http://investors.canadiansolar.com/phoenix.zhtml?c=196781&p=irol-newsArticle&ID=1695334 (accessed on 18 May 2017).
25. CSUN. 25-Year Insurance Backed Warranty. Available online: http://www.csun-solar.com/fileadmin/dateiablage/documents/PowerGuard_CSUN_2014_Flyer.pdf (accessed on 18 May 2017).
26. Trina Solar. 25 Year Insurance Backed Warranty. Available online: https://es-media-prod.s3.amazonaws.com/media/u/bad/9e9/d9b/4a377fac554a5266604e7b20285d4e78/TrinaSolar_Warranty.pdf (accessed on 18 May 2017).
27. Canadian Solar (USA) Inc. PV Module Warranty and Warranty Insurance Comparisons: A Cornerstone of Bankability. Available online: http://www.solarsouthwestflorida.com/wp-content/uploads/2012/01/PV-Module-Warranty-and-Warranty-Insurance-Comparisons-White-Paper-Sept.-2011.pdf (accessed on 18 May 2017).
28. IEC. Crystalline Silicon Terrestrial Photovoltaic (PV) Modules—Design Qualification and Type Approval. Available online: https://webstore.iec.ch/publication/4928 (accessed on 18 May 2017).
29. IEC. *Thin-Film Terrestrial Photovoltaic (PV) Modules—Design Qualification and Type Approval*; IEC: Geneva, Switzerland, 2008.
30. Osterwald, C.R.; McMahon, T.J. History of Accelerated and Qualification Testing of Terrestrial Photovoltaic Modules: A Literature Review. *Prog. Photovolt. Res. Appl.* **2009**, *17*, 11–33. [CrossRef]
31. Zielnik, A.F.; Dumbleton, D.P. Photovoltaic Module Weather Durability & Reliability—Will my module last outdoors? Available online: https://us.sunpower.com/sites/sunpower/files/media-library/white-papers/wp-atlas-25-plus-photovoltaic-module-weather-durability-reliability.pdf (accessed on 16 May 2017).
32. IEA. *Review of Failures of Photovoltaic Modules*; OECD/IEA: Paris, France, 2014.
33. Fraunhofer ISE. *Photovoltaics Report*; Fraunhofer ISE: Freiburg, Germany, 2016.
34. ITRPV/VDMA. *International Technology Roadmap for Photovoltaic*; ITRPV/VDMA: Frankfurt, Germany, 2015.
35. Rudolph, D.; Olibet, S.; Hoornstra, J.; Weeber, A.; Cabrera, E.; Carr, A.; Koppes, M.; Kopecek, R. Replacement of silver in silicon solar cell metallization pastes containing a highly reactive glass frit: Is it possible? *Energy Proced.* **2013**, *43*, 44–53. [CrossRef]
36. Lorenzo, E.; Zilles, R.; Moretón, R.; Gómez, T.; de Olcoz, A.M. Performance analysis of a 7-kW crystalline silicon generator after 17 years of operation in Madrid. *Prog. Photovolt. Res. Appl.* **2014**, *22*, 1273–1279. [CrossRef]
37. Bandou, F.; Arab, A.H.; Belkaid, M.S.; Logerais, P.-O.; Riou, O.; Charki, A. Evaluation performance of photovoltaic modules after a long time operation in Saharan environment. *Int. J. Hydrog. Energy* **2015**, *40*, 13839–13848. [CrossRef]
38. Ndiaye, A.; Kébé, C.M.F.; Charki, A.; Ndiaye, P.A.; Sambou, V.; Kobi, A. Degradation evaluation of crystalline-silicon photovoltaic modules after a few operation years in a tropical environment. *Sol. Energy* **2014**, *103*, 70–77. [CrossRef]

39. Quintana, M.A.; King, D.L.; McMahon, T.J.; Osterwald, C.R. Commonly Observed Degradation in Field-Aged Photovoltaic Modules. Proceedings of Conference Record of the Twenty-Ninth IEEE Photovoltaic Specialists Conference, New Orleans, LA, USA, 19–24 May 2002; pp. 1436–1439.
40. Skoczek, A. Long-term performance of photovoltaic modules. Available online: http://www.solar-academy.com/menuis/longtermperformanceofpvsystems032725.pdf (accessed on 16 May 2017).
41. Skoczek, A.; Sample, T.; Dunlop, E.D. The results of performance measurements of field-aged crystalline silicon photovoltaic modules. *Prog. Photovolt. Res. Appl.* **2009**, *17*, 227–240. [CrossRef]
42. Kahoul, N.; Houabes, M.; Sadok, M. Assessing the early degradation of photovoltaic modules performance in the saharan region. *Energy Convers. Manag.* **2014**, *82*, 320–326. [CrossRef]
43. Ferrara, C.; Philipp, D. Why Do PV Modules Fail? *Energy Proced.* **2012**, *15*, 379–387. [CrossRef]
44. Jordan, D.C.; Wohlgemuth, J.H.; Kurtz, S.R. Technology and Climate Trends in PV Module Degradation. Proceedings of 27th European Photovoltaic Solar Energy Conference and Exhibition, Frankfurt, Germany, 24–28 September 2012.
45. Phinikarides, A.; Kindyni, N.; Makrides, G.; Georghiou, G.E. Review of photovoltaic degradation rate methodologies. *Renew. Sustain. Energy Rev.* **2014**, *40*, 143–152. [CrossRef]
46. Peel, M.C.; Finlayson, B.L.; Mcmahon, T.A. Updated world map of the köppen-geiger climate classification. *Hydrol. Earth Syst. Sci. Discuss.* **2007**, *4*, 439–473. [CrossRef]
47. FAO. Ghana—Country Pasture/Forage Resource Profiles. Available online: http://www.fao.org/ag/agp/agpc/doc/counprof/ghana/Ghana.htm#3.%20CLIMATE%20AND%20AGRO-ECOLOGICAL%20ZONES (accessed on 21 November 2016).
48. All-India Survey of Photovoltaic Module Degradation: 2013. Available online: http://www.ncpre.iitb.ac.in/research/pdf/All_India_Survey_of_Photovoltaic_Module_Degradation_2013.pdf (accessed on 16 May 2017).
49. RETScreen International. RETScreen Clean Energy Project Analysis Software (Version 4.1) Climate Database. Available online: http://www.nrcan.gc.ca/energy/software-tools/7465 (accessed on 18 May 2017).
50. Nkrumah, F.; Klutse, N.A.B.; Adukpo, D.C.; Owusu, K.; Quagraine, K.A.; Owusu, A.; Gutowski, W. Rainfall variability over ghana: Model versus rain gauge observation. *Int. J. Geosci.* **2014**, *5*, 11. [CrossRef]
51. *PVsyst SA*; Version 5.74; PVSyst Photovoltaic Software: Satigny, Switzerland, 2012.
52. Field Applications for I-V Curve Tracers. Available online: http://solarprofessional.com/articles/design-installation/field-applications-for-i-v-curve-tracers (accessed on 16 May 2017).
53. Current-Voltage Translation Procedure for PV Generators in the German 1,000 Roofs-Programme. Available online: http://citeseerx.ist.psu.edu/viewdoc/download?doi=10.1.1.475.4370&rep=rep1&type=pdf (accessed on 16 May 2017).
54. Zaaiman, W. Solar Irradiance and Photovoltaic Measurements from Solar Radiation to PV Arrays. Proceedings of AFRETEP 3rd Regional Workshop, Cape Town, South Africa, 20–24 February 2012.
55. IEC. *IEC 60891:2009 Photovoltaic devices—Procedures for Temperature and Irradiance Corrections to Measured I-V Characteristics*; IEC: Geneva, Switzerland, 2009.
56. Outdoor PV Module Degradation of Current-Voltage Parameters. 2012. Available online: http://www.nrel.gov/docs/fy12osti/53713.pdf (accessed on 16 May 2017).
57. Tsuno, Y.; Hishikawa, Y.; Kurokawa, K. Modeling I-V Curves of PV Modules Using Interpolation/Extrapolation. *Sol. Energy Mater. Sol. Cell.* **2009**, *93*, 1070–1073. [CrossRef]
58. Marion, B. A method for modeling the current–voltage curve of a PV module for outdoor conditions. *Prog. Photovolt. Res. Appl.* **2002**, *10*, 205–214. [CrossRef]
59. Anderson, J.A. *Photovoltaic Translation Equations: A New Approach*; NREL: Golden, CO, USA, 1996.
60. Jordan, D.C.; Kurtz, S.R.; VanSant, K.; Newmiller, J. Compendium of photovoltaic degradation rates. *Prog. Photovolt. Res. Appl.* **2016**, *24*, 978–989. [CrossRef]
61. Effect of parasitic Resistances- Series Resistance. Available online: http://www.pveducation.org/pvcdrom/series-resistance (accessed on 5 December 2016).

Paper 2

INTERNATIONAL JOURNAL OF HYDROGEN ENERGY 43 (2018) 3092–3109

Available online at www.sciencedirect.com

ScienceDirect

journal homepage: www.elsevier.com/locate/he

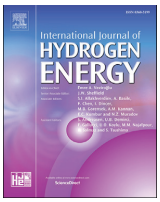

Comparative study of performance degradation in poly- and mono-crystalline-Si solar PV modules deployed in different applications

David A. Quansah [a,b,c,*], *Muyiwa S. Adaramola* [a]

[a] *Renewable Energy Group, Faculty of Environmental Sciences and Natural Resource Management, Norwegian University of Life Sciences (NMBU), 1433 Ås, Norway*

[b] *Department of Mechanical Engineering, Kwame Nkrumah University of Science and Technology (KNUST), Kumasi, Ghana*

[c] *The Brew-Hammond Energy Centre, Kwame Nkrumah University of Science and Technology (KNUST), Kumasi, Ghana*

ARTICLE INFO

Article history:
Received 11 October 2017
Received in revised form
4 December 2017
Accepted 22 December 2017

Keywords:
Solar module degradation
Field performance
Ghana
Fill factor
Crystalline silicon
Defects

ABSTRACT

Data on long-term performance and degradation of field-aged solar photovoltaic modules is widely recognized as necessary for continued technological improvement and market confidence. It is also important that such research should cover various geographical regions of the globe. This paper presents a study on twenty-nine (29) crystalline silicon modules deployed in grid-connected, battery-charging and water-pumping applications. The modules, installed at six different locations in Ghana were aged between 6 and 32 years. Peak power (P_{max}) losses ranged from 0.8%/year – 6.5%/year. The P_{max} losses were dominated by losses in fill factor (FF) and short-circuit current (I_{sc}). Visually observable defects are also reported.

Introduction

Background

Growth in the deployment of Solar Photovoltaic (PV) technology over the past three to four decades is well-documented. Watts et al. [1] reported industry growth as rising from 3.5 MW to 23.2 MW in annual shipments between 1980 and early 1985. Today, annual demand is estimated at 75 GW (75000 MW) with cumulative installed capacity of over 300 GW [2]. To put this into perspective, the annual demand in 1985 as a percentage of new installations in 2016 is only 0.03% (30 years down the lane). Nevertheless, crucial lessons from these nascent stages have contributed substantially to market development. The strength of the growth is also perceived when one considers the fact that over the past decade, new

* *Corresponding author*. Faculty of Environmental Sciences and Natural Resource Management, Norwegian University of Life Sciences, Ås, Norway.
E-mail addresses: daquansah.coe@knust.edu.gh (D.A. Quansah), muyiwa.adaramola@nmbu.no (M.S. Adaramola).
https://doi.org/10.1016/j.ijhydene.2017.12.156
0360-3199/

additions of installed capacity in each year have constituted a minimum of about 22% of the cumulative installed capacity estimated for that year (Table 1), with an average of 31%. In 2011, new additions constituted almost 43% of cumulative installations at the end of that year, and 75% of cumulative installations which had been deployed from all previous years put together.

This growth has been spurred by a number of inter-related factors such as improvements in technology, government energy policy, international climate initiatives and changing electricity consumer preferences. Continued research and development (R&D) efforts have led to reduced material usage per peak watt, an increase in cell and module efficiencies, and development of new solar cell materials [3]. Efficiency improvements in turn have multiple co-benefits - commercial, technical and ecological benefits. Increase in solar-to-electric conversion efficiency for example, could lead to less heating of the solar cells. It also implies less space requirement for a unit capacity installed. For large megawatt-scale power plants, this translates into reduced land requirements. Doubling of module efficiencies from 10% to over 20% (as currently pertains on the market) leads to halving of space/land requirements for a given installed capacity.

In Ghana, the literature traces the inception of Solar PV technology utilization to early 1980s, mainly through non-governmental entities such as religious missions [4]. It was however followed soon by state agencies such as the Cocoa Marketing Board (now Ghana Cocoa Board) for powering radio communications at its depots, the Post and Telecommunications Corporation for powering repeater stations, and later by government programmes that sought to deploy them in sectors such as health and water supply [5–7]. The number of installations in the country was estimated at 335 (160 kWp) in 1991 [5], and increased to 722 (361 kWp) by the mid-1990s [8]. At the close of 2016, official statistics indicated that installed capacity stood at 22.6 MW, which constituted less than 1% of the country's total installed electricity generation capacity of 3794.60 MW [9]. Individual and small distributed solar systems which were not directly funded by government, are usually not captured in the official statistics, even though anecdotal evidence suggests that they are significant. Earlier in 2015, the Government of Ghana in response to a power crisis rolled out a rooftop solar programme with the aim of saving 200 MW of peak power [10].

Table 1 – Evolution of solar PV module installations worldwide.

Year	Cumm. (GW)	New add (GW)	% New add
2016	303	75	24.8%
2015	228	51	22.4%
2014	177	40	22.6%
2013	137	38	27.7%
2012	99	29	29.3%
2011	70	30	42.9%
2010	40	17	42.5%
2009	23	8	34.8%
2008	16	6.6	41.3%
2007	8	2.5	31.3%
2006	6	1.4	23.3%

Like the rest of the world, Ghana hopes to maximize the benefits of a transition to a diversified and low-carbon energy system, and has over the years implemented legislation and other initiatives to promote renewable energy. The Renewable Energy Law was passed in 2011 to create an enabling environment for investment in the sector [11]. Following this, feed-in tariffs were announced by the country's Public Utilities Regulatory Commission (PURC) [12]. Additional legislation on net-metering and distributed generation were also developed by the Energy Commission [13,14]. By mid-2016, provisional licenses totaling more than 3000 MW in combined capacity had been issued for utility-scale solar PV projects [15]. Because of concerns regarding grid-stability issues, the PURC in 2014 announced some caps on allowable solar and wind power in the National Interconnected Transmission System (NITS) [16].

As Ghana, with its significant solar resource endowment (4–6/kWh/m^2/day) seeks to expand and upscale the deployment of the solar PV technologies, it is important to have some understanding of how systems already installed have performed on a long-term basis, and how they have degraded over time. An understanding of degradation and failure mechanisms, and how solar PV modules interact with various environmental stresses such as humidity, UV radiation, thermal cycling, etc., is beneficial to all actors along the solar value chain. For example, module manufacturers and research institutes involved in module development and testing are interested in understanding how module design could be improved based on failures that occur in operation on the field. Accredited testing agencies and international/national agencies involved in developing qualification test series want to be sure that failures that occur on the field could be detected by the test sequences that are in place. Hence, reporting on failure modes could help in the revision of tests and standards. Similarly, as depicted in Fig. 1, entities involved in manufacturing, market entry and field deployment can use field data for various purposes that help to improve the technology and enhance market acceptance.

Previous work

The importance of long-term climate-specific Solar PV performance loss and degradation data is widely acknowledged by industry and research community [17–22]. In spite of this acknowledgement, studies in Africa have been scant in the open literature. This geographical under-representation of available data becomes evident when one considers compilations of field studies undertaken by Jordan and Kurtz [23], Jordan et al. [24] and Phinikarides et al. [25].

The foregoing notwithstanding, some contributions have been made. Notable among these are the works which have come from Refs. [26–33]. The studies were conducted in Senegal, Algeria, Libya, South Africa and Kenya on crystalline silicon and amorphous silicon thin films (including multi-junction cells). The reported peak power (P_{max}) degradation rates are in the range of 0.22%–2.99%/year for crystalline silicon based on exposure period of 1.3–30 years. For thin films, a P_{max} degradation rate of 1%/year has been reported by Jacobson et al. [29] based on 0.9–5.9 years of exposure of amorphous silicon (a-Si) in Kenya. Radue and van Dyk [27,32] studied a-Si and CIGS modules exposed for up to 1.5 years in

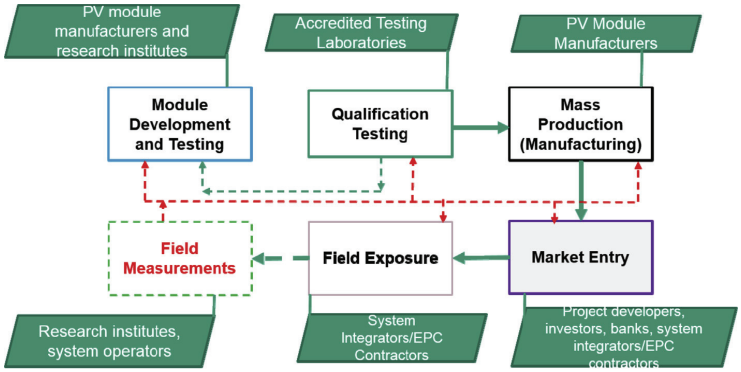

Fig. 1 – Various actors along the solar PV value chain.

South Africa and observed P_{max} decline as high as 45% in the period. The large drop in performance for the thin films was attributed to initial Light Induced Degradation (LID) [32]. An observation that one readily makes from these studies, is the rather short periods field-exposure of many of the modules [31], and in some instances very small wattage modules (e.g. 10 Wp) [29]. Degradation studies have also been conducted on new materials, as in the case of [34]. This was, however, undertaken on an experimental basis and under carefully controlled conditions of darkness and illumination and is, therefore, not considered further.

In Ghana, early contribution to this field was made by Adanu [6], who in 1994 published on the performance of a 268 W_p panel which had been monitored between 1987 and 1991. To the best of our knowledge, this was a seminal work on this subject matter in Ghana, and presented results on the performance of the mono-crystalline silicon modules. After 4 years of exposure, "several bubbles" were visible in the encapsulant, although this was not considered to have had adverse effect on the performance [6]. In a more recent work [35], also examined seasonal variation of operating temperature of silicon solar modules in the southern part of Ghana and observed that module operating temperatures sometimes exceeded 70 °C. The study however did not report the actual performance of the modules or performance loss over time. Comparative study of the technical performance of five different Solar PV module technologies installed in microclimate of Kumasi in Ghana using one-year data was presented by Ref. [36]. The technologies studied were mono-crystalline silicon (mc-Si), polycrystalline silicon (pc-Si), amorphous silicon (a-Si), Copper Indium disulfide (CIS) thin-film and heterojunction with intrinsic thin layer (HIT). Performance ratios reported were mc-Si: 67.9%, pc-Si: 76.3%, a-Si: 75.8%, CIS: 52.3% and HIT: 74.8%. Similar to the earlier observation by Ref. [35], module temperatures in excess of 70 °C were also observed in the study by Ref. [36]. Furthermore, performance degradation of 19-year-old field-exposed poly-crystalline silicon (pc-Si) modules installed in Kumasi (Ghana) was studied by Ref. [37] and also found bubble formation and delamination, as well as minor corrosion of the interconnects. A median P_{max} degradation rate of 1.3%/year was reported.

Against this background, the objective of this paper is to contribute to the body of knowledge that explores the causes of field failures and long-term performance degradation of Solar PVs and to provide data from an under-reported geographical region of the world. This work seeks to extend the study by Ref. [37] and presents assessment on twenty-nine (29) modules from six (6) locations in different micro-climatic zones of Ghana. It is hoped that this information will be useful to various actors involved in the solar PV chain, ranging from cell development to field deployment (Fig. 1).

Methodology

Description of installations and locations

In this study, twenty-nine (29) modules comprising polycrystalline (pc-Si) and monocrystalline (mc-Si) silicon technologies installed at six (6) locations in Ghana and covering four (4) administrative regions of the country (Greater Accra Region, Central Region, Eastern Region and Ashanti Region) are assessed. The applications in which they were deployed are: grid-connected systems (2), solar water pumping systems (2) and stand-alone battery-based systems (2) (Table 2). The age of the systems range from 6 to 32 years. The two grid-connected systems are installed on the premises of the Ministry of Energy (MoEN) in Accra (lat. 5.5514°, long. 0.2007°) and on the roof of the College of Engineering at the Kwame Nkrumah University of Science and Technology (KNUST) in Kumasi (lat. 6.67°, long. 1.57°). Two water-pumping systems installed by the Community Water and Sanitation Agency (CWSA) of Ghana were studied; the first is located at the headquarters of the Agency (labelled CWSA1) and the second (labelled CWSA2) is located at Mataheko, a community in the Ga South Municipal Assembly of the Greater Accra administrative Region. The final category, the off-grid battery-charging systems belong to the Ghana Cocoa Board and were part of installations that date back to the mid-1980s and are used to power radio communication systems [4,8]. The Cocoa Board solar PV installations captured in this study are located at Akim Oda (lat. 5.9142°, long. 0.9862°) in the Eastern Region

Table 2 – Location of installations and other characteristics.

Location	Geo-Coord.	Altitude (m)	Admin. region	Application	Technology	Year of inst.
Accra, Ministry of Energy (MoEN)	5.5514°, 0.2007°	54	Greater Accra	Grid-connected	mc-Si	2001
Kumasi (KNUST)	6.6735°, 1.5653°	268	Ashanti	Grid-connected	pc-Si	2008
Accra (CWSA1)	5.6253°, 0.1837°	84	Greater Accra	Water pumping	mc-Si	2006
Accra (CWSA2)	5.6264°, 0.4002°	40	Greater Accra	Water pumping	mc-Si	2011
Akim Oda	5.9142°, 0.9862°	164	Eastern	Stand-alone	pc-Si	2008
Breman Asikuma	5.5807°, 0.9929°	74	Central	Stand-alone	pc-Si	1985

and Breman Asikuma (lat. 5.5807°, long. 0.9929°) in the Central Region. The particular PV technologies deployed, year of installation, geographical coordinates and altitude of locations are presented in Table 2.

The characteristics of the modules at the various locations are presented in Table 3. The modules studied were part of installations with installed capacities ranging from 150 Wp to 3500 Wp; while the modules themselves have rated capacity ranging from 36 Wp to 170 Wp, with tolerances of ±3% to ±10%. The modules were mounted in various modes: Rooftop Free Standing (RTFS), Rooftop Roof-flushed (RTRF) and Ground Mounted (GM) – as shown in Figs. 2 and 3. Module mounting orientations were in the directions: North-South (N-S), East-West (E-W) and West-East (W-E). All the modules were inclined at angles of approximately 15°, except for the installation at Akim Oda, which was roof-flushed and installed at 6°. Module surfaces were cleaned with water prior to measurements, in order to eliminate the effect of dust and dirt accumulation. For purposes of easy identification, the modules were code-named ISF1 – ISF35 for the Isofoton modules at the Ministry of Energy (Fig. 2a) and SSKS1 – SSKS6 for the Schott Solar modules installed in Kumasi (Fig. 2b). The Cocoa Board installations were labelled CCBO1 – CCBO2 for the installation at Akim Oda and CCBA1 – CCBA4 for the modules at Breman Asikuma (Fig. 3a and b). Similarly, the solar water pumping installations were labelled CWSA1 and CWSA2 (Fig. 4). Baseline data on the modules were obtained from the nameplate where available, and complemented with data from the PV module database of the design software PVSYST® [38].

Nameplate data on the Baodin Solar modules (CCBO1 and CCBO2) had some inconsistencies. While the nameplate rating of this module stated maximum power (P_{max}) of 60 Wp, the current and voltage at maximum power suggested that it should rather be 50 Wp (Fig. 5a). These modules also did not have any certification labels, and so were the Isofoton modules (Fig. 5b) and Holec HH modules. The Holec HH modules actually predate qualification standards such as IEC 61215, which was only in draft form by 1989 [39]. There were however some European regulations such as Specification 101 and Specification 501 which had earlier been issued by the Ispra Joint Research Centre by 1981 by the Commission of European Communities (CEC) [40].

Climatic conditions

A solar PV module may be viewed as composite system comprising polymers, metals, glass and a semi-conductor. These materials make up about seven (7) key components that are common to most modules, namely: front cover, frame, encapsulation, solar cell, metallization, back sheet and junction box [41]. These materials and components are subject to various climatic and operational stresses, which include humidity and high/low temperatures, ultra-violet (UV) radiation, high-voltage bias and thermal cycling due to temperature changes [42]. Depending on the location of the installation [41] additional stress factors include salinity (along coastlines), dust and sand storms, and gases from industries and vehicular transport. These stress factors have different and varying impact on the modules. For example, high/low temperatures and associated temperature changes result in thermo-mechanical fatigue of various components of the PV modules, particularly the solder bonds and cell interconnects which result in increased series resistance and can lead to failure [43]. Humidity and moisture intrusion facilitate the onset of corrosion of the metallization and interconnects. The risk of corrosion is further enhanced by salinity levels and the presence of other gaseous compounds in the atmosphere [41]. The presence of moisture (and heat) within the module structure also reduces adhesional strength and results in defects such as delamination, which affects both optical transmission and thermal conductivity of the module. In practice, the various environmental and operational stresses act in combination and in an interactive manner.

Long-term air temperature and relative humidity data for the locations were retrieved from climate observation database of the US space agency NASA [44] and are shown in Fig. 6. For the Kumasi location, maximum monthly temperatures range from 26.7 °C (in July) to 30.1 °C (in January/February),

Table 3 – Module characteristics and related data.

Location	Inst. Size W_p	Module name	Manufacturer	P_{max} W_p	Tol. P_{max}	I_{mpp} A	V_{mpp} V	I_{sc} A	V_{oc} V	Orient
Accra (MoEN)	3500	Isofoton I-100	Isofoton, Spain	100	±10%	5.74	17.4	6.54	21.6	N-S
CWSA1	150	aleo 150-M5i	Aleo Solar GmbH, Germany	150	±3%	4.35	34.89	4.93	43.25	E-W
CWSA2	165	aleo S_03	Aleo Solar GmbH	165	±3%	4.64	35.8	5.1	43.5	W-E
Kumasi (KNUST)	2040	Schott Poly 170	Schott Solar, Germany	170	±4%	4.78	35.5	5.3	44.0	N-S
Akim Oda	300	Baodin Solar	TT Baodin Group, China	50	NA	2.9	17.2	3.2	21.6	E-W
Breman Asikuma	216	HS.40.1 N	HOLEC HH, Netherlands	36	±10%	2.1	17	2.3	22.0	E-W

Fig. 2 – Pictures of installations: (a) MoEn grid-connected system and (b) KNUST grid-connected system.

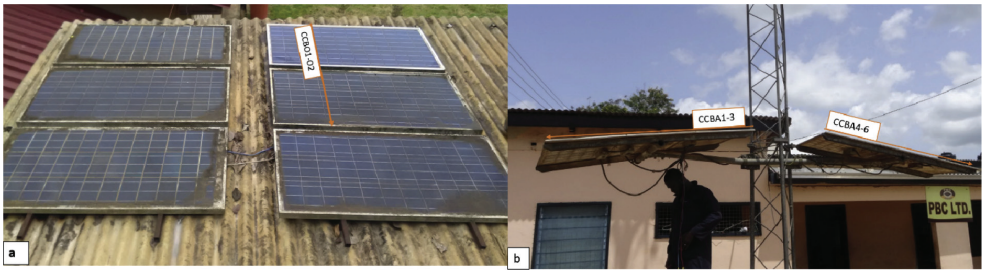

Fig. 3 – Pictures of installations: (a) Battery-charging installation at Akim Oda and (b) Battery-charging installation at Breman Asikuma.

while for Accra the range was 25.6 °C (in August) – 28.3 °C (in February). At the lower end, minimum monthly temperatures in the year were 22 °C–23.9 °C for Kumasi and 22.8 °C–25.1 °C for Accra. Similarly, relative humidity values averaged a minimum of 67% in January and maximum of 84.3% in June for Kumasi, and 76% (in January) and 85% (in October) for Accra. Queries for climate data for the four other locations (CWSA1, CWSA2, Akim Oda and Breman Asikuma) yielded temperature and humidity data similar to that of Accra (MoEN) and are therefore not shown.

Equipment and procedures

A TRI-KA current–voltage (I–V) curve tracer was used for the acquisition of I-V data on the PV modules *in situ*. The TRI-KA I-V tracer works together with a TRI-SEN (both shown in Fig. 7), which measures temperature, irradiance and inclination, thereby enabling translation of acquired data to Standard Test Conditions (STC) or other Standard Reference Conditions (SRC). Measurement range and sensitivity of the devices are shown in Table 4.

Fig. 4 – Water-pumping installations: (a) CWSA1 and (b) CWSA2.

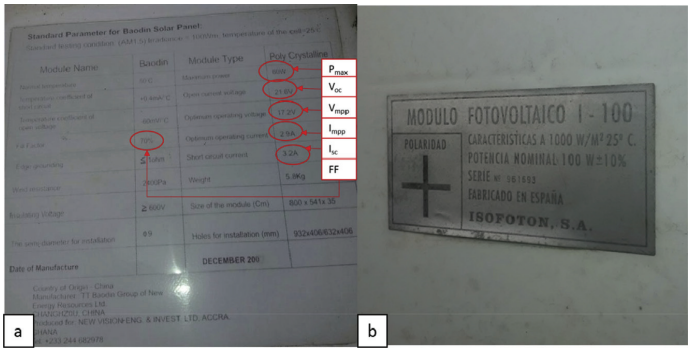

Fig. 5 – Labels of solar modules at: (a) Akim Oda and (b) Ministry of Energy.

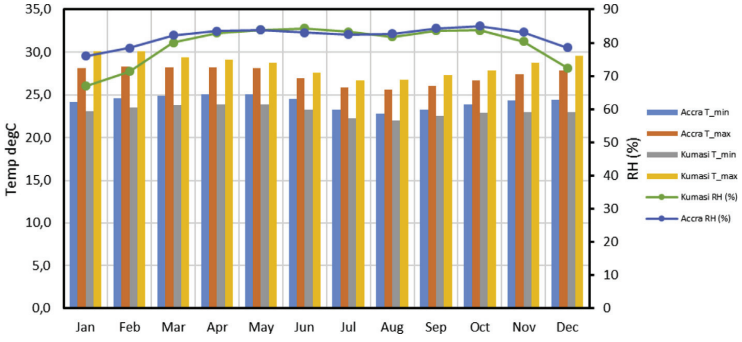

Fig. 6 – Monthly variation of air temperatures and relative humidity for Accra and Kumasi (22-year average) (Data [44]).

Translation of measured data to STC conditions is more accurate when measurements are undertaken at higher irradiance levels and as close as possible to STC conditions. Anderson [46] demonstrated that translating to STC with performance data measured at low irradiance levels have higher associated error. To minimize this error, measurements are typically undertaken at irradiance conditions of 700 W/m^2 and above (IEC 61215) [47]. Other researchers have adopted minimum irradiance levels of 500 W/m^2 – 800 W/m^2 [17,48]. In this work, minimum irradiance level adopted was 750 W/m^2. In practice however, the minimum irradiance at which measurement was taken was 766 W/m^2.

Fig. 7 – Images of TRI-KA and TRI-SEN. Photo by Ref. [45].

Table 4 – Measurement characteristics of TRI-KA and TRI-SEN.

Parameter (Unit)	Measuring range	Uncertainty
Voltage (V)	1.0–1000	±1%
Current (A)	0.1–15.0	±1%
Temperature (°C)	0–100	±3%
Irradiance (W/m^2)	100–1200	±5%

To maintain uniformity of irradiance during measurements, maximum admissible variation of irradiance was set to 5%. Therefore, irradiance variation exceeding this pre-set tolerance results in a termination of the I-V curve tracing process. Furthermore, measurements were conducted between the hours of 10 a.m. and 2 p.m. to reduce angle of incidence effects.

Calculations

A number of translation methods for I-V data exist in the literature. From early work by Sandstrom [49], a number of authors have contributed to correlations that may be used to correct I-V measurements to desired conditions [46,50–53]. Translation standards adopted by the International Electrotechnical Commission (IEC) have been largely based on the contributions of these researchers and as well as the work of national electro-technical agencies [54]. Data requirements for the implementation of the various correlations also vary and therefore affect the feasibility of implementation. For example, in outdoor measurements in locations with significant cloud movement (such as in Ghana), achieving constant irradiance while varying the temperature for determination of temperature co-efficient of short-circuit current poses significant challenges. Methods that use manufacturer-supplied temperature coefficient of peak power (%/°C) have the limitation of high uncertainty with the coefficients. Smith et al. [55] found uncertainty of about 10% in manufacturer-supplied temperature coefficient of power. In this paper, correlations presented by Kaplanis and Kaplani [56] (Equations (1)–(3)), which do not require the use of temperature coefficients are adopted for translating measured data to reference conditions. Module-specific data such as number of series-connected cells are readily obtainable. These preferences, notwithstanding, Duck et al. [54] and Herrmann & Wiesner [57] have shown that the accuracy of many I-V data translation methods in use (both algebraic and numeric) are comparable and that irradiance and temperature conditions under which measurement are made turn out to be more crucial. The open-circuit voltage at STC, $V'_{oc(STC)}$, is determined from Equation (1):

$$V'_{oc(meas)} = V'_{oc(STC)} - n_s \times 2.3 \times 10^{-3} \times (T_c - 25°C) + \frac{kT_c}{q} \ln C \quad (1)$$

where:

- $C = \frac{I_T}{10^3}$
- $k = Boltzman\ Constant = 1.38 \times 10^{-23}\ J/K$
- $n_s = number\ of\ cells\ in\ series$
- $q = electron\ charge = 1.602 \times 10^{-19}\ C$ and
- $I_T = irradiance\ in\ W/m^2$
- $V'_{oc(meas)}$ = measured open-circuit voltage

The short-circuit at STC, $I'_{sc(STC)}$, current is calculated from Equation (2):

$$I'_{sc(meas)} = I'_{sc(STC)} \times (1 + h_f \times (T_c - 25^{\circ}C)) \times \frac{I_T}{10^3} \quad (2)$$

where: $I'_{sc(meas)}$ = measured short-circuit current and $h_f = 6.4 \times 10^{-4} K^{-1}$. The power at STC, $P'_{(STC)}$, then computed from $I'_{sc(STC)}$, $V'_{oc(STC)}$ and the fill factor (FF) as:

$$P'_{(STC)} = FF \times I'_{SC(STC)} \times V'_{oc(STC)} \quad (3)$$

Series and shunt resistances are estimated from the slopes of the respective I–V curves in the neighbourhood of V_{oc} and I_{sc} respectively. The series resistance (R_s) of modules can be described as lumped quantity that accounts for resistances in solder bonds, emitter and base regions of the cells, cell metallization and interconnect busbars as well as junction-box terminations [58]. It increases with time as the metallization and interconnects become fatigued by thermo-mechanical stresses, and other components also age. It was observed by van Dyk & Meyer [58], that, a 25% reduction in fill factor and maximum power occurred when series resistance increased five-fold. Shunt resistance (R_{sh}) on the other hand represents the resistance of the module to current leakage via alternate paths. Other correlations for estimating series and shunt resistances abound in the literature (e.g. Refs. [59–61]) with varying data requirements for implementation.

Visual inspection

In addition to I-V measurements, visual inspection was undertaken to document observable physical defects. The template provided by the International Energy Agency Task 13 [62] was reviewed and used in documenting defects. This template has been adopted widely by researchers and enables the usage of consistent vocabulary in the description of observed defects in field assessments. This in turn makes it possible to compare

results of visual inspection, even though subjective judgements cannot be entirely ruled out. Observed defects for each of the modules were categorized according to the component of the PV module in which it occurred (Table 5). For each module, the number of categories in which defects were observed was recorded. For example, a module may have defect counts in 3 categories such as those observed at the front of the module and those related to wires and connectors. The actual number of defects in each category is also noted. For example, a given module might have 3 defects in the "PV Cells" category, namely, discoloured anti-reflection, broken cell and cracked cell. The occurrence of a given defect in a module was coded as 1 and non-occurrence was coded as 0. For all the modules, the number of counts in each category were aggregated to help in determining the component with most documented defects. Since not all defects lead immediately to power loss, the relationship between the occurrence of visually observable defects and performance indicators was examined using Pearson's correlation coefficient (r), Equation (4).

$$r = \frac{n\sum xy - (\sum x)(\sum y)}{\sqrt{n(\sum x^2) - (\sum x)^2}\sqrt{n(\sum y^2) - (\sum y)^2}} \quad (4)$$

where n is the number of data pairs; x represents the observation category (e.g. back of module); and y represents the performance loss (e.g. loss in P_{max} or I_{sc}).

Results and discussion

This section presents results of visual inspections and electrical characterization of the modules studied. Findings from the visual inspection process are presented first. This is followed by results of electrical performance measurements, which are presented and discussed according to the applications in which they were deployed; i.e. grid-connected systems, water-pumping and battery-charging. Correlations between electrical performance metrics and visually observable defects are also explored. The results are discussed in the context of results presented by other researchers in this domain.

Visual inspection

Visually observable defects were categorized into six broad classes according to the component of the module in which the defect was observed. The categories are defined in Table 5. Even though Table 5 has seven (7) categories, one of the categories (module frame defects) did not register any occurrence. The number of modules exhibiting defects in one or more categories are shown in Fig. 8. Out of twenty-nine (29) modules assessed in this study (Fig. 8), twenty-two (22) had one or more visually observable defects in at least one category. Similarly, five (5) of the modules had defects in all six (6) categories defined in Table 5 (with exception of frame-related defects). This implies that five modules had visually observable defects related to front of the PV module, cell metallization, back of module, junction box and wires/connectors.

In all, eighty-nine (89) defects were recorded from the twenty-nine (29) modules assessed. The distribution of the defects according to the component of the module where it was observed is shown in Fig. 9. As shown in Fig. 9, defects on the front side of the module (bubble formation, delamination, yellowing/browning of encapsulant, broken glass) were dominant. This is followed by defects in cell metallization (oxidation, burns and snail tracks) and discolouration of the cells. Junction box defects were mainly found with Isofoton I-100 modules installed in Accra and had to do with degradation of the adhesive binding the junction box to the back of the modules. Photographs of the defects are shown in Figs. A.1 and A.2 (Appendix).

These observed defects have also been reported by many who have studied field-ageing of PV modules. For example, Sastry et al. [63] studied 10-year old crystalline silicon modules installed in India and reported defects including browning of the cell encapsulants, corrosion of the metallization, delamination and defects in the junction box. In their study, no particular defect was reported as dominant, even though they suggest intensification of tests such as dump-heat (DH) and UV exposure in the qualification test series to reflect the realities of locations with harsh weather.

A similar study by Rajput et al. [64] on 22-year old monocrystalline modules identified defects in busbars, cell interconnection ribbons and string interconnection ribbons as the most frequent performance degradation modes. The study also identified hotspots, burn marks and backsheet delamination. Pozza and Sample (2016) [65] concluded after studying seventy (70) modules exposed for 22 years in Ispra, Italy, that the main failure mode was yellowing of the encapsulant. Similar observations concerning the dominance of front-of-module and metallization defects have been made by Ref. [66] (28-year old modules, Himalayan region, India) [37]; (19-year old modules in Ghana) [56]; (20 year modules in Greece) and [26] (28 year old modules in Adrar, Algeria). A literature review by Jordan et al. (2016) [67] showed that discolouration and delamination were the most reported defects. They also showed that even though hostspot formation was not the most frequently reported defect, its occurrence was associated with higher levels of power loss in modules.

Table 5 – Module components and defect categorization [62].

PV module component	Potential defects
Front of PV module	Bubbles, delamination, yellowing, browning, glass breakage
PV Cells	Discoloured anti-reflection, broken cell, cracked cell,
Cell metallization	Burnt, oxidized, snail tracks
Frame	Bent, broken, scratched, misaligned
Back of module	Delaminated, bubbles, yellowing, scratches, burn
Junction box	Loose, oxidation, corrosion
Wires – connectors	Detachment, brittle, exposed electrical parts

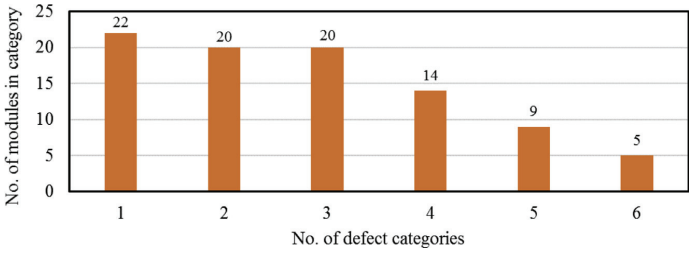

Fig. 8 – No. of modules with defects in one or more categories.

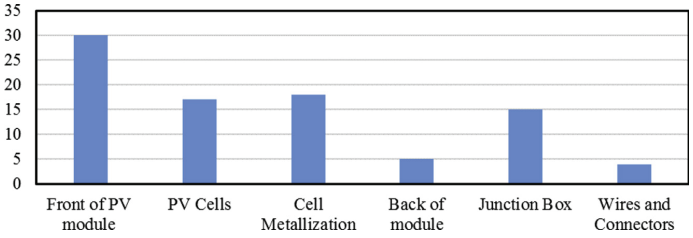

Fig. 9 – No. of defects in various module components.

Correlation between these defects and measured performance metrics are explored in later sections (Table 6).

Electrical performance indicators

Grid-connected systems

Results from measurements on the two grid-connected systems located at the Ministry of Energy (MoEN) in Accra (Lat. 5.5514°, Long. 0.2007°) and the College of Engineering at the Kwame Nkrumah University of Science and Technology (KNUST) in Kumasi (Lat. 6.68°, Long. 1.57°) are presented in this sub-section.

The decline in maximum power (P_{max}) on an annual basis (%/yr) for the monocrystalline system located in Accra is presented in Fig. 10. The decline in P_{max} varies between 1.7%/year and 4.6%/year for the 15 modules and has a median value of 1.9%/year. Degradation in the explanatory variables (I_{sc}, V_{oc} and FF), are also shown in Fig. 10. The maximum P_{max} degradation rate (4.6%/year) is more than twice the minimum (1.7%/year) and the median (1.9%/year). This wide range is due to the very high V_{oc} and FF loses incurred by the module ISF21 (Fig. 10b). Whereas the median V_{oc} and FF losses for the modules of this installation were 0.5%/year and 0.5%/year respectively, the module ISF21 showed annual losses of 3.8% and 0.6% respectively. On the other hand, the rate of decline in short-circuit current (I_{sc}) showed a much narrower range of 0.9%/year - 1.6%/year, with a median value of 1.2%/year.

Current-Voltage (I-V) curves of selected modules from the MoEN installation are shown in Fig. 11 to provide further

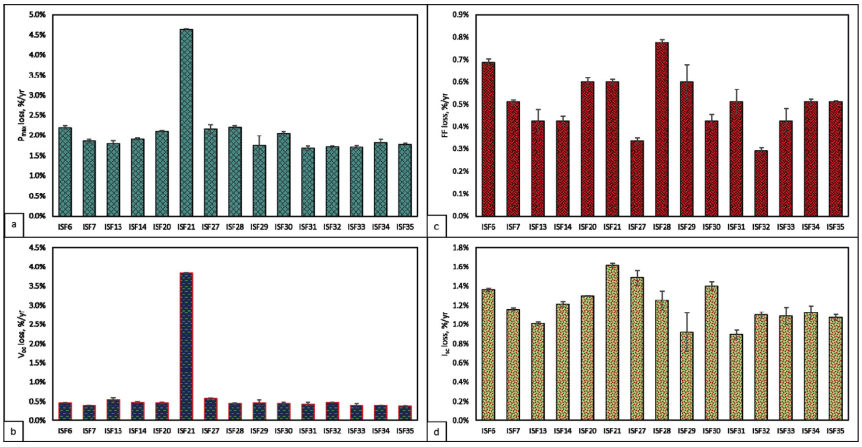

Fig. 10 – Performance loss in Isofoton I-100 modules located in Accra (MoEN): (a) P_{max}, (b) V_{oc}, (c) FF and (d) I_{sc}.

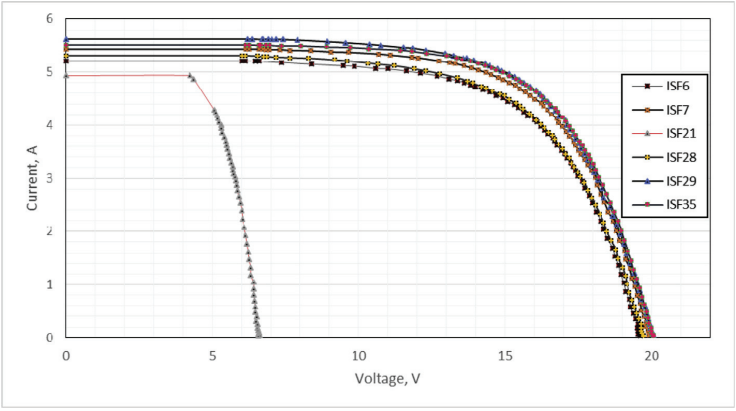

Fig. 11 – I-V curves of selected modules, showing extensive loss of V_{oc} in module ISF21 (16-year-old modules).

details on modules with comparatively high degradation. As earlier suggested by Fig. 10 (P_{max} and V_{oc}), the module labelled ISF21 indeed shows markedly lower V_{oc}. This suggests either a break in cell inter-connects or the cells, thereby failing to contribute to the build-up of voltage to the required level. Whereas the open-circuit voltage (standardized) of the remaining fourteen (14) modules are almost 93% (20.06 V) of the reference (initial) value (21.6 V), the module ISF21 on the other hand is producing just under 40% (8.35 V) of the reference value. Further investigation with techniques such as infrared thermography and electroluminescence is needed to confirm the suspicions raised by the I-V data and to identify defective cells or non-conducting regions. In general, however, module power (P_{max}) losses observed (1.9%) for this system are dominated by I_{sc} losses (1.2%), followed by FF (0.5%) and V_{oc} (0.5%) losses in comparable measure. The modules are thus producing on average 70% of rated maximum power. Notably, after 16 years of exposure, all the modules are producing well below the typical 80% (of initial P_{max}), which is normally guaranteed for a 20–25 year period.

Performance of modules in the second grid-connected system assessed in this study (located in Kumasi), is shown in Fig. 12. These modules exhibit P_{max} degradation of 0.7%/year – 1.5%/year and a median of 1.3%/year. The modules are thus, in general, operating at above 87% of P_{max} after 10 years of exposure. The least-performing module (with a 1.5%/year decline) is still above the critical 80% (of P_{max}) threshold that has characterized industry warranties for some time now. Unlike the installation in Accra, whose degradation is dominated by I_{sc} losses, the degradation in P_{max} for this installation (Kumasi) does not appear to be dominated by any one particular factor. Annual decline in I_{sc}, V_{oc} and FF respectively range from: 0.1%–0.6%, 0.3%–0.8% and 0.3%–0.5%. For all the three (3) explanatory factors, the median value is 0.4%/year. This is in contrast with a median P_{max} degradation rate of 1.9%/year for the grid-connected PV modules installed in Accra, which is dominated by I_{sc} losses (1.2%/year). The dominance of I_{sc} is consistent with the delamination and extensive discolouration that are observed for the Isofoton I-100 modules in Accra (Fig. A.1).

Water pumping systems

Modules of the two water-pumping systems installed by Ghana's Community Water and Sanitation Agency (CWSA) showed P_{max} degradation of 0.9%/year and 3.2%/year (Fig. 13). Notably, the system installed in 2011 (CWSA2), with 6 years of exposure, showed much higher degradation than the earlier one installed in 2006 (CWSA1) (11 years exposure). While CWSA1 module (aleo 150-M5i) continues to operate at above 90% of its original power rating after 11 years of continuous operation, the output of the CWSA2 module (aleo S_03) has fallen below 70% within 6 years of field exposure (5.3% P_{max}

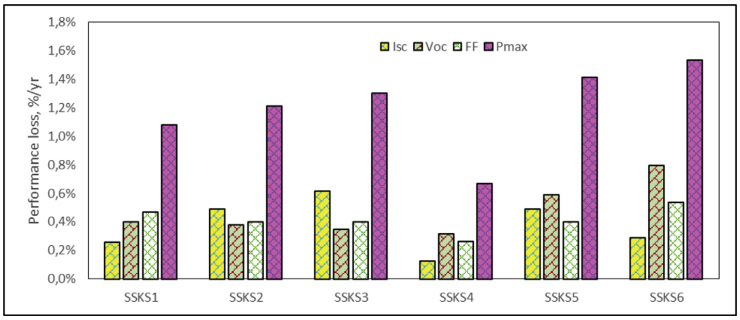

Fig. 12 – Performance characteristics of modules located in Kumasi.

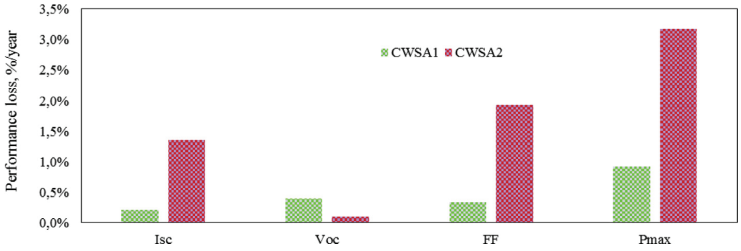

Fig. 13 – Degradation rates of electrical performance characteristics of water pumping systems.

degradation per year). At the time of field visit, the module at CWSA2 was in open-circuit mode, as the entire water pumping system was not functioning.

The module at the CWSA2 location had visible cracks on the front-glass (as shown in Fig. A.2b), which appears to explain the rather sharp decline in output after only 6 years of exposure. As shown in Fig. 13, the decline in output is influenced predominantly by losses in fill factor (FF) (3.2%/year) and short-circuit current (I_{sc}) (2.3%/year); which respectively suggest increased series resistance and optical transmission problems.

On the other hand, the module at CWSA1 has a relatively lower degradation rate of 0.8%/year with comparable contributions from V_{oc} (0.4%/year) and FF (0.3%/year); and I_{sc} at 0.2%/year. Normalized I-V curves (using translated I_{sc} and V_{oc}) of modules from the two systems (Fig. 14) provide additional insight into the high fill factor loss of the module at CWSA2. From Fig. 14, it may be observed, that, the module suffers high shunt losses and can be perceived from the slope of the curve in the neighbourhood of I_{sc}. This is further confirmed by the data in Table 7, which presents series and shunt resistances of the modules assessed. Coincidentally, these two modules are from the same manufacturer and highlight the effect that different field operating conditions and circumstances could have on modules – even from the same manufacturer.

Battery-based systems

Two (2) of the systems studied were battery-based installations, which have powered radio communications systems of the Ghana Cocoa Board over the years. The modules located at Breman Asikuma in Ghana's Central Region (CCBA1-CCBA4) and Akim Oda in the Eastern Region (CCBO1 and CCBO2) have been exposed for 32 years and 11 years respectively. Modules from the 32-year old system are performing at 45.2%–74.4% of initial $P_{max,}$ with a median value of 70.3%. On an annual basis, this implies a degradation rate of 0.8%/year - 1.7%/year (Fig. 15). The wide range is due to the performance of module CCBA2, whose performance decline (1.7%/year) may be considered an outlier as it lies rather far from the median degradation value of 0.9%/year.

Module CCBA2 is one of two modules at the location which had cracks on the front glass (as shown in Fig. A.2); the other one being module CCBA1. The crack on the front glass of module CCBA1 however does not appear to have affected its performance, as its output (71% of P_{max}) is in fact comparable to the two others which have no cracks – 69.6% and 74.4% of P_{max}. This suggests that not all cracks have perceptible effects on performance. Nonetheless, as pointed out by Ref. [68], such defect locations could create preferential nodes for accelerated module degradation. The P_{max} degradation of these modules is dominated by loss in FF, 0.5%/year - 1.1%/year, with a median value of 0.6%/year; followed by I_{sc} losses (0.2%/year – 0.8%/year), with median value of 0.4%/year. The contribution of V_{oc} losses were relatively low, with a median of 0.1%/year (Fig. 15). Overall, the modules in the CCBA series are performing at a median value of 70.3% of initial P_{max} (36 Wp) after 32 years of exposure. Except for module CCBA4, the modules in general, appear to be in a position to serve their purpose (battery charging) for some more years (Fig. 16).

On the other hand, inspection of Balance of System (BoS) components showed that even though the junction box was well fitted, with no signs of corrosion, arcing or other visible defects,

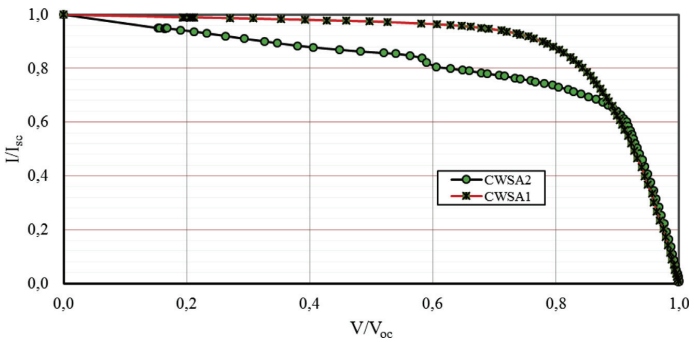

Fig. 14 – Normalized I-V curves for CWSA1 (11-year-old) and CWSA2 (6-year-old) modules (water-pumping systems).

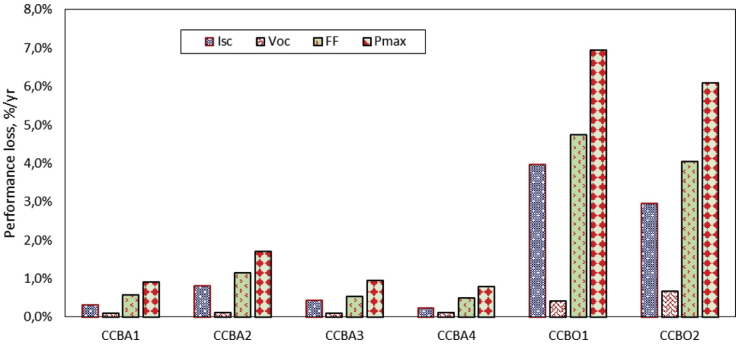

Fig. 15 – Performance characteristics of battery-based systems.

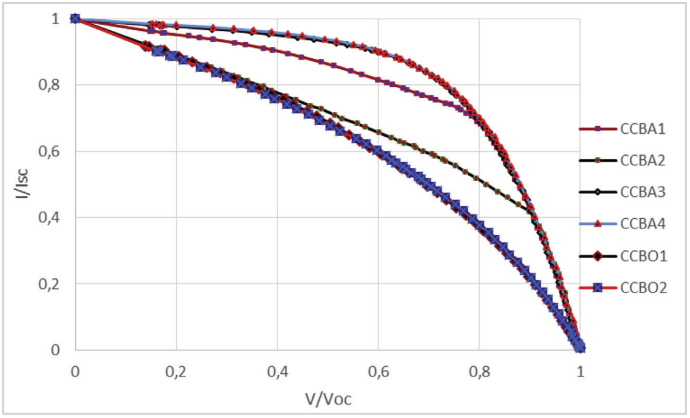

Fig. 16 – Normalized I-V curves of module CCBA1-CCBA4 (32-year-old) and CCBO1-O2 (10-year-old).

the insulation of the connecting cables had deteriorated significantly (as shown in Fig. A.2c). This poses potential safety hazard. Even though the modules were designed for a 10-year life (personal communication), they have been in service for 32 years and can still serve for some time. The unequal lifetime of different components of the PV module brings into focus current efforts at implementing component-level qualification testing for the PV industry, in the so-called *Qualification Plus* testing [69]. While the focus tends to be on the modules, the lifetime of the cables appears to be the limiting factor in this case. As noted by Watson [70], electrical cables tend to be overlooked in ageing analyses and monitoring and evaluation.

As the number of PV installations rise on an annual basis, there is the need to put in place regulatory and monitoring systems that ensure the safety of these installations, even for those that have failed. Such regulations should also consider environmental issues such as material disposal and recycling. In fulfilment of its obligations under the *Basel Convention on the Control of Transboundary Movement of Hazardous Waste* and other international protocols, Ghana passed the Hazardous and Electronic Waste Control and Management Act, (Act 917) in 2016 [71]. The aim of the Act is to provide for the control, management and disposal of hazardous waste, electrical/electronic waste and related matters. Even though Solar PV is not explicitly mentioned in the list of over 300 items for which levies are payable, it is necessary to take due cognizance of the potential hazards and opportunities that Solar PV materials present at the end of their life. The absence of well-designed O&M practices (e.g. Fig. A.3b) and end-of-life materials management plan presents both electrical hazard (e.g. Fig. A.2c) and potential environmental challenges. On the other hand, recent analysis [72] suggest significant opportunity for developing a circular economy around the recycling and re-use of solar PV materials.

Surprisingly, the output of the two (2) modules in the 10-year old system in Fig. 15 (CCBO1 and CCBO2) has dropped by almost 61% and 70% respectively; with annual decline of 6.1% and 7.0%. Compared with the typical industry warranty of 80% of P_{max} for 20–25 years, these modules have simply failed. An examination of Fig. 15 shows that the failure is attributable to losses in fill factor (FF) (4.1%/year and 4.7%/year) and short-circuit current (I_{sc}) (3%/year and 4%/year). The open-circuit voltage degradation was much less; at 0.4%/year and 0.7%/year (Fig. 15). The I-V curves of these modules (normalized to I_{sc} and V_{oc}) are shown in Fig. 16. The shape of the curves depicts

the sharp decline in the fill factor of modules CCBO1 and CCBO2 as compared with modules CCBA1-CCBA4.

Even though some minor corrosion of the metallization and browning of encapsulant are observable from the front side of the module (Fig. A.3a), the sharp decline in both I_{sc} and FF suggest more severe optical transmission and series resistance problems that are not readily visible to the unaided eye. This particular installation (CCBO1 and CCBO2) is roof-flushed and has a tilt angle of just about 6°. Such low tilt angles impede water run-off during rains, a situation which could have aided in self-cleaning of the surface. On the contrary, hardened sediments were observable on the surface of the modules (Fig. A.3b). Water retention on the surface of the modules increases the risk of water/moisture ingress into the module, which facilitates corrosion of the metallization of the modules.

Correlation between visual defects and performance loss

Losses in key performance parameters (I_{sc}, V_{oc}, FF and P_{max}) were generally positively correlated with total number of visually observable defects (Table 6). Correlation coefficients ranging from 0.07 to 0.36 were obtained between the total number of observable defects and losses in key performance metrics. This implies that the losses tend to increase as the count of visually observable defects increase. Number of defects observable from the front side of the PV module (e.g. bubbles, delamination, yellowing/browning of encapsulant and broken glass) and PV Cells (e.g. discoloured anti-reflection coating (ARC)) showed stronger positive correlation with short-short circuit current in particular (0.63 and 0.55) and P_{max} (0.52 and 0.36).

On the other hand, negative correlations are observed between the number of defects at the back of the modules, wires and Connectors, and performance indicators. These are however based on very few observations (5 and 4 respectively) and may be attributable to random error. Short-circuit current (I_{sc}) related losses are typically related to defects which are generally visible (e.g. encapsulant discolouring, delamination, glass aberration and ARC degradation), even though others such as cracks in the cells may not be readily visible [21,41,43]. This provides some explanation for the strong positive correlation of I_{sc} with defect count. However, defects related to FF (e.g. thermo-mechanical fatigue of the metallization, Cell current mismatch) and V_{oc} (e.g. line scribe errors, material deposition problems, faulty edge isolation [43,73,74]) are generally either not visually detectable or not detectable with similar levels of ease. Nevertheless, the results of this study underscore the useful role that relatively inexpensive methods such as visual inspection could play in PV module O&M practices. Indeed, as shown in Table 7, all the modules showed substantial increases in series resistance and reduction in shunt resistance.

Table 7 – Series and Shunt Resistance of modules assessed.

Module	Series resistance, Ω		Shunt resistance, Ω	
	Ref.[a]	*Measured*	Ref.[a]	*Measured*
Isofoton I-100	0.25	0.66 ± 0.02	110	52.24 ± 0.92
aleo 150-M5 i	0.55	1.31 ± 0.01	350	201.47 ± 28.38
aleo S_03	0.42	1.35 ± 0.18	400	35.11 ± 6.28
Schott Poly 170	0.55	1.20 ± 0.01	350	204.67 ± 14.10
HS.40.1 N	–	2.04 ± 0.03	–	43.63 ± 2.31
Baodin	–	3.27 ± 0.12	–	10.99 ± 0.79

[a] Reference data was obtained from database of PVSYST [38].

General discussions

Modules in the six (6) installations showed varied performance results. The grid-connected system in Accra showed a median P_{max} degradation of 1.9%/year while its 10-year-old counterpart located in Kumasi showed a median degradation of 1.3%/year. As shown in Table 8, while I_{sc} losses were dominant in the grid-connected system in Accra, all factors contributed in comparable measure to the P_{max} degradation in Kumasi. Similarly, the water pumping systems had varied module performance metrics. While the 11-year-old system (CWSA1) was performing above 90% of its rated power, with annual degradation rate of 0.8%, the output of the 6-year-old CWSA2 system had dropped below 70% of its rated capacity, having a degradation rate of 5.3%/year. The degradation at CWSA2 is dominated by losses in FF and I_{sc}. The third category of installations, the battery charging systems, on the other hand, had very contrasting outcomes, while one had entirely failed after 10 years of exposure, the 32-year system still produces above 70% of its rate output.

Except for the 32-year old system, these results do not compare favourably with the generality of results that have been published from similar work. Osterwald et al. [18] in 2005 studied modules of various technologies installed on a testbed at Golden, Colorado USA, and reported annual degradation rates of 0.3%–0.51% and 0.01%–0.91% for mono-crystalline and poly-crystalline silicon respectively. After reviewing five years of prior published work and considering their own results [18], they suggested an abandonment of the prevailing 1%/year degradation rate used as rule-of-thumb for crystalline silicon modules at the time. Instead, they considered a rate of 0.5%/year to be more realistic for crystalline silicon modules. About a decade later [24], in a review of results published over a period of 35 years involving 200 studies, found median values for crystalline silicon PV modules in the range of 0.5%–0.6%/year, in a way confirming the earlier work of [18]. Rabii et al. [75] studied twenty-four (24) polycrystalline modules installed in

Table 6 – Correlation between performance loss and defect count in module components.

Performance metric	Front of PV module	PV Cells	Cell Metallization	Back of module	Junction Box	Wires and Connectors	Total defect count
I_{sc}	0.63	0.55	0.18	−0.21	0.14	−0.30	0.36
V_{oc}	0.26	0.26	−0.13	−0.21	0.25	−0.25	0.07
FF	0.33	0.11	0.05	−0.02	−0.34	−0.07	0.07
P_{max}	0.52	0.36	0.06	−0.19	−0.04	−0.27	0.20
No of defects	30	17	18	5	15	4	89

Table 8 – Median values of electrical performance parameters of modules assessed.

Installation	Application	Exposure duration	P_{max} %/year	I_{sc} %/year	V_{oc} %/year	FF %/year
Accra (MoEN)	Grid-Connected	16 years	1.9	1.2	0.5	0.5
Kumasi	✓	10 years	1.3	0.4	0.4	0.4
CWSA1	Water pumping	11 years	0.8	0.2	0.4	0.3
CWSA2	✓	6 years	5.3	2.3	0.2	3.2
Breman Asikuma (CCBA)	Battery-charging	32 years	0.9	0.4	0.1	0.6
Akim Oda (CCBO)	✓	10 years	6.5	3.5	0.5	4.4

1990 in Tunisia after 12 years of field exposure and reported that modules had lost over 60% of their peak power – a degradation rate of more than 5%/year. They attributed the losses to degradation of encapsulant and decrease in shunt resistance. Intensive encapsulant browning was also reported by Belmont et al. [76] on 26-year old monocrystalline silicon modules installed in Phoenix Arizona. This installation had a degradation rate of 2.3%/year. Twenty-year-old polycrystalline modules studied by Polverini et al. [77] in Italy showed a degradation of 4.42% over the exposure period (an average of 0.22%/year). Over a 12-year period, Sánchez-Friera et al. [78] observed 11.5% degradation in monocrystalline silicon modules installed in Southern Europe (annual degradation rate of 0.96%). This was much higher than the observation by Polverini et al. [77], but similar to our observation for installation CWSA1 (Table 8), which has a comparable period of exposure.

In the work of Sastry et al. [63] (referred to earlier) on the 10-year old hybrid battery-charging/grid-connected system in the hot-humid climate of India (similar to Ghana), they categorized the modules studied into five (5) groups and found P_{max} degradation of up to 10% (1%/year) and more than 25% (2.5%/year) for some of the groups. Some modules had failed. They suggest an intensification of the Damp-Heat (DH) and UV exposure tests in the IEC 61215 sequence to reflect the realities of harsh locations such as India. Limmanee et al. [79] found P_{max} degradation rate of 1.2%/year for grid-connected poly-crystalline silicon modules installed in Thailand after 4 years of exposure in the hot-humid climate of the country. They [79] found that non-crystalline silicon technologies performed worse – with degradation rates of up to 6.1%/year.

A solar water pumping system assessed by Ref. [66] after 28 years of field-ageing had a degradation rate of 1.4%/year and this was attributed to encapsulant discolouration, delamination, oxidation of front grid fingers and anti-reflective coating, glass breakage and bubbles in back sheet. Quansah et al. [37] presented results of studies on 14 poly-crystalline modules in Ghana after 19 years in the climate of Kumasi and found a median P_{max} degradation of 1.3%/year; similar to results by Refs. [66,79], whose work were from climate of similar characteristics. Degradation rates of 0.8%–1%/year for crystalline silicon modules were reported by Ref. [80] for systems that they studied in the hot-humid tropical climate of Singapore.

Many of these degradation rates in the preceding paragraph, from hot-humid regions are higher than the median value of around 0.5% reported in the major reviews such as [18,23–25] for crystalline silicon systems. These reviews, as acknowledged by some of the authors have as a deficiency, a lack of geographical representativeness. This underscores the need for additional effort at obtaining data from geographically under-reported regions and more importantly, to intensify climate-specific research on the long-term performance of Solar PV modules as widely acknowledged by various authors – [17–22]. Such research will be beneficial for the implementation and revision of climate-specific module qualification tests as opined by Ref. [63]. It must be mentioned, that, even though performance loss in this study are presented in terms of average yearly percentage (%) decline (in relation to reference values), there is evidence of non-linearities at some stages, particularly in the early stages of exposure, due to light-induced degradation, and also in the wear-out phase of a module's life. A discussion on this has recently been presented by Ref. [81].

Finally, we observe that, modules at three (3) out of the six (6) installations studied, did not have any certification labels, e.g. IEC 61215. These were modules at Accra (MoEN), Breman Asikuma (CCBA) and Akim Oda (CCBO). Of these three (3) uncertified modules, two (2) (those in Accra (MoEN) and Akim Oda (CCBO)) turned out to be among the worst performing modules – with annual Pmax degradation of 1.9% and 6.5%. Although one of the remaining certified modules (IEC 61215) had annual P_{max} degradation of 5.3%, this is attributable to breakage of the front glass, resulting from impact of items such as stones. Module certification therefore appears to have some impact on long-term performance and reliability in the field. In addition to implementing module certification requirements in countries such as Ghana, certification of installers is also crucial, to provide some assurance, that the certified product will be properly installed [7].

Conclusions

This paper has presented a study on the performance loss and degradation of twenty-nine (29) crystalline silicon modules exposed across six (6) locations in Ghana, for periods ranging from 6 to 32 years, 465 module-years. The modules were deployed in three (3) types of applications: water-pumping (2), battery-charging (6) and grid-connected systems (21). This paper summarizes and concludes as follows:

- Defects observable from the front-side of modules were dominant (e.g. delamination, bubble formation, yellowing/browning of encapsulant) and showed strong positive correlation with losses in I_{sc}. Overall, the number of defects observed had positive correlation with % losses in key performance indicators (P_{max}, FF, V_{oc} and I_{sc}).
- Modules in grid-connected mode had median P_{max} degradation rates of 1.3%/year and 1.9%/year for systems located in Kumasi (poly-crystalline Si) and Accra (mono-crystalline Si) respectively. The high performance loss in modules located in Accra was mainly due to I_{sc} losses.

- Modules in off-grid, battery-charging mode had P_{max} degradation of 6.5%/year and 0.9%/year for the 10- and 32-year old systems respectively. Voltage levels are critical for battery-charging systems. Although V_{oc} loss is 0.5%/year for the 10-year-old system, heavy losses in I_{sc} and FF (3.5% and 4.4% respectively) implies battery charging will require much longer duration.
- The two solar water pumping systems studied (both mono-crystalline) showed divergent performance, with P_{max} loss of 0.8%/year and 5.3%/year for the 11-year-old and 6-year-old systems respectively. The high I_{sc} losses in the 6-year-old system has detrimental implication for the typically high surge current requirements for starting of DC pumps.
- Workmanship and installation defects were observed, notably, low tilt angle that prevents rainwater run-off and self-cleaning, and sub-optimal azimuthal orientation.
- Qualification labels were absent on some modules and it was unclear, by what standards (if any) they had been qualified for market entry.
- To ensure continued confidence in Solar PV technology, Ghana and other developing nations need to develop and implement quality management systems that provide assurance of both product quality and acceptable installation workmanship.
- As the PV industry grows and expands, end-of-life management of solar PV materials becomes more crucial. In the context of Ghana's law on *Hazardous and Electronic Waste Control and Management (Act 917 of 2016)*, appropriate measures need to be implemented to manage the waste generated by photovoltaic systems that have reached the end-of-life stage and to take advantage of the opportunities they present.

Acknowledgement

The first author gratefully acknowledges support by the Lånekassen of Norway towards his doctoral studies. The authors are thankful to the Management of the Ghana Cocoa Board, to Messrs. Wisdom Ahiataku-Togobo and Seth Mahu-Agbeve of the Renewable and Alternative Energy Directorate of the Ministry of Energy in Ghana, as well as the Management of the Community Water and Sanitation Agency (Ghana) for granting access to their respective installations for this ongoing study. The assistance of the Energy research Centre of the Netherlands (ECN) and Professor Ronald van Zolingen of the Eindhoven University of Technology in obtaining primary data on the Holec HH solar modules is much appreciated. Support from the Director of The Brew-Hammond Energy Centre at KNUST (Dr Gabriel Takyi), is likewise appreciated. Comments received from anonymous reviewers helped to improve the original manuscript. Their efforts are duly acknowledged.

Appendix A

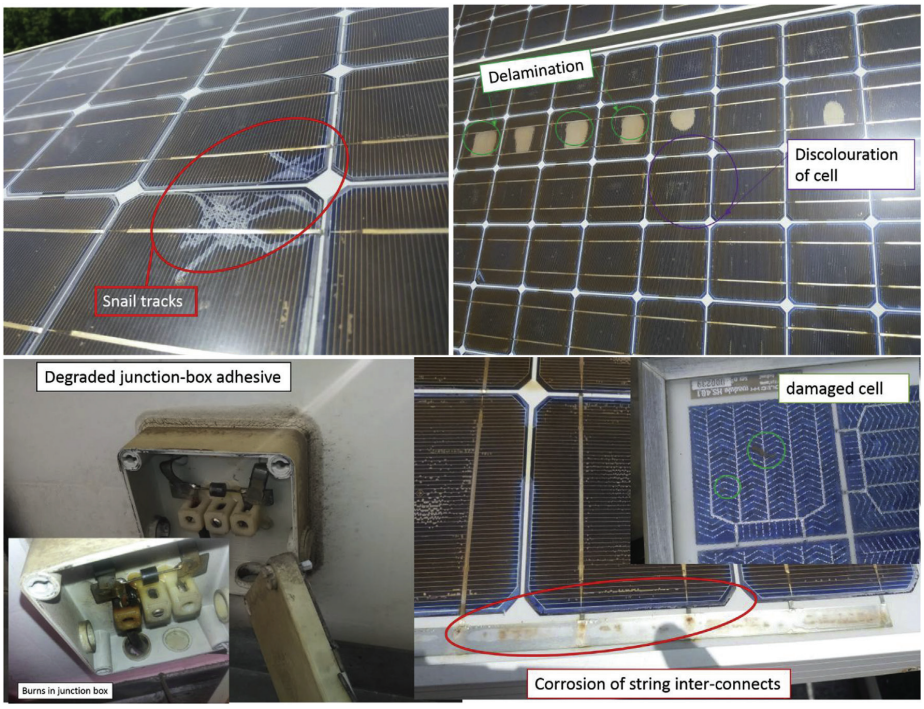

Fig. A.1 – Selected photographs of defects observed.

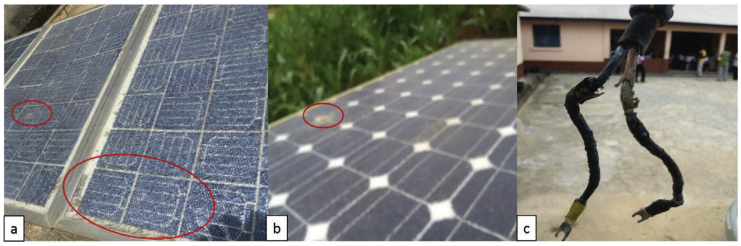

Fig. A.2 – Cracks on module front glass (a, b) and degraded cable insulators (c).

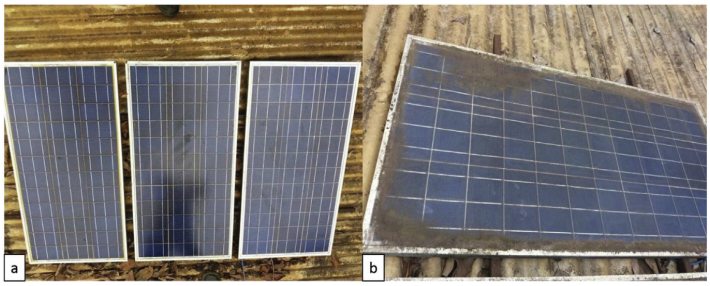

Fig. A.3 – cleaned module surface showing discolouration (a) and condition prior to cleaning (b).

REFERENCES

[1] Watts RL, Smith SA, Dirks JA. Photovoltaic industry progress through 1984. Springfield Virginia: US Department of energy (DOE); 1985.

[2] REN21 Secretariat. Renewables 2017 global status report. Paris: REN21 Secretariat; 2017.

[3] VDMA/ITRPV. International technology roadmap for photovoltaic – 2015 results. 2016.

[4] Adanu KG. Photovoltaic electricity in Ghana—current use and potential for the future. Renew Energy 1991;1(5–6):823–6.

[5] Adanu KG. Promoting photovoltaic electricity usage in developing countries — experience from Ghana. Sol Energy Mater Sol Cell 1994a;34(1–4):67–71.

[6] Adanu KG. Performance of a 268 Wp stand-alone PV system test facility. In: Proceedings of 1994 IEEE 1st world conference on photovoltaic energy conversion – WCPEC (A Joint Conference of PVSC, PVSEC and PSEC), Hawaii; 1994.

[7] Essandoh-Yeddu J. Photovoltaic R&D and applications in Ghana: current status and prospects. In: Conference record of the twenty fifth IEEE photovoltaic specialists conference – 1996, Washington, DC, USA, USA; 1996.

[8] Essandoh-Yeddu J. Current solar energy utilization in Ghana. Renew Energy 1997;10(2–3):433–6.

[9] Energy Commission Ghana. National energy statistics 2007–2016. Accra: Energy Commission Ghana; 2017.

[10] Quansah DA, Adaramola MS, Edwin IA, Anto EK. An assessment of grid-charged inverter-battery systems for domestic applications in Ghana. J Sol Energy 2016;2016.

[11] Government of Ghana. Renewable energy act (Act 832) 2011. Accra: Ghana Publishing Company Ltd, Assembly Press; 2011.

[12] PURC. Publication of feed-in tariffs for electricity generated from renewable energy sources. Accra: PURC; 2013.

[13] Energy Commission Ghana. Net metering sub-code for connecting renewable energy generating systems to the distribution network in Ghana. Accra: Energy Commission Ghana; 2015f.

[14] Energy Commission Ghana. Renewable energy sub-code for distribution network. Accra. 2015.

[15] Energy Commission. Provisional wholesale supply and generation license holders. 2016 [Online]. Available: http://www.energycom.gov.gh/licensing/register-of-licenses. [Accessed 24 August 2016].

[16] PURC. Publication of feed-in-tariff and capacity for electricity generated from renewable energy sources. Accra: Ghana Gazette; 2014.

[17] Makrides G, Zinsser B, Schubert M, Georghiou GE. Performance loss rate of twelve photovoltaic technologies under field conditions using statistical techniques. Sol Energy 2014;103(2014):28–42.

[18] Osterwald C, Adelstein J, del Cueto J, Kroposki B, Trudell D, Moriarty T. Comparison of degradation rates of individual modules held at maximum power. In: 4th IEEE world conference on photovoltaic energy conversion, Hawaii; 2006.

[19] King DL, Quintana MA, Kratochvil JA, Ellibee DE, Hansen BR. Photovoltaic module performance and durability following long-term field exposure. Prog Photovolt Res Appl 2000;8(2):241–56.

[20] Jordan DC, Wohlgemuth JH, Kurtz SR. Technology and climate trends in PV module degradation. In: 27th European photovoltaic solar energy conference and exhibition, September 24–28, 2012, Frankfurt, Germany; 2012.

[21] Skoczek A, Sample T, Dunlop ED. The results of performance measurements of field-aged crystalline silicon photovoltaic modules. Prog Photovolt Res Appl 2009:227–40.

[22] Peike C, Hoffmann S, Dürr I, Weiß K-A, Bogdanski N, Köhl M. PV module degradation in the field and in the lab - how does it fit together?. In: Proceedings of 29th european photovoltaic solar energy conference and exhibition, Amsterdam; 2014.
[23] Jordan DC, Kurtz SR. Photovoltaic degradation rates—an analytical review. Prog Photovolt 2013:12–29.
[24] Jordan DC, Kurtz SR, VanSant K, Newmiller Jeff. Compendium of photovoltaic degradation rates. Prog Photovolt Res Appl 2016;24(7):978–89.
[25] Phinikarides A, Kindyni N, Makrides G, Georghiou GE. Review of photovoltaic degradation rate methodologies. Renew Sustain Energy Rev 2014;40:143–52.
[26] Bandou F, Arab AH, Belkaid MS, Logerais P-O, Riou O, Charki A. Evaluation performance of photovoltaic modules after a long time operation in Saharan environment. Int J Hydrogen Energy 2015;40(39):13839–48.
[27] Radue C, van Dyk E. Degradation analysis of thin film photovoltaic modules. In: Proceedings of the third South African conference on photonic materials; 2009.
[28] Ibrahim IMS, Abouhdima I, Gantrari MB. Performance of thirty years stand alone photovoltaic system. In: Proceedings of 24th European photovoltaic solar energy conference, 21–25 September 2009, Hamburg, Germany; 2009.
[29] Jacobson A, Duke R, Kammen DM, Hankins M. Field performance measurements of amorphous silicon photovoltaic modules in Kenya. In: Proceedings of the American Solar Energy Society (ASES), June 16–21 2000. USA: Madison Wisconson; 2000.
[30] Kahoul N, Houabes M, Sadok M. Assessing the early degradation of photovoltaic modules performance in the Saharan region. Energy Convers Manag 2014:320–6.
[31] Ndiaye A, Kébé CMF, Charki A, Ndiaye PA, Sambou V, Kobi A. Degradation evaluation of crystalline-silicon photovoltaic modules after a few operation years in a tropical environment. Sol Energy 2014;103.
[32] Radue C, van Dyk E. A comparison of degradation in three amorphous silicon PV module technologies. Sol Energy Mater Sol Cell 2010;94(3):617–22.
[33] Ndiaye A, Kébé CMF, Ndiaye PA, Charki A, Kobi ASV. A novel method for investigating photovoltaic module degradation. In: Energy procedia – TerraGreen 13 international conference 2013-advancements in renewable energy and clean environment; 2013.
[34] Agbomahena M, Douhéret O, Kounouhewa B, Vianou A, Norbert A, Lazzaroni R. Ageing of organic photovoltaic devices in Benin environment (South-Sudanese climate). Sol Energy Mater Sol Cell 2013;117:93–7.
[35] Koffi HA, Kakane VCK, Kuditcher A, Hughes AF, Adeleye M, Amuzu J. Seasonal variations in the operating temperature of silicon solar panels in southern Ghana. Afr J Sci Technol Innov Develop 2015;7(6):485–90.
[36] Quansah DA, Adaramola MS, Appiah GK. Performance analysis of different grid-connected solar photovoltaic (PV) system technologies with combined capacity of 20 kW located in humid tropical climate. Int J Hydrogen Energy 2017;42(2017):4626–35.
[37] Quansah DA, Adaramola Muyiwa S, Takyi G, Edwin IA. Reliability and degradation of solar PV modules—case study of 19-year-old polycrystalline modules in Ghana. Technologies 2017;5(22).
[38] PVsyst SA. PVSyst photovoltaic software. 2012.
[39] Osterwald C. Standards, calibration, and testing of PV modules and solar cells. In: Markvart T, Castaner L, editors. Practical handbook of photovoltaics: fundamentals and applications. Elsevier; 2003. p. 794–809.
[40] Starr MR, Palz W. Photovoltaic power generation (solar energy R&D in the European community) – an assessment study. Dordrecht: D. Reidl Publishing Company; 1983.
[41] Ferrara C, Philipp D. Why do PV modules fail?. In: International conference on materials for advanced technologies 2011, symposium O; 2012.
[42] Dhere NG. Reliability of PV modules and balance-of-system components. In: Conference record of the thirty-first IEEE photovoltaic specialists conference, 2005. Lake Buena Vista, FL, USA, USA; 2005.
[43] Quintana MA, King DL, McMahon TJ, Osterwald CR. Commonly observed degradation in field-aged photovoltaic modules. 2002.
[44] NASA. "NASA surface meteorology and solar energy – location". 2017 [Online]. Available: https://eosweb.larc.nasa.gov/cgi-bin/sse/grid.cgi?email=skip@larc.nasa.gov. [Accessed 9 September 2017].
[45] TRITEC Group. Product overview, control and measuring instruments – TRITEC TRI-KA. 2017 [Online]. Available: http://www.tritec-energy.com/en/control-and-measuring-instruments/tri-ka-the-mobile-characteristics-analyser-now-even-more-efficient-c-62/. [Accessed 13 September 2017].
[46] Anderson JA. Photovoltaic translation Equations: a new approach. Colorado: NREL; 1996.
[47] Arndt R, Puto R. Basic understanding of IEC standard testing for photovoltaic panels. TÜV SÜD America Inc.; 2009.
[48] Sharma V, Sastry O, Kumar A, Bora B, Chandel S. Degradation analysis of a-Si, (HIT) hetro-junction intrinsic thin layer silicon and m-C-Si solar photovoltaic technologies under outdoor conditions. Energy 2014;72:536–46.
[49] Sandstrom JD. A method for predicting solar cell current-voltage curve characteristics as a function of incident solar intensity and cell temperature. In: Sixth photovoltaic Specialist conference, Cocoa Beach, Florida; 1967.
[50] Hishikawa Y, Tsuno Y, Kurokawa K. Translation of the I–V curves of various solar cells by improved linear interpolation. In: 21st European photovoltaic solar energy conference, 4–8 September, Dresden, Germany; 2006.
[51] Marion B. A method for modeling the current–voltage curve of a PV module for outdoor conditions. Prog Photovolt Res Appl 2002;10:205–14.
[52] Marion B, Rummel S, Anderberg A. Current-voltage curve translation by bilinear interpolation. Prog Photovolt Res Appl 2004;12:593–607.
[53] Tsuno Y, Hishikawa Y, Kurokawa K. Translation equations for temperature and irradiance of the I-V curves of various PV cells and modules. In: IEEE 4th world conference on photovoltaic energy conference, Waikoloa, Hawaii; 2006.
[54] Duck BC, Fell CJ, Marion B, Emery K. Comparing standard translation methods for predicting photovoltaic energy production. In: Proceedings 39th IEEE photovoltaic Specialists conference, June 16–21, 2013, Tampa Florida; 2013.
[55] Smith MR, Jordan CD, Kurtz RS. Outdoor PV module degradation of current-voltage parameters. NREL; 2012.
[56] Kaplanis S, Kaplani E. Energy performance and degradation over 20 years performance of BP c-Si PV modules. Simulat Model Pract Theor 2011;19:1201–11.
[57] Herrmann W, Wiesner W. Current-voltage translation procedure for PV generators in the German 1,000 roofs-programme. CiteSeerX; 2014.
[58] van Dyk EE, Meyer EL. Analysis of the effect of parasitic resistances on the performance of photovoltaic modules. Renew Energy 2004;29:333–44.
[59] Jia Q, Anderson WA. A novel approach for evaluating the series resistance of solar cells. Sol Cell 1988;25(3):311–8.
[60] Bashahu M, Habyarimana A. Review and test of methods for determination of the solar cell series resistance. Renew Energy 1995;6(2):129–38.
[61] Pysch D, Mette A, Glunz SW. A review and comparison of different methods to determine the series resistance of solar cells. Sol Energy Mater Sol Cell 2007;91(18):1698–706.

[62] IEA. Review of failures of photovoltaic modules. IEA/OECD; 2014.
[63] Sastry OS, Saurabh S, Shil SK, Pant PC, Kumar R, Kumar A, et al. Performance analysis of field exposed single crystalline silicon modules. Sol Energy Mater Sol Cell 2010;94(9):1463–8.
[64] Rajput P, Tiwari GN, Sastry OS, Bora B, Sharma V. Degradation of mono-crystalline photovoltaic modules after 22years of outdoor exposure in the composite climate of India. Sol Energy 2016;135:786–95.
[65] Pozza A, Sample T. Crystalline silicon PV module degradation after 20 years of field exposure studied by electrical tests, electroluminescence, and LBIC. Prog Photovolt Res Appl 2016;24:368–78.
[66] Chandel SS, Naik MN, Sharma V, Chandel R. Degradation analysis of 28 year field exposed mono-c-Si photovoltaic modules of a direct coupled solar water pumping system in western Himalayan region of India. Renew Energy 2015;78:193–202.
[67] Jordan D, Silverman T, Kurtz S. Degradation (rates) curves. In: Progress & frontiers in PV performance. Las Vegas: Nevada; 2016.
[68] Kajari-Schröder S, Kunze I, Köntges M. Criticality of cracks in PV modules. In: SiliconPV 2012, Leuven, Belgium; 2012.
[69] Kurtz S, Wohlgemuth J, Kempe M, Bosco N, Hacke P, Jordan D, et al. Qualification plus performance and durability tests beyond IEC 61215. NREL; 2014.
[70] Watson S. Service life of electrical cable and condition monitoring methods. Gaithersburg, Maryland: National Institute of Standards and Technology (NIST); 2012.
[71] Government of Ghana. Hazardous and electronic waste control and management act, Act 917 of 2016. Accra: Ghana Publishing Company Ltd; 2016.
[72] IRENA/IEA. End-of-Life management: solar photovoltaic panels. 2016.
[73] McMahon TJ, Basso T, Rummel SR. Cell shunt resistance and photovoltaic module performance. Washington DC. 1996.
[74] Hernday P. Field applications of I-V curve tracers in the solar PV industry. IEEE; 2012.
[75] Rabii AB, aidi Jr M, Bouazzi AS. Investigation of the degradation in field-aged photovoltaic modules. Osaka. 2003.
[76] Belmont J, Olakonu K, Kuitche J, TamizhMani G. Degradation rate evaluation of 26-year-old 200 kW power plant in a hot-dry desert climate. Denver, CO, USA. 2014.
[77] Polverini D, Field M, Dunlop E, Zaaiman W. Polycrystalline silicon PV modules performance and degradation over 20 years. Prog Photovolt 2012;21(5):1004–15.
[78] Sánchez-Friera P, Piliougine M, Peláez J, Carretero J, Sidrach de Cardona M. Analysis of degradation mechanisms of crystalline silicon PV modules after 12 years of operation in Southern Europe. Prog Photovolt 2011;19(6):658–66.
[79] Limmanee A, Udomdachanut N, Songtrai S, Kaewniyompanit S, Sato Y, Nakaishi M, et al. Field performance and degradation rates of different types of photovoltaic modules: a case study in Thailand. Renew Energy 2016;89:12–7.
[80] Ye JY, Reindl T, Aberle AG, Walsh TM. Performance degradation of various PV module technologies in tropical Singapore. IEEE J Photovolt 2014;4(5):1288–94.
[81] Jordan DC, Silverman TJ, Sekulic B, Kurtz SR. PV degradation curves: non-linearities and failure modes. Prog Photovoltaics Res Appl 2017;25:583–91.

Paper 3

Renewable Energy 131 (2019) 900–910

Contents lists available at ScienceDirect

Renewable Energy

journal homepage: www.elsevier.com/locate/renene

Assessment of early degradation and performance loss in five co-located solar photovoltaic module technologies installed in Ghana using performance ratio time-series regression

David A. Quansah [a, b, c], Muyiwa S. Adaramola [a, *]

[a] Renewable Energy Group, Faculty of Environmental Sciences and Natural Resource Management, Norwegian University of Life Sciences (NMBU), 1433 Ås, Norway
[b] Department of Mechanical Engineering, Kwame Nkrumah University of Science and Technology (KNUST), Kumasi, Ghana
[c] The Brew-Hammond Energy Centre, Kwame Nkrumah University of Science and Technology (KNUST), Kumasi, Ghana

ARTICLE INFO

Article history:
Received 12 April 2018
Received in revised form
20 July 2018
Accepted 23 July 2018
Available online 24 July 2018

Keywords:
Early degradation
Performance ratio
Crystalline silicon module
Thin-film module
Ghana

ABSTRACT

Long-term performance degradation in solar photovoltaic modules is generally understood to be linear. Nevertheless, there is increasing acknowledgement of sharper performance decline within the early periods of exposure. Emerging industry trend is geared toward providing multi-staged warranties that provide assurances of both early-period module output and longer-term performance. While studies on performance degradation are increasing in the open literature, there remains significant geographical imbalance. Moreover, many of the studies available are based on discrete measurements, with few resulting from continuous monitoring. This paper presents the outcome of analysis conducted to explore performance degradation of five solar photovoltaic module technologies within the first 14 months of installation in Kumasi Ghana. Based on time-series regression of the performance ratios, early degradation ranged from 8% to 13.8% of initial performance. Technologies studied were amorphous silicon, mono-crystalline silicon, polycrystalline silicon, Copper Indium Sulfide and hybrid Heterojunction with intrinsic Thin-layer (HIT).

1. Introduction

Solar photovoltaic (PV) modules experience performance decline over time once they are installed in the field and hence, exposed to real life weather conditions, which is different from those of laboratory test conditions. Over its lifetime, a PV module experiences various environmental and operational stresses that affect the integrity of its constituent materials and hence, overall performance (that is, energy yield and longevity). Some of these stresses include high/low temperature (and associated thermal cycling), moisture, UV radiation and high voltage [1,2]. Understanding performance degradation rates is important for realistic financial modelling of Solar PV projects. In addition, knowledge of mechanisms of degradation and failure on field serve as important input information for PV Research and Development (R&D) Institutes and for national and international agencies that are involved in the development of qualification test series for market entry of solar modules [3]. Researchers are increasingly studying PV module degradation, even though available research publications and data are geographically unbalanced [4].

Many studies have reported module performance degradation on the basis of average annual percentage (%) decline, and generally assume linearity, that is, it degrades at a constant rate over its lifetime (in relation to initial rated power). Indeed, industry warranty provisions are typically based on linear degradation assumptions, even though multi-staged warranties are becoming common in recent years [5–7]. In spite of the linearity assumptions embedded in many studies, it widely acknowledged, that, modules experience an initial phase of rapid degradation upon exposure to sunlight, in what is commonly referred-to as Light-Induced Degradation (LID). The LID is attributed to the Staebler-Wronski Effect (SWE) in amorphous silicon modules while its occurrence in crystalline silicon is attributed to the formation of oxygen-boron complex in p-type semi-conductors as a result of oxygen traces in molten silicon produced from the Czochralski process [8,9]. The duration of this initial degradation varies widely and depends on

* Corresponding author.
E-mail address: muyiwa.adaramola@nmbu.no (M.S. Adaramola).

https://doi.org/10.1016/j.renene.2018.07.117
0960-1481/

factors such as cell technology, method of production and irradiation at location [9,10]. The IEC 61215 qualification test process (for crystalline Si) anticipates this phenomenon by incorporating light-soaking stages in which one of eight sampled modules is exposed to 60 kWh/m^2 of outdoor irradiation (stage 10.8) [11]. All eight modules are however subjected to pre-conditioning irradiation of 5 kWh/m^2. As done for x-Si modules, thin-film technologies also undergo a light-soaking procedure, which entails exposure to outdoor irradiation of 60 kWh/m^2 (stage 10.8) (IEC 61646). In addition, thin films undergo a final light soaking stage in which they are placed under an irradiance of 600–1000 W/m^2 and a temperature range of 50 °C ± 10 °C until stabilization occurs (stage 10.19). According to IEC 61646 protocol, stability is deemed to have occurred when measurements of P_{max} (nominal power) from two consecutive periods of exposure, of at least 43 kWh/m^2 each satisfies the condition [11] (Equation (1)):

$$\frac{P_{max} - P_{min}}{P_{average}} < 2\% \quad (1)$$

Where P_{max}, P_{min} and $P_{average}$ are respectively, the maximum, minimum and average values of measured nominal power.

A number of researchers have studied the phenomenon of early degradation in solar PV modules with the view to quantifying early losses and determining when stability is attained. For example, Kenny et al. [12] studied P_{max} changes in different thin-film modules during light-soaking and suggest that irradiation level of up to 560 kWh/m^2 is required for stabilization, depending on the thin-film technology [10,12]. King et al. [13], in a study on performance characteristics of commercial amorphous silicon modules, considered stabilized power as the power level achieved after about one year of exposure and midway between seasonal oscillations. Radue and van Dyk [14] found losses of up to 30% in thin film systems installed in South Africa after 14 months. Ndiaye et al. on the other hand reported degradation of 0.22%/year for mono-silicon modules installed in Dakar Senegal after 1.3 years of exposure. Several other researchers have also explored the subject of early degradation in photovoltaic modules (e.g. Makrides and Zinsser [15], Munoz et al. [16], Hussin et al. [17]). In view of the initial rapid degradation, Jordan and Gotwalt [18] have suggested a non-linear model to describe degradation in solar PV modules. They propose a model that comprises an exponential decay component and a two-term Fourier series approximation.

The objective of this paper is to examine early performance loss observed in five different co-located solar PV module technologies installed in Kumasi, Ghana, within the first 14 months of exposure (to a hot and humid climate). Moreover, as Jordan and Kurtz [19] have observed, many of the studies available are based on discrete observations rather than continuous monitoring. This paper further seeks to contribute results based on continuous monitoring (rather than discrete) over the stated period from a geographical region that is under-represented in published research work on solar PV performance and degradation studies. This paper is organized into four (4) sections. Section 1 (this current section) provides an introduction and background to this paper. It attempts to highlight the importance of Solar PV performance degradation studies, with particular emphasis on degradation in the early period of exposure. A description of the system under study, as well as the methodology adopted in preparation of data and computational methods are presented in Section 2. The third section (Section 3) presents the results obtained and discusses them within the context of studies undertaken by other researchers. The key finding of this study are summarized in Section 4.

2. Methodology

2.1. Systems description

The grid-connected solar PV systems under study (shown in Fig. 1) were installed in March 2012 with support from the World Bank Africa Renewable Energy and Access program (AFREA) (Project P120478, TF 096613). This project was part of efforts to enhance the capacity of the Kwame Nkrumah University of Science and Technology (KNUST) and its partners in renewable energy research and education. The installation comprises five module technologies with combined capacity of 20 kWp (approximately 4 kWp each). The technologies deployed are: amorphous silicon (a-Si), monocrystalline silicon (mc-Si), polycrystalline silicon (pc-Si), hybrid Heterojunction modules with intrinsic Thin-layer (HIT, comprising a-Si and mc-Si), and Copper Indium Sulfide (CIS). The modules for the installation were selected as to include both thin-film and crystalline technologies, as well as silicon-based and non-silicon based technologies. Peak power of the modules were in the range of 50 Wp - 225 Wp, and have power temperature coefficients of −0.2%/K to −0.47%/K. Further technical characteristics of the modules are shown in Table 1. Each installation is, separately connected to the distribution grid via Sunny Boy SB3800 DC-AC inverters with integrated MPP trackers. The characteristics of the SB3800 inverters are shown in Table 2. The climate of Kumasi (as shown in Table 3) is characterized by high humidity (Rel. Hum. 65%–83.5%) and ambient air temperature of 24.4 °C - 27.8 °C. Daily irradiation on an annual basis averages 4.34 kWh/m^2 (range: 3.35–5.09 kWh/m^2). Average annual wind speeds at the location (10 m height) is 2 m/s, with lowest values recorded in the months of November, December and January (Table 3). Precipitation records a peak of 6.55 mm/day in June and records lowest values in December and January.

Module temperatures are measured with PT100 thermocouples, which are attached to the rear side of the modules. Environmental variables such as ambient temperature and plane-of-array irradiance are measured with the Sunny SensorBox from SMA. Performance data from the inverters, as well as environmental data from the SensorBox are recorded to the Sunny WebBox data logger. Further description of the installation is provided in Ref. [20].

2.2. Data cleaning and preparation

The data is logged at a 5-min time resolution, resulting in 288 data points per day and about 8640 data points per 30-day month. The data collected include power, current and voltage (AC and DC), module temperature, ambient temperature, grid frequency and operating hours of the systems. The data for each month is stored in a folder comprising csv (comma-separated values) files, which hold daily readings. In Ghana, as in many developing countries, power outages are frequent; and as such when this happens, the daily csv

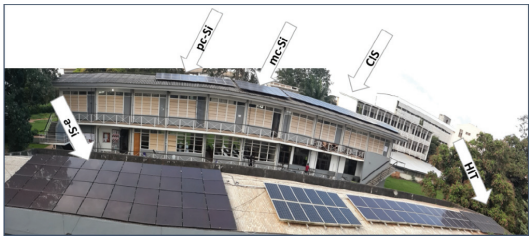

Fig. 1. Picture of 20 kWp installation at KNUST, Kumasi Ghana. Adapted from Ref. [20].

Table 1
System description and technical characteristics of modules.

Parameter	a-Si[a]	mc-Si	HIT	CIS	pc-Si
Module Type	SCHOTT ASI 100	SCHOTT MONO 190	SANYO H250	SULFURCELL SCG50–HV	SCHOTT POLY 225
Module power, P_{max}, (W)	100	190	250	50	225
P_{max} tolerance	0 W/+1.99 W	0 W/+4.99 W	(+10%/−5%)	±5%	0 W/+4.99 W
Temp. Coeff. (%/K)	−0.2	−0.44	−0.3	−0.3	−0.47
Open-circuit voltage, V_{oc} (V)	40.9	45.2	43.1	50	36.7
Short-circuit current, I_{sc} (A)	3.85	5.46	7.74	1.65	8.24
Voltage at peak power, V_{mpp} (V)	30.7	36.4	34.9	37.5	29.8
Current at peak power, I_{mpp} (A)	3.25	5.22	7.18	1.35	7.55
Module efficiency (%)	6.9	14.5	18	6.1	13.4
NOCT (°C)	49	46	46	47	47.2
Module dimension (mm)	1308 × 1108	1620 × 810	1610 × 861	1258 × 658	1685 × 993
Total capacity (W)	4000	3990	4000	4050	4050

[a] Initial P_{max} of 122 W was provided by manufacturer datasheet.

Table 2
SB3800 inverter characteristics [21].

Parameter	Value
DC Side	
Maximum DC power	4040 W
MPP voltage range	200–400 V
Minimum input voltage	200 V
Rated input voltage	200 V
Maximum input current	20 A
AC Side	
Rated power at 230 V, 50 Hz	3800 W
Maximum apparent AC power	3800 W
AC nominal voltage	220 V/230 V/240 V
AC voltage range	180 V - 265 V
Maximum efficiency, η_{max}	95.6%
European weighted efficiency, η_{EU}	94.7%

files are broken up. Therefore, a particular day could have up to five (5) files representing various periods of continuous operation. This also sometimes results in the shifting of column headings in the csv files. In the aggregation of data for each day, the "EXACT" command in MS Excel was used to test for the exactness of the column headings. This helped in ensuring that column headings were well-aligned, thereby eliminating possible human error. This procedure was repeated for each day of the month (for all 14 months). The aggregation of monthly data also followed the same procedure. As the system was connected to the grid on 20 March 2012, this day was labelled as day number one in the analysis, and similarly, March 2012 was labelled as month number one. As the accuracy of analysis is enhanced when the data used is close to peak conditions, only irradiance of 700 W/m^2 and above were retained for further analysis.

The data was further subsetted with the view to eliminating data points that do not represent optimal performance of the system. Myers [24] adopted a filtering criteria, which established a minimum power output ratio of 1.2 times the in-plane irradiance for a 1.6 kWp system installed at Golden Colorado (USA). This ratio is based on the expectation of 1.6 kW of output under irradiance condition of 1 kW/m^2 for this particular installation (a maximal power: irradiance ratio of 1.6 kW: 1 kW/m^2 under STC conditions). The threshold of 1.2 times the irradiance is approximately 75% of the expected output under peak conditions. Below this value, Myers [24] considered the system to operating in non-standard mode, due to factors such as shadowing or snow. Following the example of Myers [24], a minimum irradiance-power ratio of 1:2.8 is adopted for the 4 kWp systems under study (i.e. 1 kW/m^2 irradiance should produce no less than 2.8 kW of module power). This represents a minimum acceptable performance ratio threshold of 70% for all technologies considered in this study. Similarly, an upper limit of 1:4.8 (irradiance-power ratio) is set for each of the systems. Since this data is based on system-level monitoring and presume efficient tracking of maximum power point (MPP) by the inverters, these criteria also contribute to eliminating off-MPP performance data.

2.3. Data analysis

Performance ratio is a widely used metric for the performance assessment of solar photovoltaic installations. It normalizes the output of the PV system to its installed capacity and to available irradiance at the location, thereby enabling the comparison of the performance of systems of various installed capacities in different

Table 3
Climate data for Kumasi Ghana (lat 6.7°, long −1.6°).

Month	Daily Insolation (Horiz.), kWh/m2	RH, %	Precipitation (mm/day)	Wind speed m/s @ 10 m	Air Temp °C
January	4.18	65.0%	0.42	1.5	26.1
February	4.68	66.5%	1.12	2.1	27.2
March	5.04	71.0%	2.88	2.1	27.8
April	5.09	77.0%	4.55	2.1	27.2
May	4.97	79.5%	5.11	2.1	26.7
June	4.38	82.5%	6.55	2.1	26.1
July	3.67	83.5%	3.93	2.6	24.4
August	3.35	83.5%	3.07	2.1	24.4
September	3.80	83.0%	4.63	2.1	24.4
October	4.44	82.0%	4.83	2.1	25.6
November	4.66	76.0%	2.02	1.5	26.1
December	3.87	73.0%	0.83	1.5	25.6
Annual Av.	4.34	76.9%	3.33	2.0	26.0

Ref. [22,23].

geographical locations. The instantaneous performance ratio p_r may be determined as (Equation (2)):

$$p_r = \frac{y_f}{y_r} = \frac{P/P_{inst}}{G/G_o} \quad (2)$$

Where y_f is the final yield and y_r, the reference yield. The final yield normalizes the power output P to the PV system installed capacity, P_{inst}, while the reference yield normalizes the plane-of-array irradiance G to the irradiance under Standard Test Conditions (STC), (i.e. $G_o = 1000\ W/m^2$). In addition, performance ratio may be expressed in terms of energy output over a given period (e.g. hourly, daily, monthly or yearly). To account for the impact of temperature on the performance ratio and to minimize the impact of seasonal variations, a temperature-corrected performance ratio is defined as (Equation (3)):

$$p_{rT} = \frac{p_r}{1 + \gamma(T - 25)} \quad (3)$$

Where γ is the temperature coefficient of power (%/°C) and T (°C) is the module temperature. The temperature-corrected performance ratio is useful in forecasting output of PV systems, since it also captures thermal behaviour of the installation. Changes in its value over time points towards changes in underlying physical reality [25], and has therefore been used in studying performance degradation in installations [26–30].

The PV for Utility Systems Application (PVUSA) multiple linear regression model is also widely used ([4,31,32]) in long-term performance monitoring. It regresses plane-of-array irradiance (G), ambient temperature (T_{amb}) and wind speed (w_s) on power output (P) (Equation (4)).

$$P = G(a_1 + a_2 G + a_3 T_{amb} + a_4 w_s) \quad (4)$$

where a_1, a_2, a_3, and a_4 are regression constants derived from operational data. Systems are assigned PTC (PVUSA Test Conditions) ratings, which correspond to performance at 1000 W/m^2 (irradiance), 1 m/s (wind speed) and 20 °C (ambient temperature). The PVUSA method was developed among others to overcome challenges with extrapolation to STC conditions, which was thought to unfairly benefit technologies with higher temperature coefficients (Kimber et al. [33]). The PTC conditions were considered to be closer to actual field operating conditions. For example, ambient temperature of 20 °C is reported by Jordan and Kurtz [34] as being approximately equivalent to typical module operating temperature of 45 °C in the climate of Colorado USA. The operating conditions of the modules under study hardly make these PVUSA assumptions valid. For instance, ambient temperature of the valid data obtained for the installation is 34 °C with median module temperature of 58 °C, in the case of the CIS system, as an example (see Fig. 2).

In addition to these two approaches, classical seasonal decomposition and autoregressive integrated moving average methods have also been used in the literature for studies on PV module degradation rates, based on their ability to model and capture trends embedded in seasonal variation of module performance [27]. Typically, however, 3–5 years of data is required to capture seasonal variations. Sorloaica-Hickman et al. [32] used both PR regression and PVUSA methods to study performance degradation, based on both AC and DC power measurements. Their results showed similar degradation rates when both methods were applied. They also examined the effect of filtering in different irradiance bands (500–1200 W/m^2) and (800–1200 W/m^2) and found average difference of 0.02% for the PR method and 0.33% in the PVUSA approach. Makrides and Zinsser [15] observed four PV module technologies comprising mono-crystalline silicon (including Sanyo mono c-Si HIT), multi-crystalline silicon and amorphous silicon installed in Nicosia, Cyprus over a period of 1 year, and found early degradation of mono-crystalline silicon of 2.12%–4.73%, multi-crystalline of 1.47%–2.40%, amorphous silicon of 13.82% and Sanyo mono c-Si HIT of 4.73%. They used the both the PVUSA and PR regression methods with irradiance of 800 W/m^2 and above.

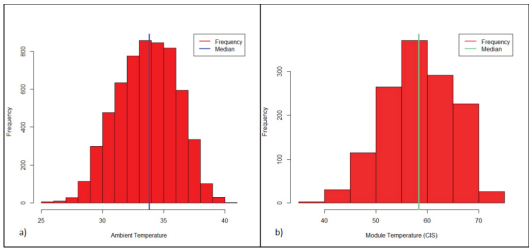

Fig. 2. (a) Ambient temperature and (b) module temperature distribution of CIS.

In this present paper, the monthly PR regression method is adopted and performance data is sorted for irradiance levels greater than 700 W/m^2. Following the examples of [17,26,28,30], the degradation rate (DR) is computed as (Equation (5)).

$$DR = \frac{m \times 12}{c} \times 100\% \quad (5)$$

Where m and c are, respectively, the slope and intercept of the linear trend line of the performance ratio (PR) versus time (in months) plot. Depending on the temporal resolution of data used in the regression, Equation (5) can be modified accordingly. For example, the slope is multiplied by 365, instead of 12, when the regression is based on daily PR values [35]. It has been noted (e.g. Meydbray et al. [36] and Reich et al. [37]), that, reference cell based PR measurements tend to be 2–4% higher than those based on pyranometer measurements. Nevertheless, these differences are systematic in nature. It should be mentioned, that, there were gaps in module temperature data records and this resulted in some monthly PR values not having corresponding temperature-corrected values. This, notwithstanding, the remaining data were used to establish trend lines for temperature-corrected PR. Prolonged data loss which occurred after the initial 14-month period influenced the cut-off point chosen for this study on early performance degradation.

3. Results and discussion

3.1. Results

The PR-based regression charts for all five technologies (CIS, a-Si, mc-Si, pc-Si and HIT) are shown in Figs. 3–7. They are shown for both temperature-corrected PR and uncorrected PR (e.g. CIS and CIS-25). For all technologies, and as expected, the temperature corrected PR values are systematically higher, since ambient temperature for the location makes cell operating temperatures much higher than 25 °C at which the modules were rated. The median monthly PR of the CIS system varied between 70% and 77% in the first few months of operation, while temperature-corrected PR (PR_25) ranged between 78.7% and 84%, suggesting temperature-related losses of about 7.85%, on average, for this module

technology (Fig. 3). Amorphous silicon technology, the other thin-film technology installed shows uncorrected PR varying between 80.4% and 94.8%, and 84.8%–99% when corrected for temperature-related losses. Similarly, for mc-Si, pc-Si and HIT respectively (Figs. 4–6), the uncorrected (*and temperature-corrected*) PR values varied between: 70.4%–77.9% *(81.1% - 88.3%)*; 73.8%–87.6% *(84.5% - 96.0%)*; and 72%–85.6% *(78.3% - 91.6%)*. The median PR over the observation period (including temperature-corrected PR) and the temperature-related losses for the various technologies are summarized in Table 4. As may be reasonably anticipated from the temperature co-efficient values (Table 1), crystalline silicon technologies exhibited the highest temperature-related losses (about 10.1%, on average, for both Silicon technologies). It should be noted that these PR values are not representative of the overall performance of the PV systems, since they exclude all performance data recorded at irradiance levels below 700 W/m^2. Nonetheless, it points to the relative performance of the technologies, as earlier reported in Ref. [20].

Based on the linear trend lines (shown on Figs. 3–7) and Equation (5), degradation rates in the first year of exposure, ranged from 7.9% to 13.8% based on monthly uncorrected PR regression (Table 5). The range widens slightly to 6.1%–13.7% when temperature-corrected PR values are used, even though its values are generally lower compared to the uncorrected PR values. Amorphous silicon showed the highest decline within the time-frame considered in this study, of 13.8%, which is consistent with expectations, based on the much-studied phenomenon of light-induced degradation. Crystalline silicon-based technologies in this study had performance loss in the region of 8%–9% based on uncorrected PR values. This reduces slightly to 6%–8% based on the corresponding temperature-corrected PR values. The HIT system, which is based on a hybrid a-Si and mc-Si PV module technology, experienced loss of 11%, which lies between the losses found for a-Si and x-Si (Table 3). Even though the amorphous silicon technology had the highest decline (13.8%), the variability in the month-on-month performance appears to decline after the first five months (Fig. 4), suggesting some resilience to seasonal variability. The monthly variability in the other technologies – mc-Si, pc-Si and HIT – are however more pronounced and result in lower R^2 values (Figs. 5–7). This variability could be the result of number of factors, including dust accumulation and the cleaning effect of rains, temporal shading and the effect of inverter operation off the maximum power point. In the case of Fig. 6 (for pc-Si), the extra deviations from the line of best-fit for the months numbered 5 and 11 could due to bias in the data, as these months had fewer valid observations than most months.

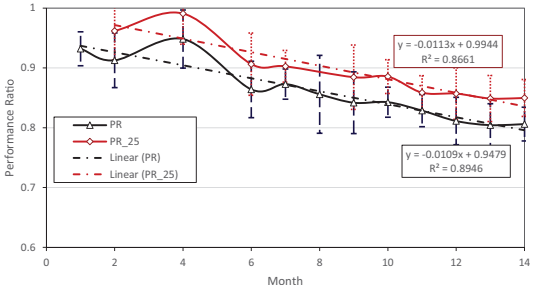

Fig. 4. Monthly PR Regression for a-Si.

The degradation rates decrease slightly for pc-Si (7.8%–8.8%) when daily median values of the PR are used in the regression (Table 6). It decreases much further for CIS, to 3.5%–4.9% (Table 6), compared with 7.3%–9.3% for monthly-based values (Table 3). Degradation values for mc-Si, a-Si and HIT, on the other hand (Table 6) showed increase (8.4%–9.4%, 14.6%–15.3% and 12.4%–13.3% respectively) compared to the counterpart monthly median values in Table 3. While high temporal resolution provides more information on data distribution, it tends to have the disadvantage of a greater number of outliers (Jordan and Kurtz [34]).

In Figs. 8–12, it can be observed that the unexplained variability in the daily data is higher, as evidenced by the lower R^2 values in comparison with the monthly values. The discussion in subsequent sections are therefore based on monthly median data.

3.2. Discussions

The degradation rates for crystalline silicon (mc-Si and pc-Si) found in this study turn out to be much higher than others found in the open literature over similar exposure periods. This study

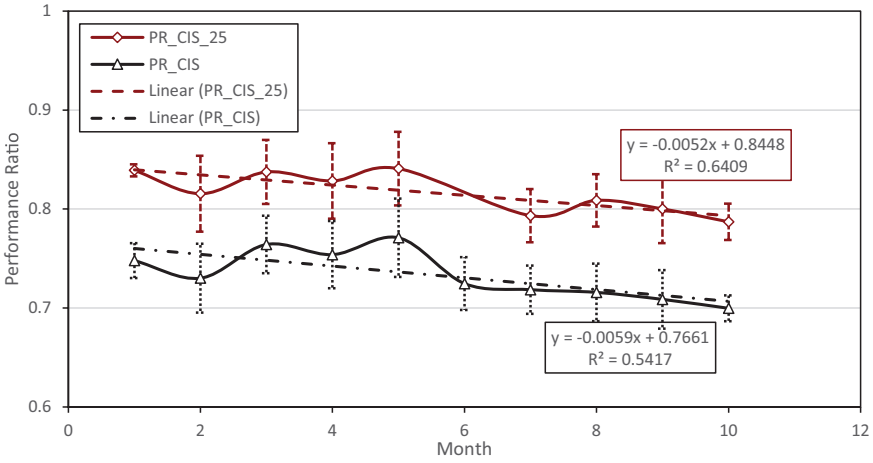

Fig. 3. Monthly PR Regression for CIS.

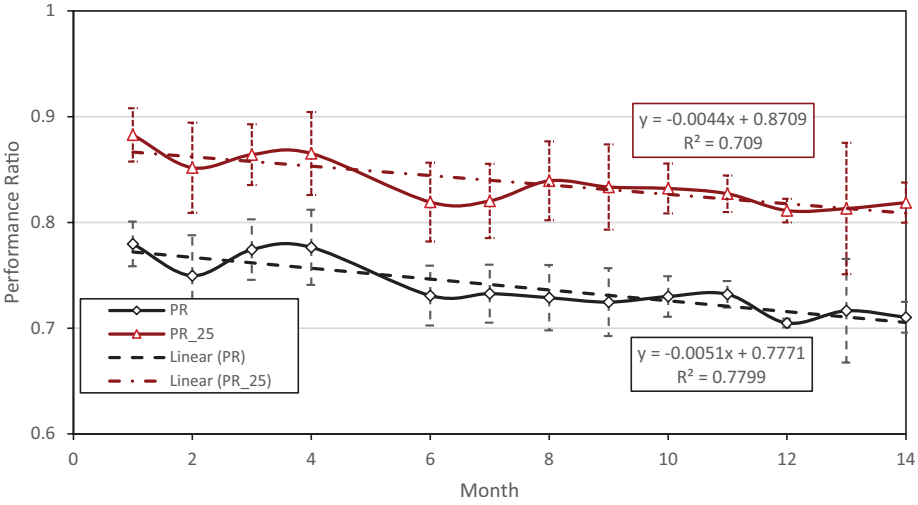

Fig. 5. Monthly PR Regression for mc-Si.

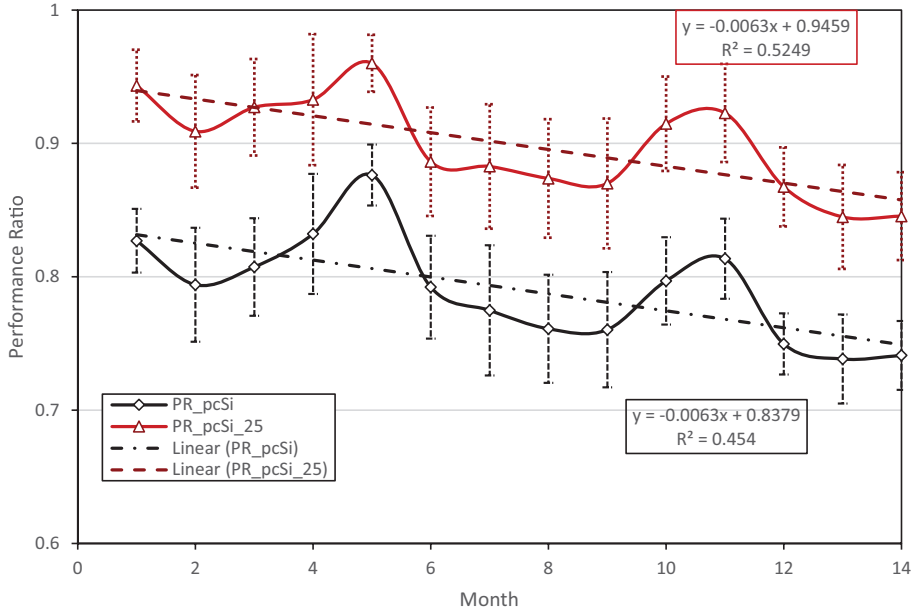

Fig. 6. Monthly PR Regression for pc-Si.

observed degradation of 7.9% for mc-Si and 9% for pc-Si. For example, Makrides and Zinsser [15] found degradation of 1.47%–2.4% for polycrystalline modules in Nicosia (Cyprus) after year of exposure. In the same study, monocrystalline modules (including HIT) recorded degradation of 2.12%–4.73%. While the literature appears to have some agreement that early degradation in crystalline silicon modules are in the range of 0%–4% (Makrides and Zinsser [15], Munoz et al. [16], Vazquez and Rey-Stolle [38] Gostein and Dunn [39]), there is significant divergence on the time-scales within which this occurs. Some studies report this early loss as occurring within few hours of exposure (e.g. Gostein and Dunn [39]); while others report timelines in weeks (Munoz et al. [40]) and up to 1 year (Vazquez and Rey-Stolle [38]).

This study found an uncorrected degradation rate of 13.8% for a-Si (as shown in Table 5), which coincides with what Makrides and Zinsser [15] also reported for a-Si (13.8%) over a similar period.

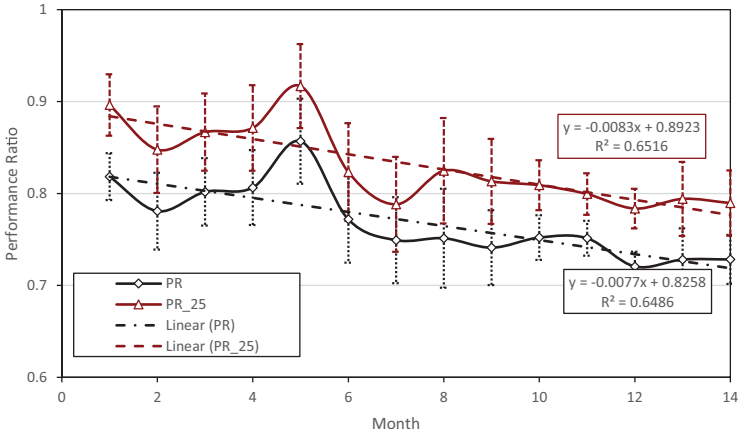

Fig. 7. Monthly PR Regression for HIT

Table 4
Median Performance Ratio of technologies.

Technology	PR (%)	PR_25 (%)	T_losses (%)
mc-Si	74.27	84.15	9.89
pc-Si	79.03	89.86	10.83
a-Si	86.84	90.49	3.64
HIT	76.84	83.03	6.19
CIS	73.01	81.18	8.17

Table 5
Performance loss based on monthly median data.

Technology	Year 1 loss (PR) (%)	Year 1 loss (PR_25) (%)
CIS[a]	9.3	7.3
a-Si[a]	13.8	13.7
mc-Si	7.9	6.12
pc-Si	9.0	8.0
HIT	11.1	11.1

[a] Temperature-corrected PR has less data points than uncorrected PR.

Table 6
Performance loss based on daily median data.

Technology	Year 1 loss (PR) (%)	Year 1 loss (PR_25) (%)
mc-Si	9.4	8.4
pc-Si	8.8	7.8
a-Si	15.3	14.6
HIT	13.3	12.4
CIS	4.9	3.5

These losses are, however, lower than degradation rate of 20%–30% found (for amorphous silicon) by Rüther et al. [41] in their round-robin study, which was conducted in four one-year periods across Arizona and Colorado (USA), and Santa Catarina in Brazil. Gostein and Dunn [39] reported a wider range (of 10%–30%) for the early degradation of amorphous silicon, based on a review study. King et al. [12], who examined early degradation in amorphous silicon modules in Albuquerque, USA, observed a similar degradation rate. In their study, King et al. [13] found that the modules lost about 20% of their power before stabilizing. They considered stabilized power as the power achieved after one year and midway between seasonal oscillations. Hussin et al. [17] on the other hand have reported a degradation rate of 4.6%/yr for amorphous silicon based on 16 months of data in Malaysia. Slower post-stabilization period degradation rate might responsible for the comparatively lower rate reported for amorphous silicon in this case. Other authors have reported initial degradation based on shorter time-scales. For instance, Astawa et al. [42] found degradation ranging between 21% and 35% in the first two weeks for amorphous silicon installed in Loughborough in the UK and attributed this to high irradiance conditions and SWE (Staebler-Wronski Effect). The decline then continued for the first 6 months, even though at a slower rate (9–11%). A summary of results from some studies on early photovoltaic module degradation, with the climatic contexts in which they were installed are presented in Table 7.

While studies on initial degradation in thin film technologies have been quite extensive, studies on crystalline silicon (x-Si) systems on the other hand have tended to focus on longer-term performance. Notwithstanding, early degradation in crystalline silicon, the dominant market technology, is an important phenomenon, particularly with cells produced by the Czochralski process [9]. Table 8 summarizes early-stage warranties that module manufacturers are providing to back their products on the market. Even though the data in Table 8 is not scientifically sampled, a majority of manufacturers appear to offer assurances of 97% or more of maximum power within the first year of exposure. This seems to be consistent with the widely reported degradation rate of 0%–4% of maximum power in year 1.

The results of this analysis show that mc-Si had the lowest performance loss (6.12%) in the period of observation. This was followed respectively by CIS (7.3%), pc-Si (8%), HIT (11.1%) and a-Si (13.8%). The order changes slightly when the ranking is done based on uncorrected PR (CIS and pc-Si swap positions, Table 5). However, the temperature-corrected PR regression approach is considered more realistic as it captures the thermal behaviour and other underlying physical realities of the system [25]. It should be noted that the results presented in this study have been based on system level monitoring over a 14-month period. Makrides et al. [27] have rightly observed, that, performance loss, instead of degradation, is a better description of the results obtained from system-level monitoring of grid-connected PV systems. They argue that the performance loss observed in these systems is influenced by other factors besides module degradation (e.g. electrical mismatch, soiling, shading, and losses in balance of system components.).

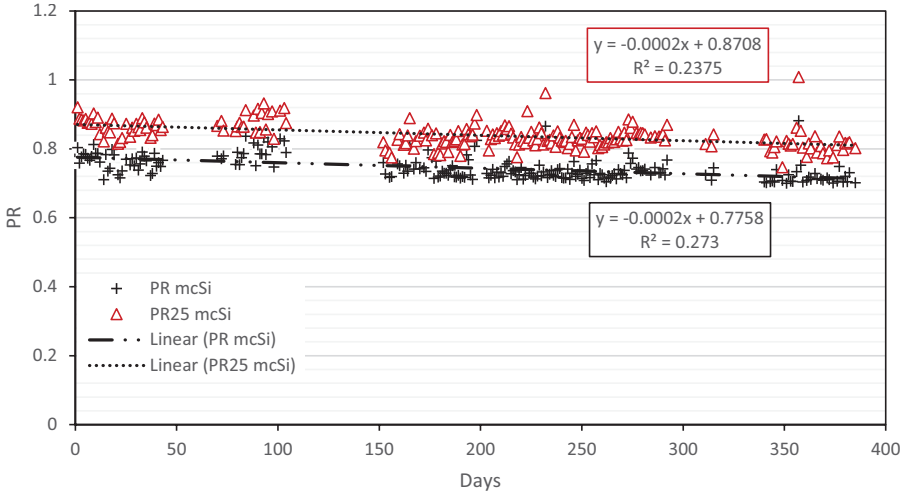

Fig. 8. Daily regression for mono-crystalline silicon.

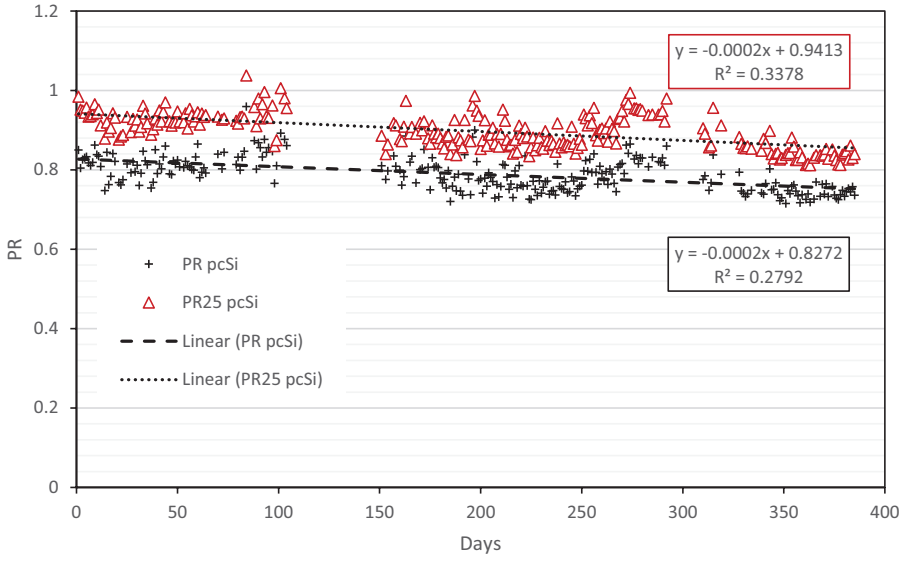

Fig. 9. Daily regression for poly-crystalline silicon.

Compared with results from PV testbeds and controlled measurements such as those found in Ref. [15,16,42], the impact of soiling on the rooftop system under consideration could be a contributor to the higher losses observed (particularly for x-Si). For example, the results presented by Munoz et al. [16] was based on controlled experiments in which modules were characterized using indoor I-V measurements after periods of outdoor exposure. Similarly, Makrides and Zinsser [15], reported results from measurements undertaken at experimental PV test site where modules were cleaned regularly. The results obtained in this present study could therefore be viewed as comprising two components: first, is the actual module degradation and second, a reversible performance loss due to factors such as accumulated soiling and other environmentally induced conditions. Even though these two components cannot be separately quantified by this current study, it is reasonable to expect the second component to vary with factors such as rainfall (self-cleaning of modules) and failure of inverter to track the maximum power point. These therefore introduce additional elements of variability in the observed performance trends (Figs. 3–7). For example, the months of May and June (month numbers 2, 3 and 4) record highest levels of rainfall in Kumasi (Table 3) and as such, the impact of dust and soiling are likely to be reduced in these

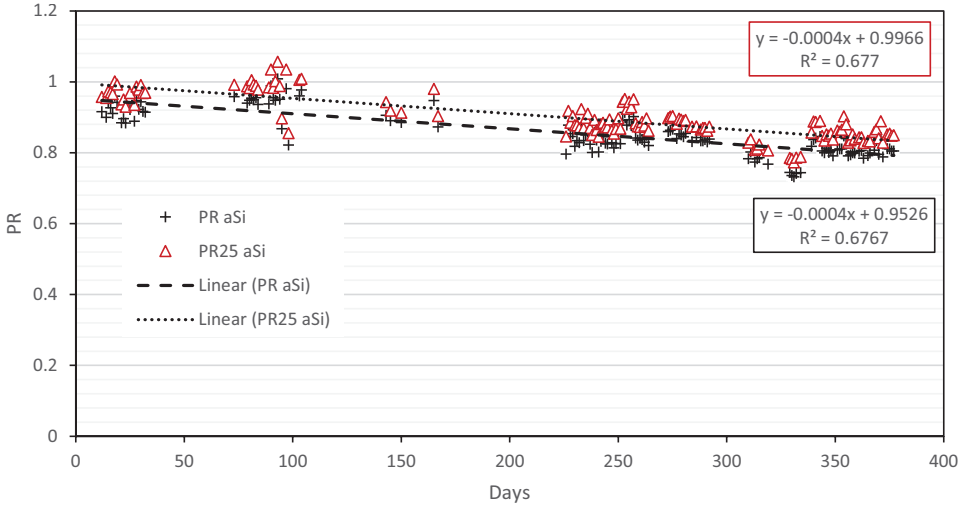

Fig. 10. Daily regression for amorphous silicon.

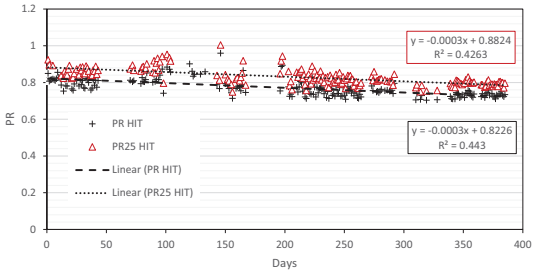

Fig. 11. Daily regression for HIT.

months, leading to higher performance ratios. Moreover, potential-induced degradation (PID) is another important mechanism that can influence the module degradation and performance loss observed. PID is generally understood to be a power loss phenomenon that is characterized by ion mobility and current leakage (shunting), and caused by high electric potential difference between solar cells and module frame [48]. It is known to depend on humidity, voltage and temperature, and therefore becomes more likely to occur in hot-humid climates such as Kumasi. The current method is however unable to isolate the presence of this mode of degradation and would rather be accounted for in the overall losses found. With exception of a-Si and CIS, results found in this study are generally higher than others reported in the literature (for mc-Si, pc-Si and HIT). Nevertheless, it is contended, that, these results are a more realistic view of early performance losses that rooftop PV system owners are likely to incur in this part of the world,

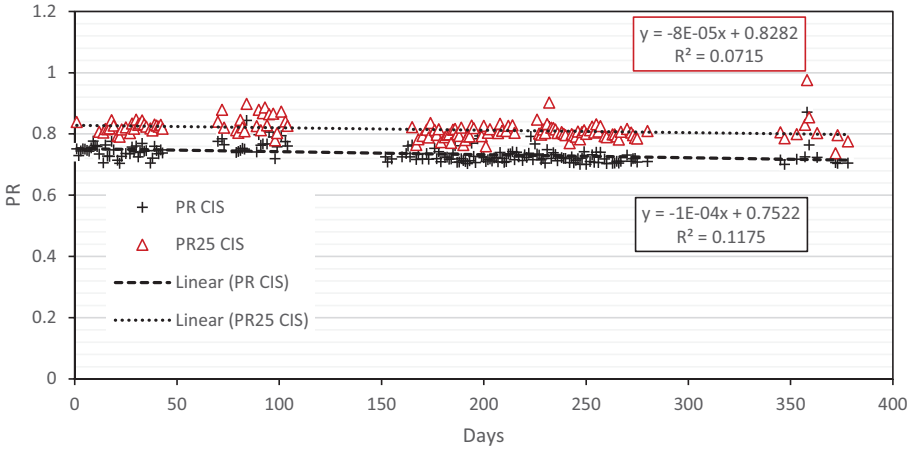

Fig. 12. Daily regression for CIS.

Table 7
A summary of Studies on Early Module Performance Degradation.

Author(s)	Location of Study	Module Technologies	Exposure Duration	Performance Reduction	Climate Characteristics[a]		
					Air temp, °C	RH, %	Irradiation, kWh/m^2
Makrides and Zinsser [15]	Nicosia Cyprus	mc-Si HIT pc-Si a-Si	1 year	mc-Si: 2.12%–4.22% HIT – 4.73% pc-Si: 1.47%–2.40% a-Si – 13.82%	11–29.4	45–64	2.2–8.12
Rüther et al. [41]	Arizona – USA Colorado – USA Santa Catarina - Brazil	a-Si ✓ ✓	1 year ✓ ✓	20–30%	10.5–30.5 0.3–23.5 16.4–25.1	20–49 47–55 80–84	3.16–8.14 2.15–6.96 2.84–6.13
Munoz et al. [16]	Madrid Spain	mc-Si	Exposed to receive 20 and 40 kWh/m^2 of irradiation.	4%	6.1–24.4	46–79	1.64–7.51
King et al. [13]	Albuquerque,	a-Si	1 year	20%	2.2–25.4	30–53	2.90–8.09
Hussin et al. [17]	Shah Alam Malaysia	a-Si	16 months	4.6%	26–27.2	79–84	4.05–4.99
Astawa et al. [42]	Loughborough UK	a-Si	2 weeks	21%–35%	4–16.5	75–85	0.51–4.5
This study	Kumasi Ghana	CIS a-Si mc-Si pc-Si HIT	14 months	CIS – 7.3% a-Si – 13.7% mc-Si – 6.12% pc-Si – 8% HIT – 11.1%	24.4–27.8	65–84	3.35–5.09

[a] Climate data compiled from Ref. [23].

Table 8
Early period performance guarantees by module manufacturers.

Manufacturer	Early performance warranty
Canadian Solar [6]	mc-Si: 97% of labelled power in first year pc-Si: 97.5% of labelled power in first year
REC Solar [43]	xSi: 97% effective power output in the first year
Trina Solar [44]	pc-Si: maximum degradation of 2.5% in the first year. mc-Si: maximum degradation of 3.0% in the first year.
Hanwha Q CELLS [45]	mc-Si: 98% of peak power in first year pc-Si: 97% peak power in first year
SunEdison [46]	mc-Si: maximum power output loss of (3.5%) in the first year.
First Solar [5]	Thin film: 97% power output in first year.
Kyocera [7]	xSi: 97% in first year.
BenQ Solar [47]	No less than 95% output of performance within first 5 years.

depending on technology, and can be reduced further with a module-cleaning schedule that addresses the contribution of soiling.

4. Conclusions

This paper examined the early performance degradation of five different solar PV technologies in the early months of exposure. In the longer-term, module degradation rate is viewed as largely linear. Nevertheless, there is increasing acknowledgement of the non-linearity that characterizes degradation in the early period of exposure. This work sought to study the phenomenon of early degradation in PV modules, using time-series regression of both temperature-corrected and uncorrected performance ratio measurements based on AC measurements. Fourteen months of data were available for this analysis, even though gaps occurred in the case of some technologies, due to system downtimes and as well as data filtering criteria adopted. The results show that early degradation (year 1) was most pronounced in amorphous silicon (13.8%), while CIS technology, the other thin-film installed, declined by 9.3%. Crystalline silicon systems lost 7.9%–9%. The HIT module technology, which is a hybrid of amorphous and monocrystalline silicon technologies, had degradation of 11.1%. Since industry practice is shifting towards multi-staged warranties that provide some assurance on module performance in the early periods of exposure, it is hoped, that this paper will serve as useful input for manufacturers and other actors in the PV value-chain. Additionally, since these installations are all roof-flushed, there will be some value in replicating this study on ground-mounted or rack-mounted installations. With increasing deployment of distributed solar PV systems, further work, focusing quantifying and minimizing the effects of shading, particularly in urban environments, will be beneficial to industry growth.

Acknowledgement

Assistance provided by the World Bank Africa Renewable Energy and Access program (AFREA) (Project P120478, TF 096613) is gratefully acknowledged. The first author also expresses gratitude to the Norwegian State Education Loan Fund (Lånekassen) for providing support toward his doctoral research.

References

[1] C. Ferrara, D. Philipp, Why do PV modules fail?, in: International Conference on Materials for Advanced Technologies 2011, Symposium O, 2012.
[2] M.A. Quintana, D.L. King, T.J. McMahon, C.R. Osterwald, Commonly Observed Degradation in Field-aged Photovoltaic Modules, 2002.
[3] D.A. Quansah, M.S. Adaramola, Comparative study of performance degradation in poly- and mono-crystalline-Si solar PV modules deployed in different applications, Int. J. Hydrogen Energy 43 (no. 6) (2018) 3092–3109.
[4] C. Osterwald, J. Adelstein, J. del Cueto, B. Kroposki, D. Trudell, T. Moriarty, Comparison of degradation rates of individual modules held at maximum power, in: 4th IEEE World Conference on Photovoltaic Energy Conversion, Hawaii, 2006.
[5] First Solar, First Solar Series 4™ PV Module, December 2015 [Online]. Available: http://www.firstsolar.com/-/media/First-Solar/Technical-Documents/Series-4-Datasheets/Series-4V2-Datasheet.ashx. (Accessed 8 November 2017).
[6] Canadian Solar Inc, Limited Warranty Statement - Photovoltaic Module Products, Canadian Solar Inc, 2017.
[7] Kyocera, Limited Warranty for Kyocera Photovoltaic Module(s), vol. 20, November 2015 [Online]. Available: http://www.kyocerasolar.com/pdf/warranty.pdf. (Accessed 8 November 2017).
[8] K.M. Broek, I.J. Bennett, M.J. Jansen, N.J.C.M. van der Borg, W. Eerenstein, Light and current induced degradation in P-type multi-crystalline cells and development of an inspection method and a stabilisation method, in: In 27th European Photovoltaic Solar Energy Conference and Exhibition, 24-28 September 2012, Frankfurt, Germany, 2012.
[9] D.C. Jordan, T.J. Silverman, B. Sekulic, S.R. Kurtz, PV degradation curves: non-

linearities and failure modes, Prog. Photovoltaics Res. Appl. 25 (2017) 583–591.
[10] N. Aste, C. Del Pero, F. Leonforte, PV technologies performance comparison in temperate climates, Sol. Energy 109 (2014) 1–10.
[11] R. Arndt, R. Puto, Basic Understanding of IEC Standard Testing for Photovoltaic Panels, TÜV SÜD America Inc, 2009.
[12] R.P. Kenny, A.I. Chatzipanagi, T. Sample, Preconditioning of thin-film PV module technologies for calibration, Prog. Photovoltaics Res. Appl. 22 (2014) 166–172.
[13] D.L. King, J.A. Kratochvil, W.E. Boyson, Stabilization and performance characteristics of commercial amorphous-silicon PV modules, in: Photovoltaic Specialists Conference, 2000. Conference Record of the Twenty-eighth IEEE, Anchorage, AK, USA, USA, 2000.
[14] C. Radue, E. van Dyk, A comparison of degradation in three amorphous silicon PV module technologies, Sol. Energy Mater. Sol. Cell. 94 (no. 3) (2010) 617–622.
[15] G. Makrides, B. Zinsser, Degradation of different photovoltaic technologies under field conditions, in: Photovoltaic Specialists Conference (PVSC), 2010 35th IEEE, Honolulu, HI, USA, 2010.
[16] M.A. Munoz, F. Chenlo, M.C. Alonso-García, Influence of initial power stabilization over crystalline-Si photovoltaic modules maximum power, Prog. Photovoltaics Res. Appl. 19 (2011) 417–422.
[17] M.Z. Hussin, A.M. Omar, Z.M. Zain, S. Shaari, Performance of grid-connected photovoltaic system in equatorial rainforest fully humid climate of Malaysia, Int. J. Appl. Power Eng. 2 (3) (2013) 105–114.
[18] D. Jordan, C. Gotwalt, JMP applications in photovoltaic reliability, in: JMP Discovery Summit 2011, Denver, Colorado, 2011.
[19] D.C. Jordan, S.R. Kurtz, Photovoltaic degradation rates—an analytical review, in: Progress in Photovoltaics, 2013, pp. 12–29.
[20] D.A. Quansah, M.S. Adaramola, G.K. Appiah, Performance analysis of different grid-connected solar photovoltaic (PV) system technologies with combined capacity of 20 kW located in humid tropical climate, Int. J. Hydrogen Energy 42 (2017) (2017a) 4626–4635.
[21] SMA Solar Technology AG, PV Inverter SUNNY BOY 3300/3800-Installation Manual, SMA Solar Technology AG, Niestetal, Germany, 2012.
[22] NASA, NASA Surface Meteorology and Solar Energy - Available Tables, NASA Atmospheric Science Data Center, 2018 [Online]. Available: https://eosweb.larc.nasa.gov/cgi-bin/sse/grid.cgi?&num=179097&lat=6.7&submit=Submit&hgt=100&veg=17&sitelev=&email=skip@larc.nasa.gov&p=grid_id&p=swvdwncook&p=ret_tlt0&p=wspd10arpt&p=RAIN&step=2&lon=-1.6. (Accessed 5 June 2018).
[23] RETScreen International, RETScreen Climate Database, 2014.
[24] D. Myers, Evaluation of the Performance of the PVUSA Rating Methodology Applied to DUAL Junction PV Technology, NREL, Golden, Colorado, 2009.
[25] IEA, Analytical Monitoring of Grid-connected Photovoltaic Systems: Good Practices for Monitoring and Performance Analysis, IEA, Paris, 2014.
[26] A. Limmanee, N. Udomdachanut, S. Songtrai, S. Kaewniyompanit, Y. Sato, M. Nakaishi, S. Kittisontirak, K. Sriprapha, Y. Sakamoto, Field performance and degradation rates of different types of photovoltaic modules: a case study in Thailand, Renew. Energy 89 (2016) 12–17.
[27] G. Makrides, B. Zinsser, M. Schubert, G.E. Georghiou, Performance loss rate of twelve photovoltaic technologies under field conditions using statistical techniques, Sol. Energy 103 (2014) (2014) 28–42.
[28] T. Ishii, A. Masuda, Annual degradation rates of recent crystalline silicon photovoltaic modules, Prog. Photovoltaics Res. Appl. (2017).
[29] S. Silvestre, S. Kichou, L. Guglielminotti, G. Nofuentes, M. Alonso-Abella, Degradation analysis of thin film photovoltaic modules under outdoor long term exposure in Spanish continental climate conditions, Sol. Energy 139 (2016) 599–607.
[30] J.K. Copper, K. Jongjenkit, A.G. Bruce, Calculation of PV system degradation rates in a hot dry climate, in: Proceedings of the Asia Pacific Solar Research Conference 29 November - 02 December 2016, Canberra, Australia, 2016.
[31] V. Sharma, O. Sastry, A. Kumar, B. Bora, S. Chandel, Degradation analysis of a-Si, (HIT) hetro-junction intrinsic thin layer silicon and m-C-Si solar photovoltaic technologies under outdoor conditions, Energy (72) (2014) 536–546.
[32] N. Sorloaica-Hickman, K. Davis, A. Leyte-Vidal, S. Kurtz, D. Jordan, Comparative study of the performance of field-aged photovoltaic modules Located in A Hot and humid environment, in: Photovoltaic Specialists Conference (PVSC), 2012 38th IEEE, Austin, TX, USA, USA, 2012.
[33] A. Kimber, T. Dierauf, L. Mitchell, C. Whitaker, T. Townsend, J. NewMiller, D. King, J. Granata, K. Emery, C. Osterwald, D. Myers, B. Marion, A. Pligavko, A. Panchula, T. Levitsky, J. Forbess, F. Talmud, Improved test method to verify the power rating of a photovoltaic (PV) project, in: 2009 34th IEEE Photovoltaic Specialists Conference (PVSC), Philadelphia, PA, 2009.
[34] D.C. Jordan, S.R. Kurtz, Photovoltaic Degradation Risk, NREL, Colorado, 2012.
[35] A. Phinikarides, G. Makrides, G.E. Georghiou, Initial performance degradation of an a-Si/a-Si Tandem PV array, in: 27th European Photovoltaic Solar Energy Conference and Exhibition, Frankfurt, Germany, 2012.
[36] J. Meydbray, E. Riley, L. Dunn, K. Emery, S. Kurtz, Pyranometers and Reference Cells: Part 2: what Makes the Most Sense for PV Power Plants? NREL, Golden, Colorado, 2012.
[37] N.H. Reich, B. Mueller, A. Armbruster, W.G.J.H.M. van Sark, K. Kiefer, C. Reise, Performance ratio revisited: is PR>90% realistic? Prog. Photovoltaics Res. Appl. 20 (2012) 717–726.
[38] M. Vazquez, I. Rey-Stolle, Photovoltaic module reliability model based on field degradation studies, Prog. Photovoltaics Res. Appl. (2008).
[39] M. Gostein, L. Dunn, Light soaking effects on photovoltaic modules: overview and literature review, in: Photovoltaic Specialists Conference (PVSC), 2011 37th IEEE, Seattle, WA, USA, 2011.
[40] M.A. Munoz, M.C. Alonso-García, N. Vela, F. Chenlo, Early degradation of silicon PV modules and guaranty conditions, Sol. Energy 85 (2011) 2264–2274.
[41] R. Rüther, J. d. Cueto, G. Tamizh-Mani, A.A. Montenegro, S. Rummel, A. Anderberg, B. von Roedern, Performance test of amorphous silicon modules in different climates - year four: progress in understanding exposure history stabilization effects, in: Photovoltaic Specialists Conference, 2008. PVSC '08. 33rd IEEE, San Diego, CA, USA, USA, 2008.
[42] K. Astawa, T.R. Betts, R. Gottschalg, Effect of loading on long term performance of single junction amorphous silicon modules, Sol. Energy Mater. Sol. Cell. 95 (1) (2011) 119–122.
[43] REC, 25-year Linear Power Output Warranty, REC, 2013.
[44] Trina Solar, Limited Warranty for Trina Solar Brand Crystalline Solar Photovoltaic Modules, Trina Solar, Changzhou, 2016.
[45] Q CELLS, Warranty Terms and Conditions for Crystalline Photovoltaic Modules, 2016 [Online]. Available: https://www.q-cells.com/us/index/service/warranty. (Accessed 8 November 2017).
[46] SunEdison, Photovoltaic Module Limited Warranty, 15 July 2014 [Online]. Available: http://www.sunedison.com/sites/default/files/file-uploads/solar-material-resource/SE_Mono_Limited_Warranty_35mm_72cell_v4.pdf. (Accessed 8 November 2017).
[47] BenQ. Solar, Warranty and Performance Guarantee Conditions of BenQ Solar PV Module, July 2013 [Online]. Available: http://benqsolar.com/download.php?file=..%2Fupload%2Fmedia%2Fbenqsolarfile%2Fwarrantyletter%2FWarranty_letter_PM096B00_en.pdf. (Accessed 8 November 2017).
[48] W. Luo, Y.S. Khoo, P. Hacke, V. Naumann, D. Lausch, S.P. Harvey, J.P. Singh, J. Chai, Y. Wang, A.G. Aberle, S. Ramakrishna, Potential-induced degradation in photovoltaic modules: a critical review, Energy Environ. Sci. 10 (2017) 43–68.

Paper 4

Solar Energy 173 (2018) 834–847

Contents lists available at ScienceDirect

Solar Energy

journal homepage: www.elsevier.com/locate/solener

Ageing and degradation in solar photovoltaic modules installed in northern Ghana

David A. Quansah[a,b,c,1], Muyiwa S. Adaramola[a,*,1]

[a] Renewable Energy Group, Faculty of Environmental Sciences and Natural Resource Management, Norwegian University of Life Sciences (NMBU), 1433 Ås, Norway
[b] Department of Mechanical Engineering, Kwame Nkrumah University of Science and Technology (KNUST), Kumasi, Ghana
[c] The Brew-Hammond Energy Centre, Kwame Nkrumah University of Science and Technology (KNUST), Kumasi, Ghana

ARTICLE INFO

Keywords:
Photovoltaic module
Degradation
Encapsulant
Mono-crystalline
Fill factor
Ghana

ABSTRACT

Understanding field failure and degradation modes in solar photovoltaic (PV) modules is important for various actors along the value chain. This paper presents results from field studies on performance degradation in twenty-two mono-crystalline silicon modules exposed for 16 years in three communities in the northern part of Ghana, prior to electricity grid extension. The results show, that, maximum power of the modules (P_{max}) had declined by 18.2–38.8% (median – 24.6%) over the period, which translates to an annual linear degradation rate of 1.54%. The losses in module power output are dominated by losses in short-circuit current (I_{sc}) and fill factor (FF), which are 0.75%/year and 0.54%/year respectively (median values). Discolouration of the encapsulant and degradation of the junction-box adhesive were the most frequently occurring visually observable defects on the modules.

1. Introduction

Solar photovoltaic (PV) technology has become a mainstream technology, characterized by phenomenal and sustained growth for well over a decade, with cumulative global installed capacity reaching 402 GW by end of 2017 (REN21, 2018). In 2017, the annual installed capacity was almost 100 GW, which constitutes almost a quarter of this cumulative capacity (REN21, 2018; Schmela, 2017). The importance of the technology takes on added significance as the world pursues low-carbon development pathways through initiatives such as the sustainable energy for all (SEforALL) and the adoption of the sustainable development goals (SEforALL, 2018). In Africa, where access to electricity remains low, solar PV is once again widely acknowledged as one of the important technologies that can help in addressing the crucial problems of energy poverty, particularly with the deployment of solar home systems and mini-grids (Quansah et al., 2016). Peculiar features of solar PV, such as modularity and short deployment lead times, makes it a well-suited technology, as the challenges of energy access and climate goals have taken on renewed urgency.

Ghana currently has one of the highest rates of access to electricity in sub-Saharan Africa (80% (World Bank Group, 2016)) and seeks to attain universal electrification by 2020 - 10 years ahead of the SE4ALL target year of 2030. The medium-to-long-term plans of the country emphasize an important role for renewables in general and solar PV in particular. To give further push to its quest to harness the potential of solar energy, Ghana recently ratified its membership of the newly-formed International Solar Alliance, which was conceived at the COP21 Paris climate conference in 2015 (Government of Ghana, 2018).

Deployment of solar PV systems require investment and sound investment decisions in turn depend on the availability of reliable information regarding risk-return profiles. Understanding and minimizing technology risks associated with PV investments underpin the need for ongoing studies on operational performance and reliability of field-deployed systems. Indeed, such data is important to various actors along the solar PV value-chain; from institutions involved in basic research to those that are engaged in project development, system integration, field deployment and operations and maintenance (O&M) services (Quansah and Adaramola, 2018).

Globally, investments in solar PV have been rising, increasing from $11bn in 2004 to $160bn in 2017, with cumulative annual growth rate of 23% (Frankfurt School-UNEP Centre/BNEF, 2018). Along with this, is the increased interest in monitoring, acquisition and interpretation of operational data on fielded modules and from testbeds managed by many National Laboratories and other Research Institutes. For example, Osterwald et al. (2006) in 2005 conducted a review in which they identified only 10 studies that had researched the subject of

* Corresponding author.
E-mail addresses: daquansah.coe@knust.edu.gh (D.A. Quansah), muyiwa.adaramola@nmbu.no (M.S. Adaramola).
[1] An ISES member.

https://doi.org/10.1016/j.solener.2018.08.021
Received 30 May 2018; Received in revised form 6 August 2018; Accepted 9 August 2018

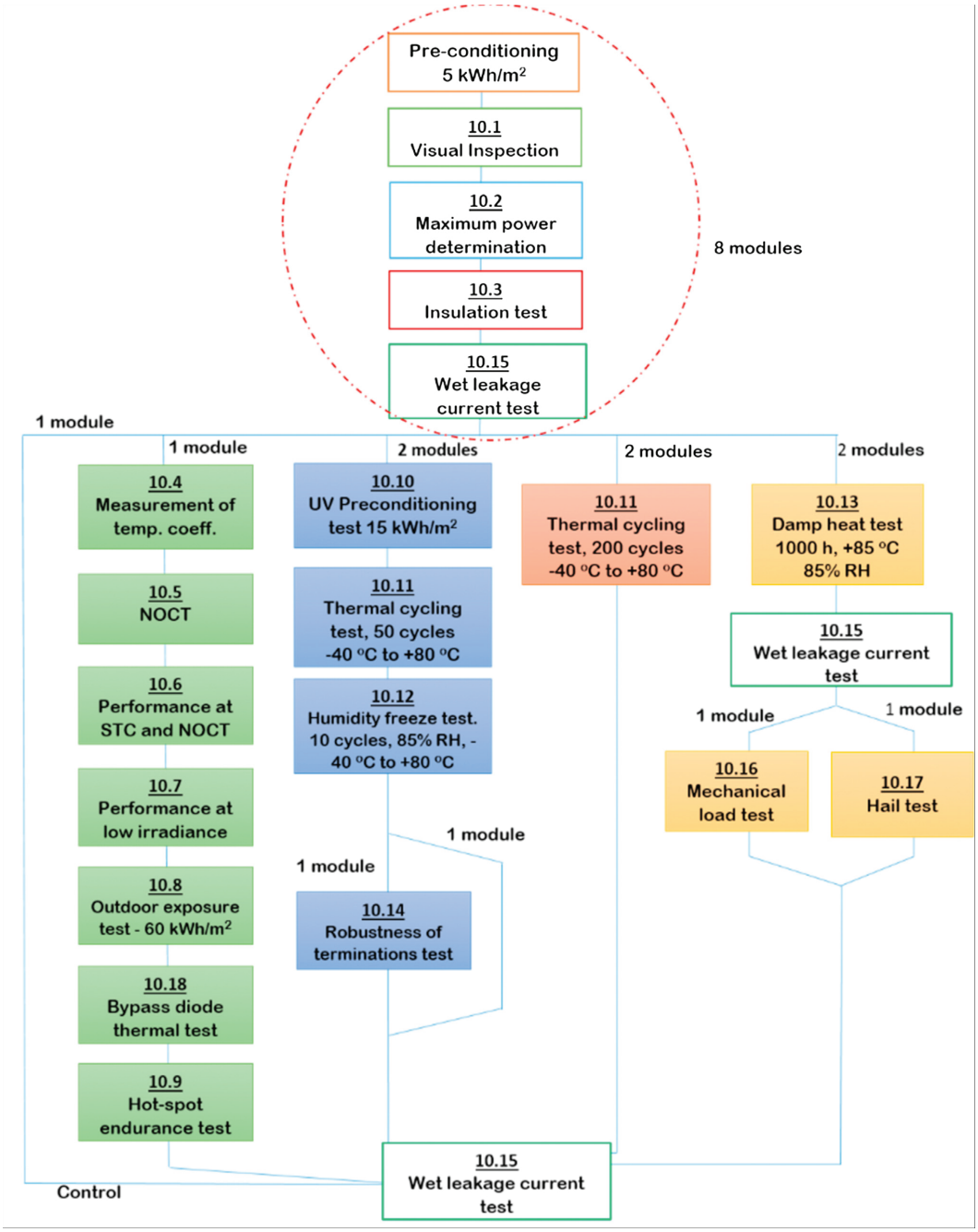

Fig. 1. IEC 61215 test series. Adapted from Arndt and Puto (2009).

photovoltaic performance degradation. By 2016 (after a decade), Jordan et al. (2016) reviewed almost 200 studies reporting more than 11,000 degradation rates from 40 countries. These meta-studies (Jordan et al., 2016; Jordan and Kurtz, 2013) have also highlighted the geographical imbalance of available data and made a case for an expanded representation of high-quality data on field performance and degradation of solar photovoltaic modules. Currently, the IEC 61215 qualification test series (Fig. 1) is widely accepted by market actors as a

minimum entry requirement for crystalline silicon solar photovoltaic modules (Ishii and Masuda, 2017). It is the result of several years of iterations and has benefited greatly from early lessons from space programmes and also from initiatives such as the block procurements of the US Jet Propulsion Laboratory (JPL) and the European Solar Test Installation (ESTI) programme (Hoffman and Ross, 1978; Osterwald and McMahon, 2009). While, the IEC 61215 has been credited with significantly reducing infant failures in fielded PV modules, it does not provide information regarding longevity and long-term performance of the modules (Osterwald and McMahon, 2009). However, as industry players seek greater assurance on product reliability, it has been suggested (Wohlgemuth and Kurtz, 2011), that, module designs which have proven resilient on field exposure could serve as control modules in stress-testing of new module designs and provide a means of predicting how long the new module designs could last. Field measurements and studies on module performance degradation in various geographical locations and climatic conditions therefore become crucial, since ageing and performance degradation constitute an important phenomenon that affect system output and consequently financial figures of merit.

In Ghana, recent studies (Quansah and Adaramola, 2018; Quansah et al., 2017) have reported on module degradation and long-term performance of systems installed in the southern and middle parts of the country (Fig. 2). These studies, together reported on 43 modules installed in off-grid (battery-charging and water-pumping) and grid-connected applications. The technologies comprised mono-crystalline silicon (mc-Si) and poly-crystalline silicon (pc-Si) modules with 6–32 years of field exposure (Quansah and Adaramola, 2018; Quansah et al., 2017). The objective of this current paper is to present results of further studies conducted in the northern part of Ghana, on 16-year old modules installed under a Government programme to provide energy services for domestic and communal purposes. The systems were installed in the early 2000 s under a project titled *"Renewable Energy-Based Electricity for Rural Social and Economic Development (RESPRO)"* and jointly implemented by the Government of Ghana (GoG), United Nations Development Programme (UNDP) and the Global Environment Facility (GEF) (UNDP/GEF, 2002). Nassen et al. (2002) and Bawakyillenuo (2009) have previously reported on the socio-economic and other aspects of installations undertaken under this project.

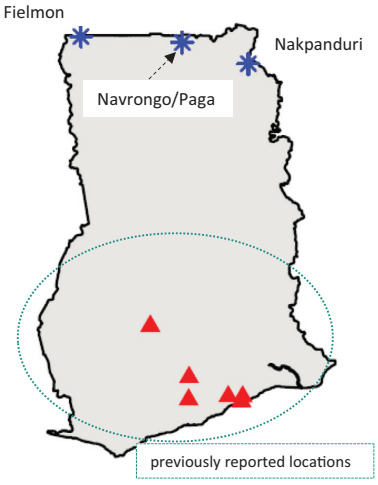

Fig. 2. Map of Ghana, showing locations of study, *red – previously reported* (Quansah and Adaramola, 2018; Quansah et al., 2017), *blue – current study*. (For interpretation of the references to colour in this figure legend, the reader is referred to the web version of this article.)

The results of this present study show a median degradation rate of 1.54%/year, with encapsulant discolouration and its attendant loss in short-circuit current emerging as the dominant mode of module power degradation. All the once off-grid communities are now connected to the national grid, and most systems studied were in open-circuit mode following failure of the batteries. An economic assessment on the viability of restoring PV-based energy services by investing in balance of system (BoS) components showed positive results. The northern part of the country is host to the first megawatt-scale solar PV plant constructed in Ghana and features high annual irradiation values (an average of 6.07 kWh/m^2/day (Natural Resources Canada, 2004)). Moreover, the northern regions of Ghana are expected to host additional solar power plants, for which provisional licenses with proposed capacities totaling over 1000 MW have already been acquired, by both state-backed utilities and private developers (Energy Commission Ghana, 2018). It is hoped, that, this study provides some insight to project developers on long-term module performance and degradation in Ghana and specifically in the northern part of the country.

2. Material and methods

After reviewing background documentation on RESPRO and other early solar PV projects implemented by the Ministry of Energy (UNDP/GEF, 2002), actual locations of the installations studied in this work were obtained with the assistance field officers who were closely associated with the implementation of the project (see Acknowledgements section). The communities visited were Nakpanduri and Navrongo/Paga in the Upper East Region and Fielmom in the Upper West Region (Fig. 2). Long-term (22-year) climatic data for the locations were retrieved from the database of NASA (NASA, 2018) and shown in Fig. 3. Temperature and humidity data for Navrongo/Paga (lat. 10.897°, long. −1.086°) were similar to those of Nakpanduri (lat. 10.584°, long. −0.102°) and Fielmon (lat. 10.987°, long −2.605°), and is therefore considered as representative of these two other communities from which measurements were made. Indeed, all three locations, falling between latitudes 10–12°N, are classified into the same sub-climate zone (sub-humid dry) by researchers (Beckley et al., 2016).

Average daily ambient temperature ranges from 24.7 °C in August (relative humidity of 82%) to 29.8 °C in March (relative humidity of 43.2%). Maximum daily temperatures however reach a high of about 35 °C occurring (in around March), while minimum daily temperatures are recorded in the months of December and January. At these sites (Fielmon, Navrongo/Paga, and Nakpanduri), the modules encountered in the study were mainly Isofoton I-110/12 modules, but others were also found (Isofoton I-100 and I-50, in single occurrences). Maximum power of the modules were 110 W, 100 W, and 50 W respectively for I-110/12, I-100 and I-50. The short-circuit current (I_{sc}), open-circuit voltage (V_{oc}), fill factor (FF) and other characteristics of the modules are presented in Table 1. The data shown in this table (which serve as references values) are manufacturer-supplied values. They are were obtained from module nameplates, and complemented with data from database of the photovoltaic module design and simulation software PVsyst (PVsyst, 2012), as shown in Fig. 4. The systems were deployed at a time when the communities were not connected to the national grid. They were therefore installed with charge controllers and batteries, to power direct current (dc) lamps for lighting and provide other basic services.

Even though most of the systems were out of operation, some homes had the original batteries and (or) charge controllers that came with the installations still in place. Charge controller and battery that were used in the installations are shown in Fig. 5 and their technical characteristics are presented in Table 2. The modules, installed at different locations, were generally mounted on poles (except one, which was roof-flushed) and faced due south at locations in the houses that ensured that

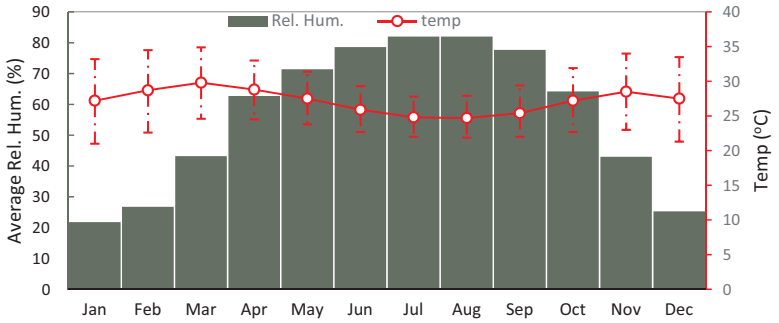

Fig. 3. Monthly average daily relative humidity and temperature variation in Navrongo (NASA, 2018).

Table 1
Module types and characteristics.
Source: Field data and database of PVSYST® (PVsyst SA, 2012).

Module parameter	Unit	Value		
Commercial				
Manufacturer	–	Isofoton	Isofoton	Isofoton
Model	–	I-110/12	I-100	I-50
Electrical				
I_{sc}	A	6.76	6.54	3.27
V_{oc}	V	21.6	21.6	21.6
FF	%	75.3	70.70	70.70
P_{max}	W	110	100	50
Tol	%	10	10	10
I_{mpp}	A	6.32	5.74	2.87
V_{mpp}	V	17.4	17.4	17.4
No. of cells in series	–	36	36	36
No. of cells in parallel	–	2	2	1
Thermal				
Temp. coeff. of I_{sc}	%/°C	−0.034	−0.035	−0.07
Temp. coeff. of P_{mpp}	%/°C	−0.44	−0.46	−0.42
Dimensions				
Length	mm	1310	1310	1290
Width	mm	651	651	328
Thickness	mm	34	34	34
Weight	kg	11	11	5.7
Module area	m^2	0.853	0.853	0.423
Construction				
Frame	–	Anodized Al	Anodized Al	Anodized Al
Front	–	Tempered glass	Tempered glass	Tempered glass
Encapsulation	–	EVA	EVA	EVA
Back sheet	–	Polymer	Polymer	Polymer

they were unshaded in the east-west apparent direction of the sun (see Fig. 6 for typical pole-mounted installation). All the communities now have grid-based electricity and as such, some previously known installations had been decommissioned by their owners at the time of visit and the modules sold in near-by communities without electricity (particularly across the border). Some modules had also suffered theft, while most of the remaining systems were in open-circuit mode (Table 3).

2.1. Instrumentation and measurement

Measurement of electrical characteristics of the modules was undertaken with a TR-KA I-V (current-voltage) curve tracer and its accompanying TRI-SEN sensor for temperature and irradiance measurement. The TRI-SEN maintains a wireless communication with the TRI-KA during the I-V sweep and automatically synchronizes temperature and irradiance variables to the performance data. This enables translation of acquired data to Standard Test Conditions (STC) or other desired reference conditions. Standard test conditions for solar PV modules for terrestrial applications are: irradiance – 1000 W/m^2, module temperature – 25 °C and air mass – 1.5. Minimum required irradiance level for measurement was set to 700 W/m^2 and maximum tolerance was 5% during measurement. Measurement range, accuracy and other characteristics of the measuring devices are shown in Table 4.

To reduce the impact of angle-of-incidence effects, measurements were conducted between 10 am and 2 pm local time (within the solar window). Documentation of visually observable defects were undertaken with the aid of the NREL/IEA template ((IEA, 2014; NREL, 2012), in order to maintain consistent vocabulary with the research works found in the open literature as well as earlier observations made in this ongoing research (Quansah and Adaramola, 2018; Quansah et al., 2017).

2.2. Degradation rate analysis

Current-voltage (I-V) measurements obtained under field conditions were translated to STC conditions by applying Eqs. (1)–(3) (Kaplanis and Kaplani, 2011).

$$V_{oc(meas)} = V_{oc(STC)} - n_s \times 2.3 \times 10^{-3} \times (T_c - 25\,^{\circ}\mathrm{C}) + \frac{kT_c}{q} \ln C \quad (1)$$

where:

$V_{oc(meas)}$ and $V_{oc(STC)}$ are respectively, the open-circuit voltage at measured and at STC conditions, and:

- $C = \frac{I_T}{10^3}$,
- $T_c = cell\ \ temperature$
- $k = Boltzman\ \ Constant = 1.38 \times 10^{-23}$ J/K,
- $n_s = number\ \ of\ \ cells\ \ in\ \ series$,
- $q = electron\ \ charge = 1.602 \times 10^{-19}$ C, and
- $I_T = irradiance\ \ in$ W/m^2

The short-circuit current at STC, $I_{sc(STC)}$, is calculated from Eq. (2):

$$I_{sc(meas)} = I_{sc(STC)} \times (1 + h_f \times (T_c - 25\,^{\circ}\mathrm{C})) \times \frac{I_T}{10^3} \quad (2)$$

where:

$$h_f = 6.4 \times 10^{-4} K^{-1}$$

The maximum power at STC, P_{STC}, is computed from $I_{sc(STC)}$, $V_{oc(STC)}$ and the measured fill factor (FF) using Eq. (3):

$$P_{STC} = FF \times I_{sc(STC)} \times V_{oc(STC)} \quad (3)$$

The average annual degradation rate of the module's maximum power ($DR_{P_{max}}$) is determined as per Eq. (4):

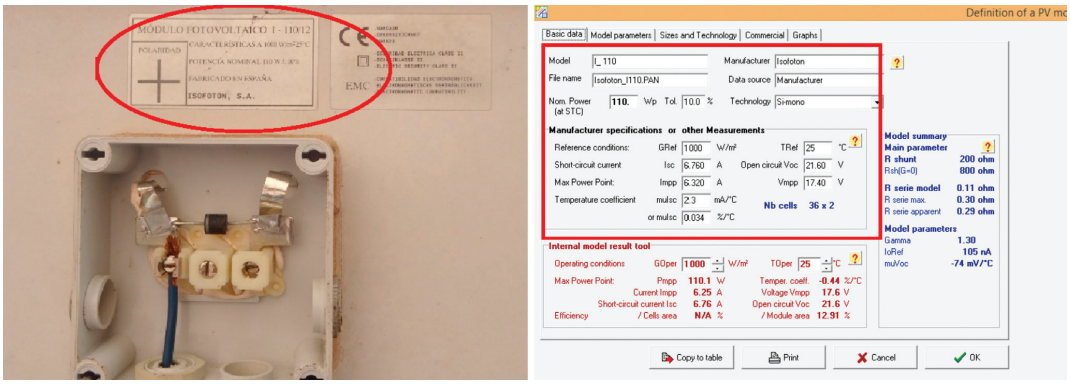

Fig. 4. Backside of the module showing the nameplate data and snapshot of PVsyst software showing module's specifications.

$$DR_{Pmax} = \left(\frac{P_{Max_{Ref}} - P_{STC}}{y \times P_{Max_{Ref}}}\right) \times 100\% \quad (4)$$

where $P_{Max_{Ref}}$ is the reference performance data (Table 1), y is field exposure duration (in year), and P_{STC} is from Eq. (3). The degradation rates of the explanatory variables (i.e. V_{oc}, I_{sc} and FF) are assessed in an analogous manner.

2.3. Economic analysis

Due to the failure of the balance of system (BoS) components, mainly batteries in this case, most systems were not operational, even though the modules were working. A techno-economic analysis based on the prevailing performance data and economic parameters, is therefore conducted to assess the viability of investing in BoS to restore energy services. The annual energy output (in year n) from the system, (E_n), is estimated as (Eq. (5)):

$$E_n = P_{STC} \times PSH \times 365 \times \eta_{sub\_sys} \times f_{d\_n} \times f_{derate} \times f_{avail} \quad (5)$$

where:

- P_{STC} is the current reference performance of the module
- PSH is the peak sunshine hours
- η_{sub_sys}, the conversion efficiency of subsystems
- f_{d_n} is the degradation factor for year *n*
- f_{derate}, the derating factor, and
- f_{avail} is the availability factor

Table 2
Description of balance of system components.
Data Sources: (Hawker Group, 1999; PVsyst SA, 2012).

Parameter	Value
Battery	
Manufacturer/model	VARTA, Vb 12,106
Capacity (at C10)	120 Ah
Nominal voltage	12 V
Floating voltage	13.38 V
Charge controller	
Manufacturer model	Isofoton, Isoler 30
Nominal battery voltage	12 V/24 V
Maximum input current	30 A
Maximum output current	30 A
Charging thresholds (whole battery)	13.7 V
Load disconnecting threshold	10.9 V

With exception of early stages of module exposure and end-of-life stages, module degradation is generally considered linear (Osterwald et al., 2006). That is, power loss may be visualized as a fixed annual wattage loss in relation to the initial performance of the module. The annual loss in Watts is then:

$$P_{loss} = \%DR_{Pmax} \times P_{Max_{Ref}} \quad (6)$$

The degradation factor in year n, as a function of P_{STC} is computed as:

$$f_{d\_n} = \left(1 - \frac{n \times P_{loss}}{P_{STC}}\right) \quad (7)$$

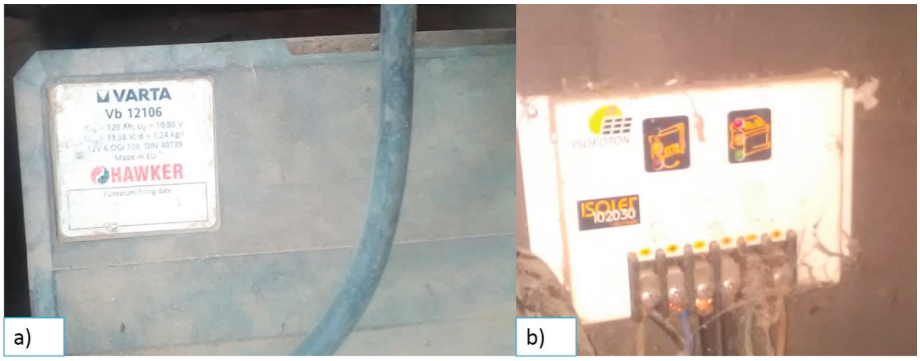

Fig. 5. Battery and charge controller.

Fig. 6. Selected installations in the communities (Nakpanduri and Navrongo/Paga).

Table 3
Summary of installations assessed in various communities.

Community	No. of installations	No. operational
Bimbagu	5	1
Navrongo/Paga	13	1
Fielmon	4	3
Total	22	5

Table 4
Measurement characteristics of TRI-KA I-V curve tracer and TRI-SEN.

Parameter (Unit)	Measuring range	Uncertainty (%)
Voltage (V)	1.0–1000	± 1
Current (A)	0.1–15	± 1
Temperature (°C)	0–100	± 3
Irradiance (W/m^2)	100–1200	± 5

The concepts of Net Present Value (NPV) and Payback period are used in the assessment of the financial viability of further investments. The NPV is computed as per Eq. (8).

$$NPV = \sum_{n=0}^{N} PVal\_Benefit\_n - \sum_{n=0}^{N} PVal\_Cost\_n \quad (8)$$

where $PVal\_Benefit\_n$ is the present value of benefits in year n and $PVal\_Cost\_n$ represents the present value of costs in year n. The benefits in year n consist of the avoided cost of electricity from the grid and is estimated per Eq. (9):

$$PVal\_Benefit\_n = \frac{P_{STC} \times PSH \times 365 \times \eta_{sub\_sys} \times \left(1 - \frac{n \times P_{loss}}{P_{STC}}\right) \times f_{derate} \times f_{avail} \times \tau(1+r)^n}{(1+d)^n} \quad (9)$$

where τ, r and d are respectively the electricity tariff, escalation rate of electricity tariff and discount rate.

Costs consist mainly of initial investment required to restore energy services. These include the cost of battery ($Cost_{batt}$), charge controller ($Cost_{cc}$) and installation service ($Cost_{install}$) (Eq. (10)). All costs are assumed to be incurred in year 0. The cost of the photovoltaic module is treated as a sunk cost, since the investment has already been made.

$$PVal_{Cost_n} = Cost_{batt} + Cost_{cc} + Cost_{install} \quad (10)$$

The NPV then becomes (Eq. (11)):

$$NPV = \sum_{n=0}^{N} \frac{P_{STC} \times PSH \times 365 \times \eta_{sub\_sys} \times \left(1 - \frac{n \times P_{loss}}{P_{STC}}\right) \times f_{derate} \times f_{avail} \times \tau(1+r)^n}{(1+d)^n} - \sum_{n=0}^{N} (Cost_{batt} + Cost_{cc} + Cost_{install}) \quad (11)$$

The payback period (in years) is determined graphically with cumulative annual cash flows of the project. A summary of input parameters for economic model is presented in Table 5.

3. Results and discussion

This section presents results based on measured data and computations undertaken with the set of equations presented in Section 2. Technical performance characteristics of the modules studied are presented and discussed within the context of previously reported results by other researchers and in the context of earlier results by ongoing research (mainly from the southern parts of Ghana). Visually observable defects that were documented in the study are presented next. Attempt is made to explore the relationship between observed defects and explanatory variables for module power losses (i.e. I_{sc}, V_{oc} and FF). Finally, results of economic analysis on the viability of additional investment to restore energy services are presented.

3.1. Performance characteristics

Applying Eqs. (1)–(4), with relevant data in Table 1 and measured data, yields annual decline in P_{max} of 1.14–2.43% with a median of 1.54% (Fig. 7). The modules are therefore performing at 61.2–81.8% of the initial rated power (median – 75.4%), having lost 18.2–38.8% of power (median – 24.6%) over a 16-year period. Studies in this domain tend to prefer the median to the mean as a measure of central tendency due to the former's resilience to the impact of outliers. This view is adopted in this paper, and, as such, subsequent discussions on the general performance characteristics of the modules are based on median values. As shown in Figs. 8–10, I_{sc} losses are in the range of 0.32–1.84%/yr (median 0.75%/yr), while FF and V_{oc} respectively range from 0.15% - 0.98%/yr (median 0.54%/yr) and 0.25–0.52%/yr (median 0.35%/yr). Losses in P_{max} are attributable (Figs. 8–11) mainly to losses in I_{sc}; and to lesser extents, on losses in FF and V_{oc} (recalling Eq. (3)), i.e. $P_{max} = f(I_{sc}, V_{oc}, FF)$).

The degradation (in P_{max}) values found in this study compare favourably with 1.9%/yr found in Ref. (Quansah and Adaramola, 2018)

Table 5
Summary of economic analysis input parameters.

Parameter	Description	Value	Remarks
P_{max}	Maximum power of module	Calculated	Based on field data
PSH	Peak sunshine hours	6 h	SWERA/RETSCREEN Climate database (Natural Resources Canada, 2004)
η_{sub_sys}	Efficiency of subsystems	85%	95% charge controller, 90% round-trip battery efficiency (Luo et al., 2015)
n	Current year	0–10	–
N	Project life	10 years	Chosen to reflect maximum expected battery life
P_{loss}	Annual module power loss	Calculated	Eq. (6)
f_{derate}	factor to account for system operation at non-STC conditions	80%	Accounts for temperature, soiling and other losses.
f_{avail}	Availability factor	98%	(Klise and Balfour, 2015)
τ	Average end-user tariff in Ghana	$0.2/kWh	(Energy Commission Ghana, 2017)
r	Electricity tariff escalation rate	1%	(Energy Commission Ghana, 2017)
d	Discount rate	5%	(Quansah and Adaramola, 2016)
$Cost_{batt}$	Cost of battery	$200/kWh	(Luo et al., 2015; Quansah et al., 2017)
$Cost_{cc}$	Cost of charge controller	$20	(Quansah et al., 2017)
$Cost_{install}$	Cost of labour	$30	(Opoku et al., 2018)

for 16-year old modules (Isofoton I-100) installed in grid-connected mode in the Southern part of Ghana, which were also produced by the same manufacturer. However, performance degradation also needs to be interpreted in the context of warranty provisions on the module. Currently, modules manufactured and sold on the market come with 25-year warranties (multi-staged), during which period they are expected to produce at a minimum of 80% of initial power. However, this has not always been so. Warranty durations have evolved over the past four decades, from about 5 years in the 1980 s to current duration of 25 - 30 years, during which 80–90% of initial module P_{max} is promised (Jordan and Kurtz, 2013; Meydbray and Dross, 2016). Even though warranty information for this module (I-100/12) is not readily available, modules of this era typically came with 10–20 year warranties. In fact, a study conducted by the IEA on EU-funded PV systems installed for schools in rural South Africa using Isofoton I-110/12 modules suggest a warranty period of 10-years for this module (IEA, 2004). As shown in Fig. 11, an annual degradation rate of 1.54% suggests about 13 years of module operation before performance falls below 80% of P_{max} (Quansah et al., 2017). Therefore, these modules could be considered as having met (and exceeded) warranty expectations. For a 10-year warranty period, degradation rate must not exceed 2%/yr (Fig. 12).

In a global perspective, Jordan and Kurtz (2013) found from their review, that, 78% of nearly 2000 reported degradation rates were below 1%. They found a mean of 0.8% and median of 0.5% for all technologies studied. Although the study was not based on scientific sampling of publications (and not geographically representative), it provided an insightful synthesis of the increasing number of studies on module degradation. The results of the meta-analysis by Jordan and Kurtz (2013) agreed with earlier work by Osterwald et al. (2006) who studied various module technologies in the climate of Golden Colorado (USA) and found degradation rates of 0.3–0.51% per year for mono-crystalline (mc-Si) modules after almost 10 years of exposure. They suggested that module degradation is linear over time, but requires a minimum observation period of 3 years to establish long-term trends (Osterwald et al., 2006; Osterwald and McMahon, 2009). Based on their results, they advocated that the prevailing 1%/year rule-of-thumb for degradation rate should be abandoned, in favour of 0.5%/year (Osterwald et al., 2006). Skoczek (2008) reported on performance measurements involving 204 crystalline silicon modules after 19–23 years of exposure at the European Solar Test Installation (ESTI) in Italy and found an average degradation rate of 1%/yr. The work by Skoczek (2008) is of particular interest in this current study, as their work also observed modules which were in open-circuit mode. Their results showed a statistically significant difference in degradation rates of modules were under load, compared with those in open circuit mode (0.6%/yr). Current-carrying grids and inter-connects of modules under load are considered to endure higher levels of thermo-mechanical fatigue due to the so-called Joule heating effect. This in turn, compared with those in open-circuit mode, accelerates the coarsening of solder bonds and changes in the geometry of solder-joints, thereby increasing the series resistance of the modules, resulting in higher fill-factor losses (Skoczek, 2008; Park et al., 2014).

The foregoing suggests, that, the degradation rate of 1.54%/yr found in this study could reasonably be expected to be higher if the modules were under load throughout the exposure period.

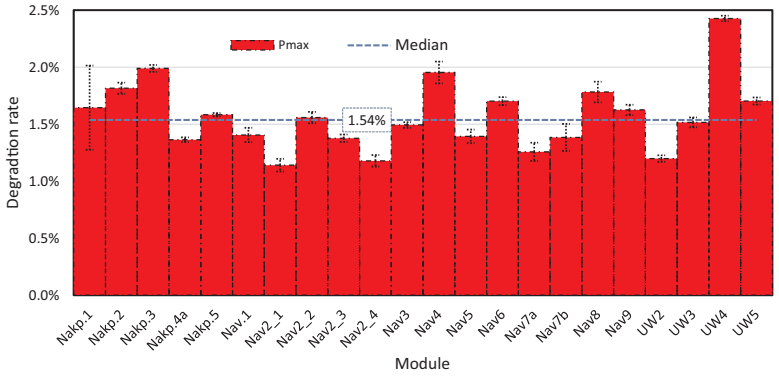

Fig. 7. Degradation in nominal maximum power (P_{max}).

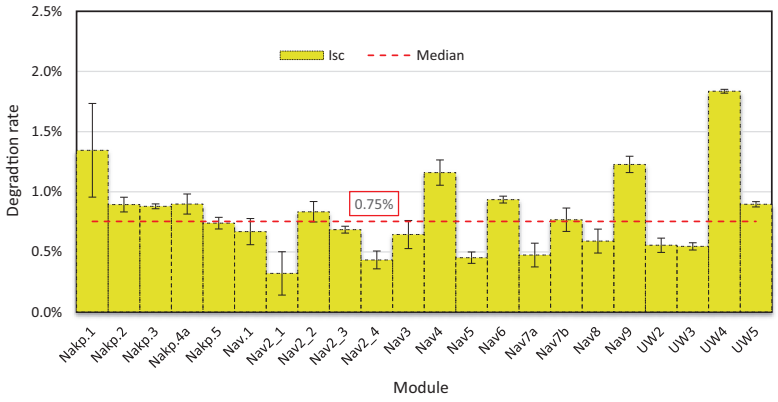

Fig 8. Degradation in short-circuit current (I_{sc}).

Furthermore, the degradation rate of 1.9%/yr found for similar modules in (Quansah and Adaramola, 2018) (same manufacturer) could be a more accurate reflection of the long-term performance of the modules. Degradation rates of 1.3%/yr and 0.8%/yr have also been found for PV modules in battery-charging applications in Ghana after 19 and 32 years respectively of outdoor exposure (Quansah et al., 2017; Quansah and Adaramola, 2018). Kaplanis and Kaplani (2011) found a lower degradation rate of 0.5%/yr for 20-year-old mc-Si systems installed in Greece. Lorenzo et al. (2014) also observed a similar rate (0.53%/yr) for 17-year modules installed Madrid Spain – these were deployed in grid-connected mode. An even lower degradation rate has been reported from 20-year grid-connected systems in Italy (Pozza and Sample, 2016; Polverini et al., 2012). After 3-years of monitoring of grid-connected PV systems in the Saga Prefecture of Japan, Ishii and Masuda (2017) reported no observed degradation (± 0.2% uncertainty) beyond an initial 2% light-induced degradation. The results found in this current study does not compare favourably with the generality of results found in the literature. Yet, it is important to note that many of the studies are from regions of Europe and North America with moderate environmental conditions (Jordan and Kurtz, 2013).

However, module degradation is known to depend (inter alia) on factors such as climate, technology, age and mounting type, and it has been observed that studies coming from harsher climatic regions tend to report higher degradation rates (Jordan et al., 2016). For instance, studies by Bandou et al. (2015) in the Adrar Region of Algeria, on a 30.24 kW_p installation showed an annual degradation rate of 1.22% after 28 years and was dominated by losses in I_{sc} and FF. Belmont et al. (2014) have reported modules in hot-dry desert of Arizona (United States) as having degraded at a rate of 2.3%/yr after 26 years of operation. Analysis conducted by Limmanee et al. (2017), on systems installed in Thailand, a country with a tropical climate (as Ghana), showed a degradation rate of 1.2%/yr for polycrystalline (pc-Si) modules after 4-years of operation. Other module technologies had higher degradation rates (up to 6.1%) (Limmanee et al., 2017). A Similar study, by Ye et al. (2014), in tropical Singapore, found a degradation rate of 0.8% for mc-Si and 1% for pc-Si modules, and were attributed mainly to losses in short-circuit current.

Following 5 years of continuous monitoring of systems installed at different locations in the hot and humid environment of Florida by the Florida Solar Energy Centre (United States), Sorloaica-Hickman et al. (2012) reported degradation rates up to 2.5% for crystalline silicon modules. A degradation rate of 1.9% was reported by Rajput et al. (2016) following their study of a 22-year old battery-charging installation at Gurgaon, India.

Skoczek et al. (2008), presented results from stress-testing of modules according to the IEC 61215 protocol and showed that thermal cycling (TC200), UV exposure and dump heat (DH) tests were the most severe tests on candidate modules and were the cause of most failures

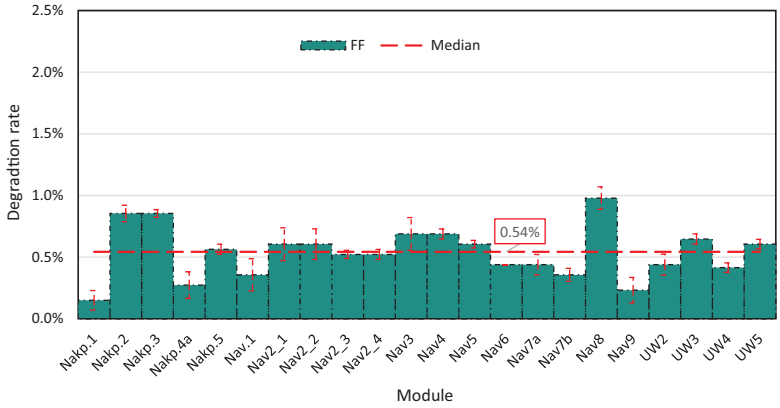

Fig. 9. Degradation in fill factor (FF).

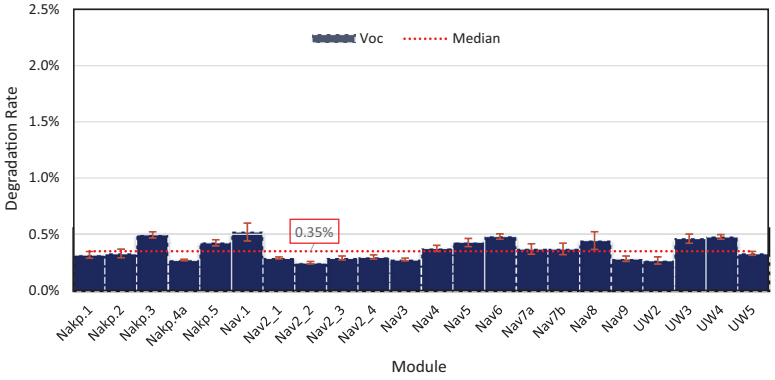

Fig 10. Degradation in open circuit voltage (V_{oc}).

recorded. These results have been corroborated by results from other testing laboratories (Bogdanski and Herrmann, 2011). Together, these tests (TC200, DH and UV) attempt to induce field failure and degradation modes that would be expected, and are indeed prevalent in desert and hot-humid climates (Wohlgemuth and Kurtz, 2011; Meydbray and Dross, 2016).

3.2. Visually observable defects

The defects observed in the studied modules include degraded junction box adhesive, snail track, browning of the encapsulant, delamination, cracks on front-glass and degraded cabling (shown in Fig. 13). Summary statistics of observed defects in various components of modules are presented in Fig. 14 and show discolouration of encapsulant as the most recurrent defect, occurring in about 45% of the modules, followed by degraded adhesion of the junction box Fig. 14.

These observed defects are consistent with observations in the explanatory factors for module power loss (as shown in Figs. 8–11), which show losses in short-circuit current as the dominant factor. Discolouration of cell encapsulant and delamination, tend to have detrimental impact on I_{sc}, as they alter the refractive indices of the materials and cause optical decoupling and mismatch, leading to reduced light transmission to the solar cells (Quintana et al., 2002). Even though degradation of junction box adhesion is also prominent (Fig. 14), this in itself might not directly lead to power loss. An earlier study in Ghana (Quansah and Adaramola, 2018) also registered encapsulant browning as a major mode of module degradation. It (Quansah and Adaramola, 2018) also found delamination to be more extensive compared with the findings of this current study, in which delamination occurs in under 10% of the modules studied (Fig. 14). This contrast is likely a result of the relatively higher levels of humidity (RH of 76–85%) and atmospheric salinity due to its proximity to the sea (Quansah and Adaramola, 2018). High humidity and high temperature are known to accelerate the onset of defects such as delamination and electrochemical corrosion (Ferrara and Philipp, 2011; King et al., 2000).

Encapsulant discolouration has been widely reported by many researchers as a leading cause of module degradation. For example, Pozza and Sample (2016) found yellowing of the encapsulant as the main failure mode in their study. Intensive encapsulant browning was reported of modules in the desert of Arizona by Belmont et al. (2014). Bandou et al. (2015) also observed yellowing and browning of encapsulant, delamination, broken front-glass and discolouration of grid fingers when they studied the 28-year-old system in Adrar, Algeria. Even though studies from Africa on PV module have been scant, those found in the open literature, reporting on long-term degradation have mostly come from locations in the Northern part of the continent (e.g. Rabii et al., 2003; Kahoul et al., 2014; Ibrahim et al., 2009) and have highlighted detrimental impact of high temperatures on module life.

High ambient temperature, and subsequently, high module operating temperatures have adverse impact on various module component materials (e.g. the solder bonds and the metallization) (Ferrara and Philipp, 2011). Since, temperatures also vary diurnally and seasonally,

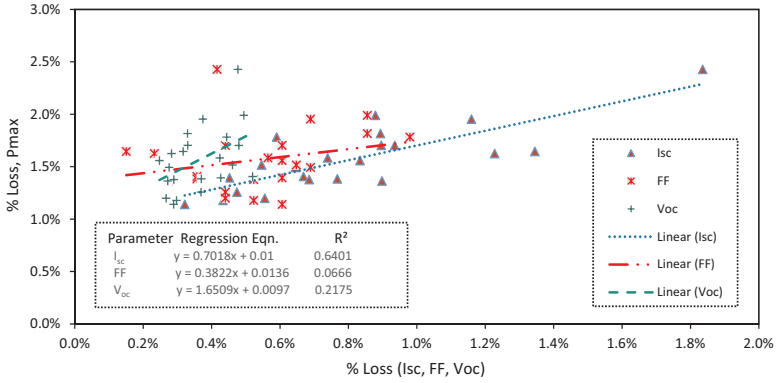

Fig. 11. Variation of P_{max} losses with losses in I_{sc}, FF and V_{oc}.

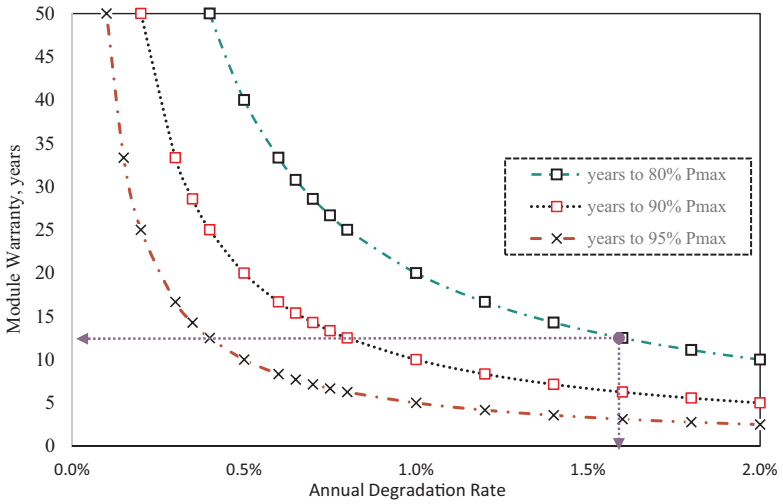

Fig. 12. module warranty period vs minimum degradation rates.
Adapted from Quansah et al. (2017).

it results in thermo-mechanical stresses which are exacerbated by the different thermal expansion coefficients of various constituent materials the solar module (e.g. glass, semiconductor, metallization, polymers) (Bogdanski and Herrmann, 2011; Dhere, 2005). Additionally, encapsulant degradation modes, such as discolouration, loss of elasticity and adhesional strength, have been attributed to the combined action of UV radiation and high temperatures, as they alter the chemical structure of EVA (ethylene-vinyl acetate) – the most widely used cell encapsulant in the PV industry (Bandou et al., 2015) (Wohlgemuth and Kurtz, 2011). In general, as noted by, Ferrara and Philipp (Ferrara and Philipp, 2011), polymer-related defects are the most obvious and widespread degradation and failure modes in field-aged photovoltaics. However, cell-related defects such as micro-cracks, breaks in cells and hot spots tend to have higher impact on module power output. Additional studies from various locations, with degradation rates and dominant modes of degradation reported by these studies are presented in Table 6.

3.3. Economic analysis

Results of the financial viability of further investment to restore energy services are presented in this section. For the 110 W_p modules, the performance is rated at 75 W_p currently, having degraded by 24.6% in the last 16-years of exposure. Even though the modules have fallen below the typical warranty threshold of 80% of P_{max} (and currently at 75.4% of P_{max}), this in itself does not constitute the end-of-life of the modules. Osterwald and McMahon (2009) viewed the lifetime of a module as the point in time when the module is no longer acceptable for reasons such as safety and appearance, or when the output has fallen below a minimum acceptable level. Yet, this definition, particularly, in terms of minimum power output, does not readily lend itself to quantitative and numerical description, especially from the perspective of an end-user. As Skoczek et al. (2008) have argued, the system is not at the end of its life if it continues to produce energy to meet the user's needs. However, for the purpose of this analysis, a definition by Rosenthal

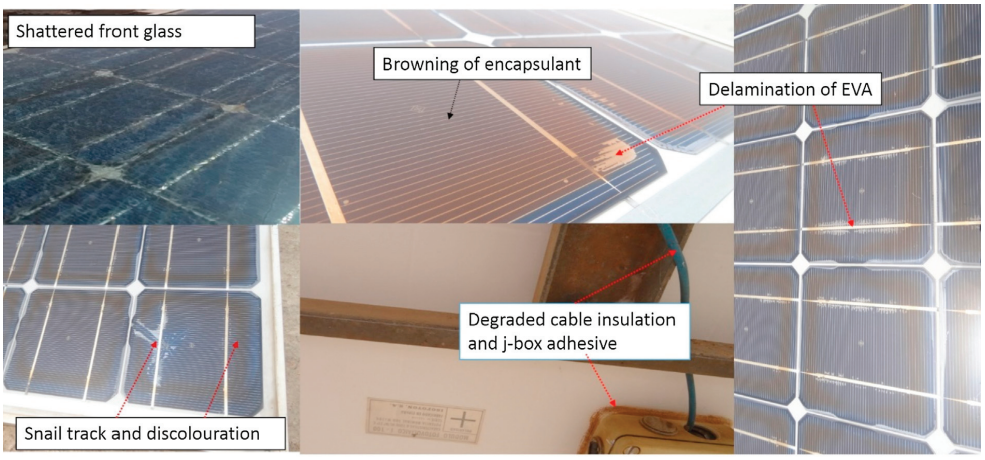

Fig. 13. Samples of observed defects in modules.

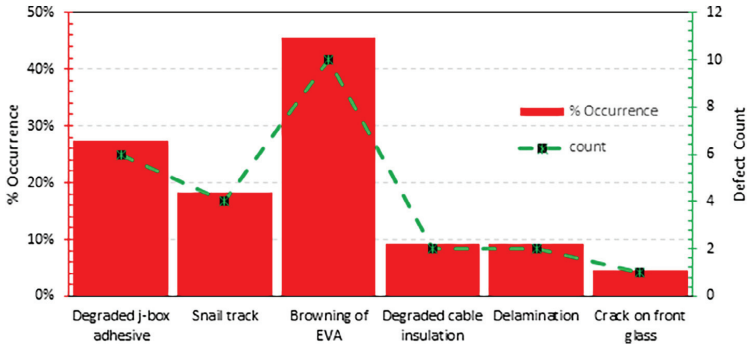

Fig. 14. Occurrence rate of observed defects.

Table 6
Summary of field degradation studies at various locations.

Author(s)	Module technology	Location	Exposure duration	Losses reported	Dominant defects observed
Sastry et al. (2010)	mc-Si	India	10 years	up to 2.5%/yr	Browning of EVA, Corrosion of metallization, Delamination and Junction box defects.
Makrides et al. (2014)	mc-Si pc-Si thin film	Nicosia, Cyprus	5 years	mc-Si: 0.64%/yr pc-Si: 0.62%/yr thin film: 1.78%/yr	–
Sharma and Chandel (2016)	pc-Si	India	2.5 years	0.6–2.5% in duration. Three modules had 50% degradation.	Snail trails, cell browning, junction box failure. Three modules had hotspots, disconnected cells and string interconnect ribbons.
Lorenzo et al. (2014)	mc-Si	Madrid, Spain	17 years	0.53%/yr	Backsheet delamination, Cracks in junction box,
Kaplanis and Kaplani (2011)	mc-Si	Greece	20 years	0.526%/yr (11% in 20 years)	Cell discolouration, Corrosion of connectors, encapsulant delamination
Rabii et al. (2003)	pc-Si	Tunisia	12 years	over 60% loss	Encapsulant degradation
Belmont et al. (2014)	mc-Si	Phoenix, Arizona	26 years	2.3%/yr	intensive encapsulation browning
Bandou et al. (2015)	mc-Si	Adrar, Algeria	28 years	1.22%/yr	yellowing of encapsulant
Limmanee et al. (2017)	pc-Si HIT Micromorph CIGS	Thailand	4 years	pc-Si – 1.2%/yr HIT – 1.3%/yr micromorph – 1.8–6.1%/yr CIGS – 1.7%/yr	–
Kahoul et al. (2014)	mc-Si	Algeria	11 years	0.45–1.%/yr	cracks cell, breaks in interconnect busbar, hot spot
Ibrahim et al. (2009)	mc-Si	Libya	30 years	0.5–1%/yr	cracks in the cover material, deterioration in packaging material, degraded cable insulation
Chandel et al. (2015)	mc-Si	Himalayan region, India	28 years	1.4%/year	Encapsulant discolouration, delamination, oxidation of front grid fingers and anti-reflective coating, glass breakage and bubbles in back sheet.
Rajput et al. (2016)	mc-Si	India	22 years	1.9%/yr	Hotspots, defects in busbar, cell interconnection ribbons, burn marks and backsheet delamination
This study	mc-Si	Ghana	16 years	1.54%/yr	Encapsulant browning, degraded junction box adhesive

et al. (1993) is adopted, which considers a module to have failed, and therefore at the end of its life, if its power output falls below 50%. By this definition, and considering the rate of degradation (1.54%/year), the modules under study could serve for up to 33 years from the year of installation (i.e. 17 years more), (Fig. 15). This, notwithstanding, a 10-year additional life is used in the analysis, and chosen mainly to reflect the longest duration that a deep-cycle solar battery might be expected to last. As shown in Table 7, an estimated investment of $140 will be required for households to restore energy services of each unit (now rated 75 W_p). These costs comprise the cost of batteries, charge controllers and labour (earlier described in Table 5).

The simple payback time for the investment is 5 years and 6 years when cash flows are discounted (Table 7), which is less than the 10-year analysis horizon adopted for the economic analysis under the reference scenario defined in Table 5. The annual cash flows are shown in Fig. 16. The module degradation rate of 1.54%/year is interpreted in reference to original module rating (110 W_p) and translates to an annual wattage loss of 1.7 W_p. This annual wattage loss is assumed to continue, and is applied to the new reference value of 75 W_p in the investment analysis, and results in an energy production of 1351.32 kWh over the analysis period.

The NPV of the cash flows is positive ($116.98) and points to the viability of the investment, in view of a cost of $140 and benefits estimated at $0.2/kWh, escalating at 1% per year (Table 5). The benefit could be higher, depending on the electricity tariff category in which the system owner falls. In Ghana, the categorization is based on facility

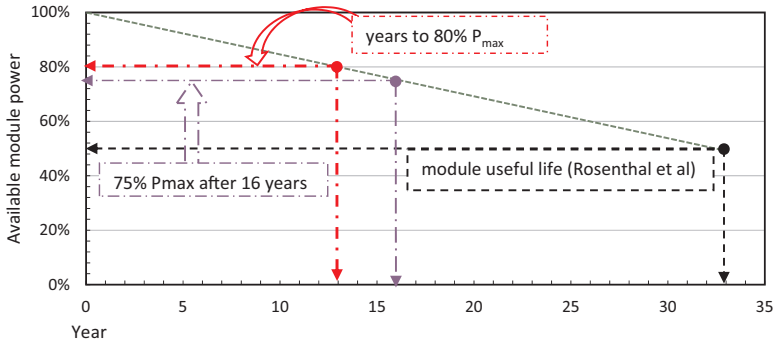

Fig. 15. Module performance degradation curve.

Table 7
Economic viability indicators.

Parameter	Value
Investment cost, $	140
Energy production, kWh	1 351
Present value of benefits, $	257
NPV, $	117
Payback [Simple], yr	5
Payback [Discounted], yr	6

type and electricity consumption level (PURC, 1999). Using 2017 as base year, electricity tariffs range between $0.1–0.3$/kWh depending on customer class and monthly consumption (Electricity Company of Ghana, 2018). A sensitivity analysis is conducted with these tariff assumptions. On the other hand, lower tariffs (below $0.2/kWh), particularly in the residential category could reduce the returns and even make the investment not viable, in which case the modules become a "stranded asset".

A sensitivity analysis conducted on the tariffs (Fig. 17) suggest, that, below, 0.1/kWh, it is not worthwhile putting further money to restore the system, as both the simple and discounted payback times increase significantly and the NPV turns negative. Nevertheless, other benefits that are difficult to quantify (such as reliability of supply, security issues, etc.) could over-ride suggestions by these indicators of financial merit (NPV and payback). Furthermore, after 16 years of module exposure and the possibility of a non-viable financial case for restoring the system to service, the issue of end-of-life management of solar PV modules and related components come into sharp focus. Future work

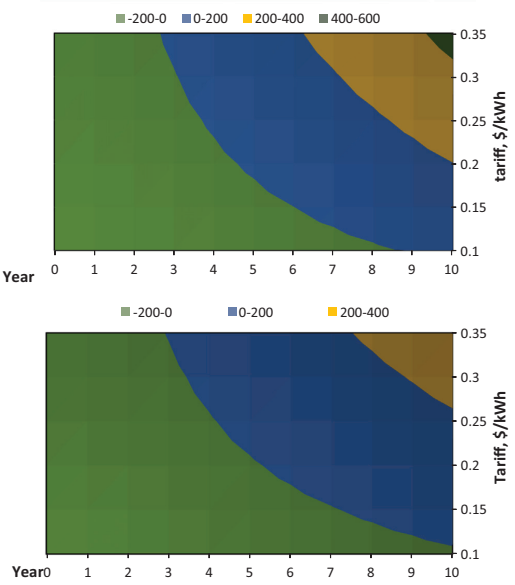

Fig. 17. Sensitivity of cumulative cash flows ($) to tariffs: (top) – simple and (bottom) - discounted.

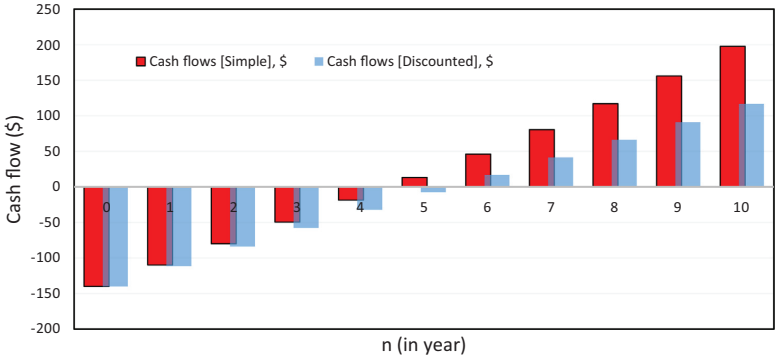

Fig. 16. Cumulative cash flow (discounted and simple).

will consider these aspects of the solar PV life cycle in Ghana, as opportunities for PV-based circular economy are becoming clearer and better understood (IRENA/IEA, 2016).

4. Conclusion

This paper has examined module output degradation in 16-year-old modules exposed in the northern part of Ghana with the view to finding the linear rate of degradation and assessing the causative factors. The modules were deployed in early 2000s under a project titled "*Renewable Energy-Based Electricity for Rural Social and Economic Development (RESPRO)*" to provide basic energy services to households in communities that were yet to be electrified. Twenty-two installations from three communities were assessed, and the results show:

- A linear P_{max} degradation of 1.14–2.43%/yr with a median of 1.54%/yr. The losses are dominated by decline in I_{sc} (0.75%/yr) and FF (0.54%/yr).
- Discolouration of the encapsulant was the most recurrent defect, occurring in 45% of modules studied, followed by degradation of junction-box adhesive (27% occurrence).
- Most of the systems were in open-circuit mode, following the failure of the batteries and the arrival of grid-based electricity.
- An economic analysis conducted on the systems, suggests that at an average end-user tariff of $0.2/kWh, it is viable to invest further in balance-of-system components to restore systems to useful service.

The degradation rates found in this study may be viewed as understated, since available data and methods used are unable to separately account for module degradation under load and degradation while in open-circuit mode. Future work will aim at obtaining data from continuous monitoring of PV modules (including I-V characterization), in order to better understand the evolution of degradation with time under Ghanaian climatic conditions, particularly in the early periods after installation.

Acknowledgements

The authors are grateful to the Norwegian State Educational Loan Fund (Lånakassen), the Kwame Nkrumah University of Science and Technology (KNUST) Ghana and the Faculty of Environmental Sciences and Natural Resource Management of the Norwegian University of Life Sciences (NMBU) for providing financial support for this work. Facilitation provided by the following (all in Ghana) towards, and during the field measurements is much appreciated: Directorate of Renewable and Alternate Energy of the Ministry of Energy, Mr. Isaac A. Edwin (Solar Energy Applications Laboratory, KNUST), Mr. Amadu Mahama (New Energy, Tamale), Mr. Joe Addae (Tamale), Mr. Isaac Yamdogo (Navrongo), Mr. Duut Konlanbik (Nakpanduri) and Mr. Cornelius Yadle (Fielmon). Field support provided by Mr. Joseph Oti-Bio of The Brew-Hammond Energy Centre (KNUST), is likewise appreciated.

References

REN21, 2018. Renewables 2018 Global Status Report. REN21 Secretariat, Paris.
Schmela, M., 2018. Looking Back & Forth: Big Solar Surprises in 2017 & 2018. SolarPower Europe. Available: <http://www.solarpowereurope.org/newsletter/editorial-looking-back-forth-big-solar-surprises-in-2017-2018/> (accessed 17 May 2018).
Sustainable Energy for All (SEforALL), 2018. Our Mission - Going further, faster – together. Sustainable Energy for All. Available: <https://www.seforall.org/our-work> (accessed 3 May 2018).
Quansah, D.A., Adaramola, M.S., Mensah, L.D., 2016. Solar photovoltaics in sub-saharan Africa – addressing barriers, unlocking potential. Energy Procedia 106, 97–110.
World Bank Group, 2016. Access to electricity (% of population). World Bank Group. Available: <https://data.worldbank.org/indicator/EG.ELC.ACCS.ZS?locations=GH> (accessed 3 May 2018).
Government of Ghana, 2018. Ghana ratifies framework agreement on International Solar Alliance. Information Services Department. Available: <http://www.ghana.gov.gh/index.php/media-center/news/4044-ghana-ratifies-framework-agreement-on-international-solar-alliance> (accessed 3 May 2018).
Quansah, D.A., Adaramola, M.S., 2018. Comparative study of performance degradation in poly- and mono-crystalline-Si solar PV modules deployed in different applications. Int. J. Hydrogen Energy 43 (6), 3092–3109.
Frankfurt School-UNEP Centre/BNEF, 2018. Global Trends in Renewable Energy Investment 2018. Frankfurt School of Finance & Management gGmbH, Frankfurt.
Osterwald, C., Adelstein, J., del Cueto, J., Kroposki, B., Trudell, D., Moriarty, T., 2006. Comparison of degradation rates of individual modules held at maximum power. In: 4th IEEE World Conference on Photovoltaic Energy Conversion, Hawaii.
Jordan, D.C., Kurtz, S.R., VanSant, K., Newmiller, Jeff, 2016. Compendium of photovoltaic degradation rates. Prog. Photovolt.: Res. Appl. 24 (7), 978–989.
Jordan, D.C., Kurtz, S.R., 2013. Photovoltaic degradation rates—an analytical review. Prog. Photovolt. 12–29.
Ishii, T., Masuda, A., 2017. Annual degradation rates of recent crystalline silicon photovoltaic modules. Prog. Phtovoltaics: Res. Appl.
Hoffman, A.R., Ross, R.G.J., 1978. Environmental qualification testing of terrestrial solar cell modules. In: Photovoltaic Specialists Conference; 13th; June 5–8, 1978, Washington, DC.
Osterwald, C.R., McMahon, T.J., 2009. History of accelerated and qualification testing of terrestrial photovoltaic modules: a literature review. Prog. Photovolt.: Res. Appl. 17, 11–33.
Wohlgemuth, J.H., Kurtz, S., 2011. Using accelerated testing to predict module reliability. In: 37th IEEE Photovoltaic Specialists Conference (PVSC 37), Seattle, Washington.
Arndt, R., Puto, R., 2009. Basic Understanding of IEC Standard Testing For Photovoltaic Panels. TÜV SÜD America Inc.
Quansah, D.A., Adaramola, M.S., Takyi, G., Edwin, I.A., 2017. Reliability and degradation of solar pv modules—case study of 19-year-old polycrystalline modules in Ghana. Technologies 5 (22).
UNDP/GEF, 2002. Renewable Energy-Based Electrcity for Rural Social and Economic Development (RESPRO).
Nassen, J., Evertsson, J., Andersson, B.A., 2002. Distributed power generation versus grid extension: an assessment of solar photovoltaics for rural electrification in northern Ghana. Prog. Photovolt.: Res. Appl. 10, 495–510.
Bawakyillenuo, S., 2009. Policy and institutional failures: photovoltaic solar household system (PV/SHS) dissemination in Ghana. Energy Environ. 20 (6), 927–947.
Natural Resources Canada, 2004. Clean Energy Project Analysis: RETSCREEN Engineering & Cases Textbook.
Energy Commission Ghana, 2018. Provisional Wholesale Supply and Generation License Holders. Energy Commission Ghana, Accra.
NASA, 2018. NASA Surface meteorology and Solar Energy - Location. Available: <https://eosweb.larc.nasa.gov/cgi-bin/sse/grid.cgi?email=skip@larc.nasa.gov> (accessed 2 April 2018).
Beckley, C.S., Shaban, S., Palmer, G.H., Hudak, A.T., Noh, S.M., Futse, J.E., 2016. Disaggregating tropical disease prevalence by climatic and vegetative zones within tropical west africa. Plos One 11 (3).
PVsyst SA, 2012. PVSyst Photovoltaic Software. Satigny.
Hawker Group, 1999. Hawker Batteries Handbook - Standby Batteries for Telecommunications. Hawker Group, Wiltshire.
IEA, 2014. Review of Failures of Photovoltaic Modules. IEA/OECD.
NREL, 2012. Development of a Visual Inspection Data Collection Tool for Evaluation of Fielded PV Module Condition. NREL, Golden.
Kaplanis, S., Kaplani, E., 2011. Energy performance and degradation over 20 years performance of BP c-Si PV modules. Simul. Model. Pract. Theory 19, 1201–1211.
Luo, X., Wang, J., Dooner, M., Clarke, J., 2015. Overview of current development in electrical energy storage technologies and the application potential in power system operation. Appl. Energy 137, 511–536.
Klise, G.T., Balfour, J.R., 2015. A Best Practice for Developing Availability Guarantee Language in (PV) O&M Agreements. Sandia National Laboratories, Albuquerque, New Mexico.
Energy Commission Ghana, 2017. National Energy Statistics 2007–2016. Energy Commission Ghana, Accra.
Quansah, D.A., Adaramola, M.S., 2016. Economic assessment of a-Si and CIS thin film solar PV technologies in Ghana. Sustain. Energy Technol. Assess. 18, 164–174.
Quansah, D.A., Woangbah, S.K., Anto, E.K., Akowuah, E.K., Adaramola, M.S., 2017. Techno-economics of solar pv-diesel hybrid power systems for off-grid outdoor base transceiver stations in Ghana. Int. J. Energy Clean Environ. 18 (1), 61–78.
Opoku, R., Mensah-Darkwa, K., Samed Muntaka, A., 2018. Techno-economic analysis of a hybrid solar PV-grid powered air-conditioner for daytime office use in hot humid climates – a case study in Kumasi city, Ghana. Sol. Energy 165, 65–74.
Meydbray, J., Dross, F., 2016. PV Module Reliability Scorecard 2016. DNV GL, Oslo.
IEA, 2004. Managing the Quality of Stand Alone PV Systems:Case Studies. IEA, Paris.
Skoczek, A., 2008. Long-term performance of photovoltaic modules.
Park, N., Jeong, J., Han, C., 2014. Estimation of the degradation rate of multi-crystalline silicon photovoltaic module under thermal cycling stress. Microelectron. Reliab. 54, 1562–1566.
Lorenzo, E., Zilles, R., Moretón, R., Gómez, T., Martínez de Olcoz, A., 2014. Performance analysis of a 7-kW crystalline silicon generator after 17 years of operation in Madrid. Prog. Photovolt.: Res. Appl. 22 (12), 1273–1279.
Pozza, A., Sample, T., 2016. Crystalline silicon PV module degradation after 20 years of field exposure studied by electrical tests, electroluminescence, and LBIC. Prog. Phtovolt.: Res. Appl. 24, 368–378.
Polverini, D., Field, M., Dunlop, E., Zaaiman, W., 2012. Polycrystalline silicon PV modules performance and degradation over 20 years. Prog. Photovolt. 21 (5), 1004–1015.
Bandou, F., Arab, A.H., Belkaid, M.S., Logerais, P.-O., Riou, O., Charki, A., 2015. Evaluation performance of photovoltaic modules after a long time operation in

Saharan environment. Int. J. Hydrogen Energy 40 (39), 13839–13848.
Belmont, J., Olakonu, K., Kuitche, J., TamizhMani, G., 2014. Degradation rate evaluation of 26-year-old 200 kW power plant in a hot-dry desert climate. Denver, CO, USA.
Limmanee, A., Songtrai, S., Udomdachanut, N., Kaewniyompanit, S., Sato, Y., Nakaishi, M., Kittisontirak, S., Sriprapha, K., Sakamoto, Y., 2017. Degradation analysis of photovoltaic modules under tropical climatic conditions and its impacts on LCOE. Renewable Energy 102 (2017), 199–204.
Ye, J.Y., Reindl, T., Aberle, A.G., Walsh, T.M., 2014. Performance degradation of various PV module technologies in tropical Singapore. IEEE J. Photovolt. 4 (5), 1288–1294.
Sorloaica-Hickman, N., Davis, K., Leyte-Vidal, A., Kurtz, S., Jordan, D., 2012. Comparative study of the performance of field-aged photovoltaic modules located in a hot and humid environment. In: Photovoltaic Specialists Conference (PVSC), 2012 38th IEEE, Austin, TX, USA.
Rajput, P., Tiwari, G.N., Sastry, O.S., Bora, B., Sharma, V., 2016. Degradation of mono-crystalline photovoltaic modules after 22 years of outdoor exposure in the composite climate of India. Sol. Energy 135, 786–795.
Skoczek, A., Sample, T., Dunlop, E.D., Ossenbrink, H.A., 2008. Electrical performance results from physical stress testing of commercial PV modules to the IEC 61215 test sequence. Sol. Energy Mater. Sol. Cells 92 (12), 1593–1604.
Bogdanski, N., Herrmann, W., Weighting of climate impacts on pv-module degradation - comparison of outdoor weathering data and indoor weathering data. In: 26th European Photovoltaic Solar Energy Conference and Exhibition, Hamburg.
Quintana, M.A., King, D.L., McMahon, T.J., Osterwald, C.R., 2002. Commonly Observed Degradation in Field-Aged Photovoltaic Modules.
Ferrara, C., Philipp, D., 2012. Why do PV modules fail? In: International Conference on Materials for Advanced Technologies 2011, Symposium O.
King, D.L., Quintana, M.A., Kratochvil, J.A., Ellibee, D.E., Hansen, B.R., 2000. Photovoltaic module performance and durability following long-term field exposure. Prog. Photovolt.: Res. Appl. 8 (2), 241–256.
Rabii, A.B., Jraidi, M., Bouazzi, A.S., 2003. Investigation of the degradation in Field-Aged Photovoltaic Modules. Osaka.
Kahoul, N., Houabes, M., Sadok, M., 2014. Assessing the early degradation of photo-voltaic modules performance in the Saharan region. Energy Convers. Manage. 320–326.
Ibrahim, I.M.S., Abouhdima, I., Gantrari, M.B., 2009. Performance of thirty years stand alone photovoltaic system. In: Proceedings of 24th European Photovoltaic Solar Energy Conference, 21–25 September 2009, Hamburg, Germany.
Dhere, N.G., 2005. Reliability of PV modules and balance-of-system components. In: Conference Record of the Thirty-first IEEE Photovoltaic Specialists Conference, 2005, Lake Buena Vista, FL, USA.
Sastry, O.S., Saurabh, S., Shil, S.K., Pant, P.C., Kumar, R., Kumar, A., Bandopadhyay, B., 2010. Performance analysis of field exposed single crystalline silicon modules. Sol. Energy Mater. Sol. Cells 94 (9), 1463–1468.
Makrides, G., Zinsser, B., Schubert, M., Georghiou, G.E., 2014. Performance loss rate of twelve photovoltaic technologies under field conditions using statistical techniques. Sol. Energy 103 (2014), 28–42.
Sharma, V., Chandel, S.S., 2016. A novel study for determining early life degradation of multi-crystalline-silicon photovoltaic modules observed in western Himalayan Indian climatic conditions. Sol. Energy 134, 32–44.
Chandel, S.S., Naik, M.N., Sharma, V., Chandel, R., 2015. Degradation analysis of 28 year field exposed mono-c-Si photovoltaic modules of a direct coupled solar water pumping system in western Himalayan region of India. Renewable Energy 78, 193–202.
Rosenthal, A.L., Durand, S.J., Thomas, M.G., 1993. A ten year review of performance of photovoltaic systems. In: Conference Record of the Twenty Third IEEE Photovoltaic Specialists Conference - 1993 (Cat. No.93CH3283-9), Louisville, KY, USA.
PURC, 1999. Electricity Rate Setting Guidelines. PURC, Accra.
Electricity Company of Ghana, 2018. Electricity Tariff Reckoner Effective 15th March, 2018. Electricity Company of Ghana, Accra.
IRENA/IEA, 2016. End-of-Life Management: Solar Photovoltaic Panels.

ISBN: 978-82-575-1550-8
ISSN: 1894-6402

Norwegian University
of Life Sciences

Postboks 5003
NO-1432 Ås, Norway
+47 67 23 00 00
www.nmbu.no